Title
Modeling Myopia in Guinea Pigs

Author
Kochik, Sarah Elizabeth

Publication Date
2019

Peer reviewed|Thesis/dissertation

Modeling Myopia in Guinea Pigs

by

Sarah Kochik

A dissertation submitted in partial satisfaction of the
requirements for the degree of
Doctor of Philosophy

in

Vision Science

in the

Graduate Division

of the

University of California, Berkeley

Committee in charge:

Associate Professor Yue (Maria) Liu, Chair
Professor Christine Wildsoet, Co-chair
Professor Austin Roorda
Professor John Colford

Summer 2019

Modeling Myopia in Guinea Pigs

Abstract

Modeling Myopia in Guinea Pigs

by

Sarah Kochik

Doctor of Philosophy in Vision Science

University of California, Berkeley

Associate Professor Yue (Maria) Liu, Chair

Professor Christine Wildsoet, Co-chair

Myopia, or nearsightedness, is a common vision disorder characterized by an abnormal increase in eye elongation, leading to a mismatch in the refractive power of the eye and the location of the retina. Myopia has dramatically increased in prevalence over the last 50 years, currently affecting half of college-aged individuals in the United States and almost all young adults in certain Asian populations. This trend is not a temporary aberration; myopia is projected to afflict nearly half of the global population by the year 2050.

Traditionally, myopia is "corrected" using glasses, contact lenses, or refractive surgery. Although these solutions allow for clear vision, they do not rectify the underlying structural changes associated with myopia, including the lengthening of the eye and the thinning of its layers. As a result, there remains an increased risk of vision-threatening complications, such as glaucoma, retinal detachment, myopic maculopathy, and choroidal neovascularization. In the past, these complications were regarded as characteristic of "pathological" myopia. However, it is now known that no amount of myopia is considered safe; the more severe the myopia, the greater the risk, starting from even the smallest measurable amounts.

In addition, not all myopes have access to refractive correction. Uncorrected refractive error accounts for over half of global vision impairment. It has also been estimated that uncorrected myopia is associated with an annual global potential productivity loss of $244 billion.

With these startling figures, there have been renewed efforts to develop and prescribe treatments for myopia. Inspired by the influence of animal models on myopia research thus far, we sought to further one of the most popular mammalian models of myopia, the guinea pig, to allow for mechanistic exploration that is not possible in human clinical trials.

Chapter 1 reviews the process of emmetropization and refractive error development as understood from observations in humans and experiments in animal models. Current clinical recommendations are also summarized.

Chapter 2 presents a qualitative synthesis of the known relevant ocular characteristics of the guinea pig myopia model. Guinea pigs have emerged as a popular mammalian model

because of the relative ease of housing and husbandry, larger eyes, and better visual acuity compared to other laboratory rodents. However, guinea pigs aren't perfect subjects for the human condition we are attempting to model. Knowledge of the optical quality of the guinea pig eye isn't firmly established, and experimental models of myopia depend on manipulating the visual experience.

In Chapter 3, we detail the optical aberrations of the guinea pig eye. Using a custom-built Shack-Hartmann wavefront sensor, we fit a Zernike polynomial function to the images collected from adolescent guinea pigs. The optical quality of the eyes was assessed in terms of individual Zernike coefficients, and data were further analyzed to derive root-mean-square wavefront errors, modulation transfer functions, point spread functions, and depth of focus. These data are compared with visually normal young adult human eyes. While visual acuity is much poorer in the guinea pig eye compared to the human eye, high order aberrations do not appear to be major sources of image quality degradation. It is still unknown what optical information the eye is using to generate growth modulatory signals. However, the measurement of the optical aberrations of the guinea pig eye is an important step forward, allowing the nature of the defocus stimuli and their effects on retinal image quality to be better understood in this mammalian model.

Chapter 4 presents the results of a novel method of inducing myopia in the guinea pig model. Historically, spectacle-mounted lenses and diffusers are used to induce myopia in guinea pigs. These lenses are typically mounted on Velcro ring supports, which are then glued to the fur surrounding the guinea pigs' eyes. While shown to be safe and effective, there are significant limitations with this process. The lenses (or diffusers) can be removed by the guinea pigs if they scratch at the velcro site, requiring very frequent monitoring and reapplication. As a result, experiments using spectacle-mounted lenses cannot be conducted over a long period of time. We designed and tested rigid gas permeable contact lenses as an alternative method for inducing myopia in guinea pigs, which will also allow for testing contact lens treatments in this animal model.

Finally, the ability of atropine to prevent the development of myopia is a fairly consistent finding in animal studies. However, important exceptions have been noted. In Chapter 5, we establish that topically applied 1% atropine is effective in reducing myopia progression in guinea pigs. After two weeks of treatment with either daily or weekly applied atropine, guinea pigs treated with our contact lens-induced myopia model developed significantly less myopia compared to those treated with a placebo drop.

The overarching goal of this research is to further our basic understanding of the guinea pig eye so that we can continue to use this model to test translational clinical treatments.

To Arjun

Quand tu veux construire un bateau, ne commence pas par rassembler du bois, couper des planches et distribuer du travail, mais reveille au sein des homes le desir de la mer grande et large.
- Antoine de Saint-Exupry

Translation:
If you want to build a ship, don't get people together to collect wood and don't assign them tasks and work, but rather teach them to long for the endless immensity of the sea.

Contents

List of Figures

List of Tables

Acknowledgments

I would like to thank the excellent mentors that made up my qualifying exam committee as well as my thesis committee: Dr. Deborah Orel-Bixler, Dr. Nancy McNamara, Dr. Austin Roorda, Dr. Jack Colford, and Dr. Nick Jewel. You have imparted a healthy skepticism into everything that I read and do. Because of you, I have confidence in my ability to conduct and evaluate rigorous scientific work. I would especially like to thank my advisors, Dr. Maria Liu and Dr. Christine Wildsoet. You have been truly inspiring role models. You have been selfless with your knowledge and time and foster a welcoming and lively lab group.

I am grateful to have gotten to know and work with such talented undergraduate research assistants: Niathi Kona, Pawanjot Kaur, and Brandon Kim. Thank you for your time and commitment to the projects described here and to the efforts that went into the work that (as so often is the case in science) did not make it to these pages. Your dedication is truly appreciated. I would also like to recognize the optometry student research assistants that I had the great honor of working with: Natalia Santizo, Jennifer Nguyen, Irene Tan, Michelle Holmes, Connie Chen, and Elysia Ison, thank you for your interest and enthusiasm for optometric research. I hope that what you learned in the lab will continue to serve you in clinical practice.

There are many people that I'd like to acknowledge for many reasons, and I won't be able to fit everything here. I would like to recognize my family for their endless support of my education and my friends for being such a positive source of energy and light in my life. Mom, thank you for teaching me that it is better to be resourceful than to have resources. Baba, thank you for being my biggest cheerleader for my whole life! Ashley, you've become such a source of inspiration and support - you're always there for me when I need you. Sasha, thanks for being such a great friend for so long. Jazzi, I could not and would not have done any of this without you by my side! Sean, thank you for getting me over the finish line with your careful proofreading, editing, and comical commentary. Leo & Luna, thanks for always cheering me up and reminding me that work isn't always the most important thing.

And finally, Arjun. Former Supreme Court Justice Sandra Day O'Connor once said that the key to a fulfilling life is meaningful work. Thank you for supporting me on my quest for meaningful work over these past twelve years, and for allowing me to feel protected and cared for throughout this long journey. Let this serve as a permanent record of how great of an inspiration you have been on my life.

Chapter 1

Introduction

Myopia (nearsightedness) is a condition that occurs when the length of the eye becomes too long for its optical power, causing distant objects to appear blurred. Correcting this visual problem requires collecting a few data points, measuring refraction, and then prescribing optical correction. However, we have learned that this simple solution does not prevent comorbid diseases associated with myopia, and in fact, we may be unintentionally exacerbating the disease process with traditional prescribing methods.

1.1 Emmetropization and the Development of Myopia

Normal ocular development for humans, like most animals, is toward emmetropia, where the refracting optical power of the eye is matched to the length of the eye, resulting in perfect focus. When there is a mismatch between these ocular components, the result is either hyperopia (farsightedness), in which the eye is relatively too short, or myopia (nearsightedness), in which the eye is relatively too long. Examples are shown in Figure 1.1.

Human eye growth continues from birth throughout childhood development and has some interesting properties compared to other measures of growth such as height or weight. Although most growth variables follow a Gaussian distribution, the distribution of human refractive errors becomes leptokurtic, in which the average amount and the variance in the distribution of refractive errors are reduced (Figure 1.2). This change cannot be accounted for by scaled growth alone, the so called passive emmetropization. Therefore, it is generally accepted that active emmetropization, guided by visual experience, accounts for part of this change; however, the precise mechanisms that coordinate this process are not completely understood.

Newborn infants have a broad distribution of refractive errors, with a mean refractive error of +2.00 D of hyperopia [120]. Over the next 6-12 months, emmetropization leads to a reduction in both the magnitude of hyperopia and the variance, towards a more leptokurtic distribution. Changes to corneal curvature (flattening), axial length (increasing), and lens power (decreasing) all contribute to the process of emmetropization in infancy [120]. By 5-7

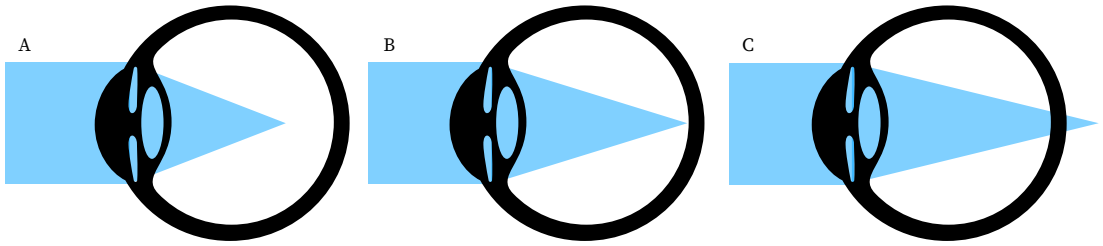

Figure 1.1: Schematic illustration of myopic (A), emmetropic (B), and hyperopic (C) eyes. In a myopic eye, the axial length is too long for the optical power, causing the image to come into focus in front of the plane of the retina. In an emmetropic eye, images come into focus on the retina, while in a hyperopic eye, images focus behind the retina.

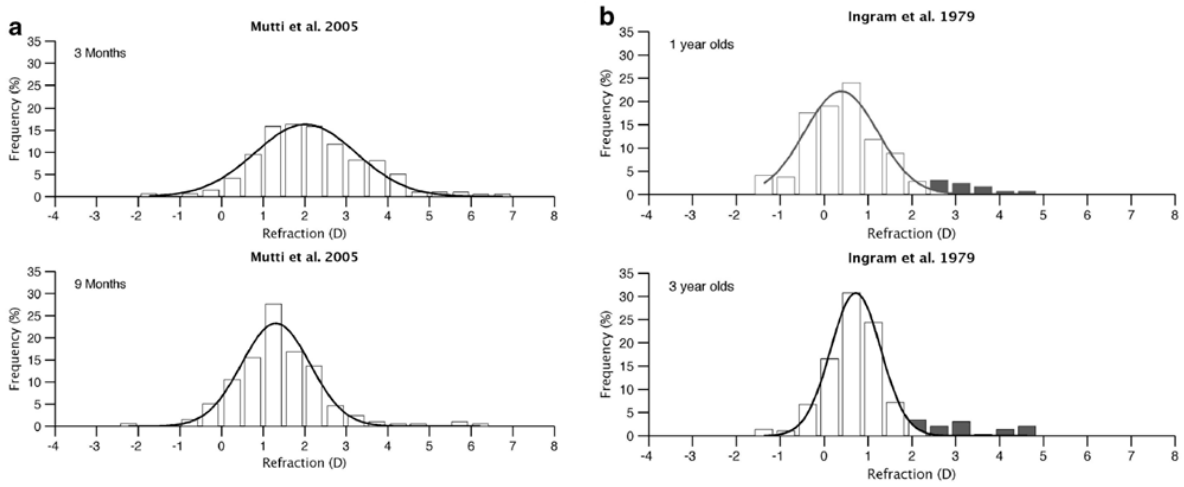

Figure 1.2: (a) Shift in refraction between 3 months and 9 months of age. (b) Leptokurtic shift in refraction between 1 year and 3 years of age. [120] [68]

years of age, most American children have relatively low residual hyperopic refractive errors.

After 5-7 years of age, refractive development appears to vary dramatically depending on genetics, location, and culture. Non-pathological myopia follows an initial linear course of refraction change, followed by a rapid increase in myopia, then relative stability beginning in the late teenage years. The development and progression of myopia during these juvenile years is attributable to excessive axial elongation. In rare cases, myopia appears to occur as an early failure of emmetropization, due to a disruption of the normal visual experience, such as with congenital cataracts or ptosis, or resulting from other systemic conditions such as Stickler Syndrome.

1.2 Myopia as a Threat to Public Health

Myopia is now the most common human eye disorder in the world and has seen unprecedented increases in prevalence in recent decades around the world [195, 136]. Just 60 years ago, only 10-20% of the Chinese population was estimated to be nearsighted [36]. In some Asian countries today, the prevalence of myopia is approaching 100% in young adults; for example, a prevalence of 86.1% was reported in a recent survey of military conscripts in Taiwan [89] and 96.5% for a similar cohort in Seoul, South Korea [80]. Myopia currently affects half of young adults in the United States [195], Europe [36], and Asia, [136] and it is projected to affect half of the world population by the year 2050 [58].

Not only is the overall prevalence of myopia increasing [195, 58], but the onset of myopia appears to be occurring earlier in life. In the past, the onset of myopia typically occurred between 8-12 years of age. However, in a 2004 Taiwan-based study, the prevalence of myopia was reported to have already reached 20-30% among 6-7 year-olds, further increasing to 84% in high school students [97]. Estimates are thought to be even higher today.

Myopia has historically been seen as more of an inconvenience than a disease and is traditionally corrected with glasses, contact lenses, or refractive surgery, which allows for clear distance vision. However, the anatomical changes associated with myopia - lengthening of the eye, thinning of the retinal, choroidal, and scleral tissues, which are exaggerated in high myopia - are not treated by optically or surgically correcting refractive errors. Any amount of myopia increases the risk of retinal detachment, glaucoma, and other vision-threatening complications [44], and high myopia is now a leading cause of preventable blindness [221]. In addition, not all myopic individuals have access to correction for their refractive error. Uncorrected refractive errors (including myopia, hyperopia, presbyopia, and astigmatism) accounts for over half of global visual impairment [9]. It has been estimated that uncorrected myopia alone is associated with an annual global potential productivity loss of $244 billion [121].

For centuries, eye care professionals have proposed methods of intervening in an attempt to slow myopia progression. However, the first evidence-based review of such methods, published in 2002 and based on 10 randomized controlled trials, concluded that there were no recommended interventions for controlling myopia [163]. Nonetheless, the growing myopia epidemic has driven a renewed interest in controlling this disease, and there have been more than 170 peer-reviewed articles on myopia control in humans and hundreds more in animal models since that first review was published.

1.3 Clinical Myopia Control

There is now convincing evidence that it is possible to slow the progression of myopia in children through optical and/or pharmaceutical interventions.

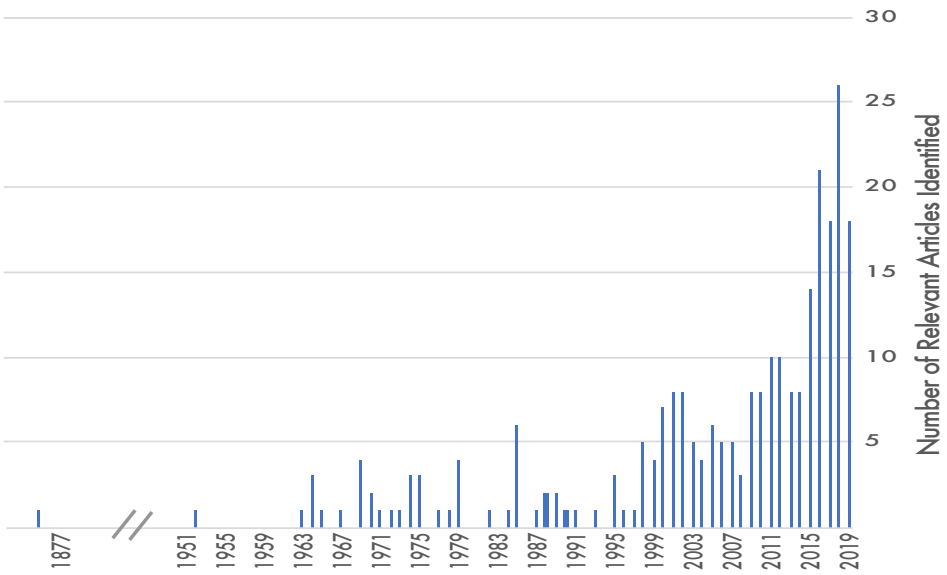

Figure 1.3: Frequency of relevant medline publications concerning atropine and myopia

Atropine for Myopia Control

Topical atropine, a non-selective and irreversible muscarinic antagonist, has proven to be the most effective in reducing myopia progression of all interventions in current clinical use, although the mechanism underlying its anti-myopia effect remains unclear [179]. A renewed interest in this application of atropine is evident from my initial search conducted for this report: A keyword search for the terms atropine and myopia yields 259 results, the earliest published in 1874, with a much higher frequency of publications in the past decade as shown in Figure 1.3.

In the late 21st century, several randomized trials were attempted that demonstrated some promising clinical effects on the progression of myopia [226, 171, 170]. However, these studies were small and suffered from important methodological flaws, such as lack of regular and detailed follow-up examinations, absence of appropriate controls, and absence of masking of participants or investigators. In addition, the safety and long-term efficacy was not followed.

The Atropine in the Treatment of Myopia (ATOM) study was a randomized, double-masked, placebo-controlled trial designed primarily to study whether topical 1% atropine sulfate can prevent the progression of myopia effectively and safely in children 6 to 12 years of age [30]. Four hundred children were enrolled in the study between April 1999 and September 2000 and were randomized with equal probability to either the atropine group or the placebo-control group. One eye of each child was chosen at random to be treated. Results of this study demonstrated that a once-nightly dose of 1% atropine was highly effective in reducing progression of myopia compared to placebo treatment. Over the two-year period of the study, children treated with atropine achieved a 77% reduction in the mean progression of

myopia compared with the placebo treatment and no change in axial length. However, while no serious adverse effects were observed and the monocular treatment was well-tolerated, blurred near vision and light sensitivity prevent this treatment from being widely adopted as a myopia treatment.

The same group continued with a new randomized trial to assess the efficacy, safety, and functional impact of three different atropine concentrations for the bilateral treatment of myopia in children of a similar age range. Atropine for the Treatment of Childhood Myopia: Safety and Efficacy of 0.5%, 0.1%, and 0.01% Doses (ATOM 2) was a single-center, double-masked, randomized trial in which 400 children were randomized to receive bilateral treatment of one of the above-listed doses of atropine nightly for two years [27]. Results revealed a dose-dependent response, with 0.5% and 0.1% doses showing a very similar efficacy as the 1% dose in controlling myopia both in terms of refractive error change and axial length change. Interestingly, the 0.01% dose, which was originally intended to be a placebo treatment, showed some efficacy in slowing myopia progression, although there appears to be a difference between the controlling effect on refractive error, compared to axial length. The axial elongation in the 0.01% group remained significant, leading to uncertainty in the role of very low concentration atropine in myopia control. A summary of both trials is shown in Figure 1.4.

Atropine appears to be highly effective in the short-term (1-2-year treatment period). However, 0.01% atropine is not a universal solution for myopia control. A major limitation to this being a widely-adopted treatment are the side effects of the drug. The primary ocular side effects include mydriasis and cycloplegia, resulting in symptoms of glare, light sensitivity, and blurred near vision. Side effects are important to consider, not only for their primary effect on patient comfort, but also because side effects may lead to poor compliance [171].

The ATOM studies also found an important effect when atropine treatment was discontinued. Both concentration- and age-related rebound myopia was observed in children followed for a year after termination of atropine treatment [26, 190, 25]. The pharmacodynamics of atropine would suggest that long-term exposure to a competitive antagonist will cause an upregulation of receptors, resulting in a loss of efficacy to the applied drug over time and exaggerated symptoms when treatment is ended [45]. Younger children and those treated with higher concentrations were shown to have the highest risk of rebound myopia progression in these studies [25].

Additionally, studies have shown that as atropine concentration decreases, the percent of "nonresponders" (children who continue to experience rapid myopia progression despite atropine treatment) increases [27, 171]. Finally, although meta-analyses have supported that the efficacy of atropine does not vary between high (0.5% - 1%), moderate (0.01% - 0.5%), and low (0.01%) concentrations [65, 53], a recent trial of three low concentrations of atropine (0.05%, 0.025%, and 0.01%) found that efficacy did increase with concentration, at least over a short-term (1-year) period [225]. Clearly, we are still uncertain of the exact relationship between atropine concentration and myopia control efficacy.

In summary, topical 0.01% atropine appears to show some efficacy in controlling myopia

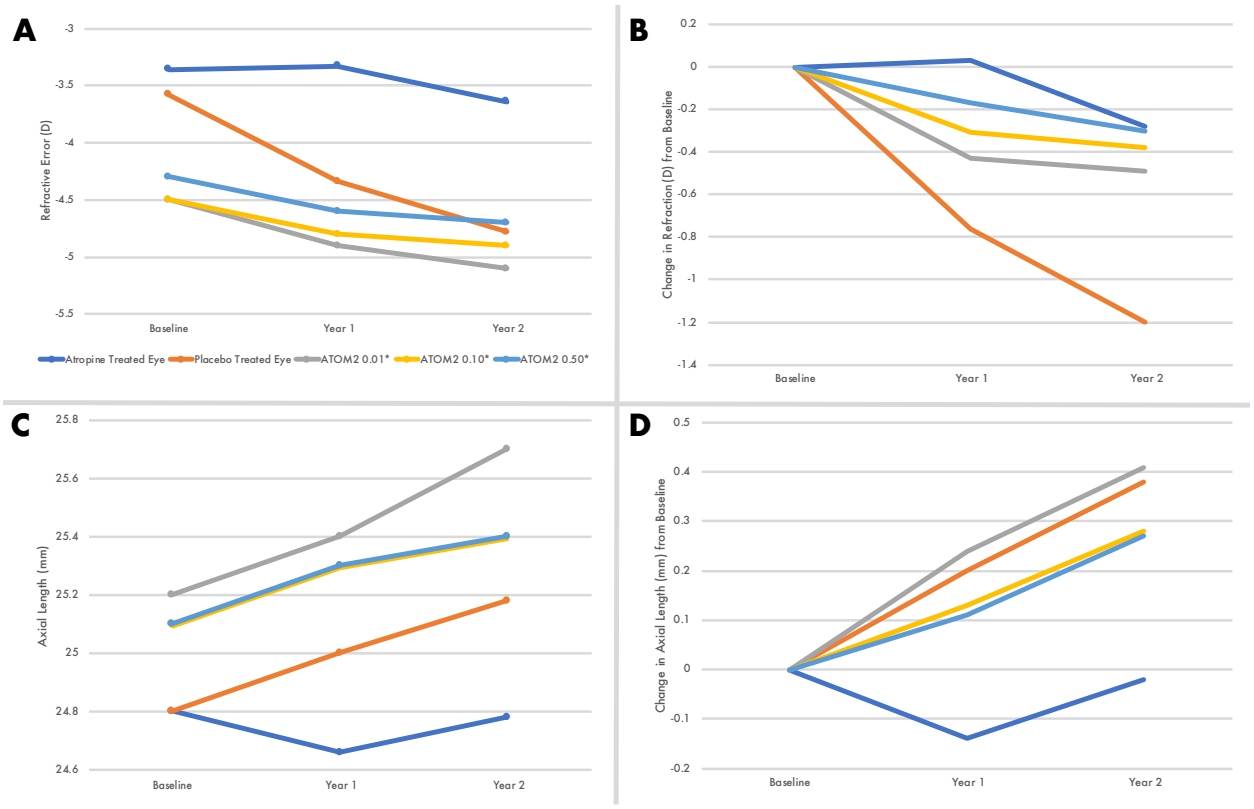

Figure 1.4: Combined results from ATOM1 and ATOM2. The top row shows the raw change in refractive error over the two-year study periods (panel A) and relative change normalized to the baseline (panel B). The bottom row represents the raw change in axial length (panel C) and relative change normalized to the baseline (panel D). It is important to note that ATOM1 and ATOM2 occurred at different points in time (separated by nearly 10 years) and different instrumentation was used to measure axial length (a partial coherence interferrometer in ATOM2 as opposed to an ultrasound in ATOM1).

progression and has far fewer side effects and less risk of rebound compared to the other doses tested. Two meta-analyses have been performed in an attempt to better characterize the concentration-dependent responses of atropine on myopia progression. The first of these reviews concluded that that while atropine was effective, there was no concentration-dependent effect [65]. Similarly, the second meta-analysis suggests that even if the effect of atropine is not concentration-dependent, the side effects are [53]. Despite the remaining questions, the American Academy of Ophthalmology supports the use of low-concentration atropine in myopia control [141], and this has become a common clinical practice in the United States.

Optical Treatments for Myopia Control

Studies employing orthokeratology and multifocal contact lenses, which involve peripheral defocus manipulations, have also shown consistent and clinically significant benefits [59], although reductions in myopia progression remain limited to around 50% at best. Orthokeratology (ortho-k), represents one of the most effective optical approaches to myopia control [199, 65], as reflected in its increasing use with pediatric patients. Ortho-k was originally introduced as a method of improving uncorrected daytime vision in myopic patients, involving specifically designed rigid gas permeable lenses that are worn overnight to temporarily flatten the central cornea. With the advent of more sophisticated lens designs (e.g., reverse geometry lenses), faster and more accurate correction is achievable. In addition, numerous clinical trials have demonstrated reduced myopia progression with ortho-k lenses compared to spectacles or single-vision contact lenses, as indicated by slowed axial elongation [172].

This treatment effect has been attributed to the altered optical defocus profile induced by corneal topographical changes. Supporting evidence for this interpretation comes from observed strong inhibitory effects of imposed myopic defocus on axial elongation in animal models, even when limited to the peripheral retina [201, 174]. Such results are also consistent with other animal studies demonstrating local (ocular) regulation of eye growth and refractive errors, and importantly, a significant influence of the peripheral retina on overall ocular growth and central refractive development [103, 178]. Furthermore, a review of the relevant literature pertaining to optical treatment strategies for controlling myopia suggests that the effectiveness of control treatments involving imposed myopic defocus is influenced by the extent of the exposed visual field [175]. Specifically, the efficacy of optical treatment strategies for myopia may be improved by increasing the retinal area exposed to imposed myopic defocus. However, few studies have formally addressed this possibility in humans. If the above interpretation is correct, then it should be possible to improve myopia control efficacy for individual patients through appropriate manipulation of imposed peripheral defocus, either in area or duration of exposure.

Although eye care practitioners worldwide are concerned about myopia and understand that there are methods of intervention that have been repeatedly found to be effective in slowing progression of myopia, the majority still prescribe single-vision spectacles and contact lenses to progressing myopes [217]. There is a need for evidence-based guidance informed by animal models as well as human trials that can inform clinical practice and future research.

1.4 Study Rationale and Dissertation Approach

Much of our current understanding of the characteristics and mechanisms of eye growth and the development of myopia has come from experiments using animal models. These models include primates (macaque and marmoset monkeys), tree shrews, guinea pigs, mice, chickens, fish, and squids [193]. All have been shown to have visually-guided eye growth and can compensate for optically imposed myopic or hyperopic defocus by altering axial length.

The fact that visually-guided eye growth is preserved across these varied species suggest that this is a fundamental property of the camera-type eye [193]. Each species provides experimental advantages to study the mechanism of eye growth and refractive development despite differences in ocular anatomy and vision function. However, it is important to consider anatomical and physiological differences when interpreting and translating results to the human eye.

The work described in this dissertation raises important considerations when using the guinea pig model as a mechanism to study the human condition of myopia.

This dissertation is organized into four sections with four distinct goals (Chapters 2, 3, 4, and 5):

Chapter 2 briefly reviews animal models of myopia and provides an anatomical comparison of the human eye and the guinea pig eye. Key features, advantages, and disadvantages of using the guinea pig for refractive error research are highlighted.

Chapter 3 describes a study using the Shack-Hartmann wavefront sensor, which allows for rapid, accurate, and objective measurements of wave aberrations. Wave aberration data collected from one eye of each of eight young guinea pigs were used to derive image quality metrics over a 4 mm pupil, which were compared with known wavefront error trends in humans.

Chapter 4 describes the design of rigid gas permeable contact lenses that can be used as an alternative method of inducing myopia in guinea pigs.

Chapter 5 establishes the guinea pig as an animal model for topical dosing of atropine. The ability of atropine to prevent the development of myopia is a fairly consistent finding in animal studies, however, important exceptions have been noted. The work described in this chapter demonstrates that guinea pigs respond to topical doses of atropine in a similar way to humans.

Chapter 6 summarizes the main findings described in this dissertation and their clinical implications are discussed. Future research directions are also outlined.

Chapter 2

Animal Models of Myopia

2.1 Introduction

Across the animal kingdom, both during development and afterwards, most body parts actively regulate their size and shape through homeostatic mechanisms [201]. In this context, the eye faces many challenges. The length of the eye must precisely match the focal length of its optics for images of distant objects to be imaged on the retina in order to achieve sharp focus (i.e. emmetropia), rather than in front of or behind it.

While ocular dimensions could be, at least in part, genetically determined as with other organs in the body, observations of human infants and from animal models indicate that vision guides the growth (elongation) of the eye. For example, if a lens is placed in front of a young eye and causes images to consistently fall behind the retina (hyperopic defocus) or in front of the retina (myopic defocus), then the rate of eye growth is up- or down-regulated to compensate for this optical effect [165, 69, 67, 209, 114].

What mechanisms control this process? Are there differences between developmental stages in the regulation of eye growth? What external or environmental factors contribute to this process? To answer these questions, we rely on careful experimentation using appropriate animal models. This chapter reviews the factors considered important for the research questions that follow in this dissertation and the rationale for selecting the guinea pig for future studies.

Why Develop an Animal Model for a Disease?

Animals are very complex organisms in which organs serve apparently distinct physiological functions, yet are highly interdependent. Relationships between tissues and organ systems involve complex networks of cells, with cross-talk between cells, mediated by various molecular signals, including hormones. Therefore, it is necessary to study organisms at multiple levels: molecules, cells, organs, and physiology in health and disease to better understand the mechanisms underlying disease. The first two levels can be investigated *in vitro* (e.g., cell culture), and research at this level has become very advanced, now addressing questions

once limited to studies of live animals. However, exploration of complex physiological processes, such as the development of vision, requires studies of the intact organism in order to comprehensively characterize such processes.

What are important qualities of an animal model?

It is important to consider many factors when selecting an animal model to use for a particular research question. Results obtained from animal studies may not necessarily be confirmed in further human studies due to critical differences between the chosen animal model and humans. Therefore, the selection of an animal model should strategically mimic the human condition under study. In addition, animals should not be used whenever non-animal-based experimental approaches are available. The number of animals used should be adjusted to the minimum needed to reach a conclusion, while not being reduced to an extent that studies are under-powered statistically and results are unclear. All provisions must be taken to minimize harm, and all efforts should lead to replacement and reduction of animal use and refinement of animal models to improve the reliability of the data and information gained.

2.2 Animal Models in Refractive Error Research

The cause of myopia has been debated for more than a century. Excessive near work, accommodation, inadequate or altered lighting, and genetics have all been suggested as culprits. Because the development of refractive error is such an insidious process, and there are so many potential environmental influences, the condition is best studied in an animal model, where much of the environment can be very carefully and systematically controlled.

The first model for human myopia developed out of an incidental observation by Wiesel and Raviola (1977) in an unrelated study that lid-sutured eyes had become myopic [210]. Beginning in the mid-1970s, several animal models were developed to study the mechanisms underlying refractive error involving primates (old and new world monkeys), tree shrews, guinea pigs, mice, chickens, fish, and squids. Much of our current understanding of the characteristics and mechanisms of eye growth and the development of myopia has come from experiments using animal models. For example, although it was once generally believed that normal growth of the eye and the development of refractive error was controlled by genetics [180, 182, 181], it is now widely accepted that both genetic and environmental influences contribute to refractive development due to animal research. Evidence from a wide range of animals indicates that normal, unrestricted vision tends to grow toward an emmetropic refractive state [200, 131, 211], but disruptions to early visual experience may alter the emmetropic state.

Studies in animal models have established two highly important findings that have been transformative in the study of refractive error development. First, that eye growth is regulated by visual experience and this is highly conserved across species. Second, eye growth regulation is mediated by mechanisms that are located entirely within the eye [201, 129].

Each species used in studies of refractive error development provides unique experimental advantages to the study of underlying mechanisms of eye growth regulation, reflecting differences in ocular anatomy and/or vision function. It is important to consider these differences when interpreting results from animal studies and attempting to translate results to the human eye.

The process of emmetropization is completed in all species over a relatively short period of time, relative to the life span of the animal. For example, marmosets and macaques achieve stable refractive errors around 2 and 5 months of age, respectively, while guinea pigs, tree shrews, mice, and chicks achieve stable refractive errors within the first few weeks of life [193]. Importantly, however, these vision-dependent mechanisms appear to remain active into adult life [176, 192, 173, 137], which represent important features of these animal models given that in humans, myopia may continue to progress after the emmetropization process is largely complete. As a result, the ages of the animals used must be carefully considered in studies targeting potential interventions at these later stages to control myopia.

These animal studies have laid the foundation for the development of many of the optical and pharmaceutical treatments in clinical use today, aimed at reducing the prevalence and progression of myopia. Animal studies may allow testing of treatments that could even prevent myopia in the future.

Comparative Anatomy of the Guinea Pig Eye

Cavia porcellus has been so frequently used in scientific studies that its common name, guinea pig, is used as a term denoting any sort of experimental subject. Guinea pigs are mammals that belong to the order Rodentia, which are characterized by a single pair of continuously growing incisors in both the upper and lower jaws [153]. Rodents are the most diversified mammalian order and live in a variety of habitats, man-made environments, as pets, research subjects, and occasional food sources [153].

Guinea pigs first appeared in research laboratories in the 1800's [15]. Among rodents, guinea pigs are favored both as research subjects and pets for their small size, short breeding cycles, and ease of handling [153]. Pups can be weaned as early as 5-7 days of age, must be weaned by three weeks of age, and become fully mature in two to three months [81]. Their typical lifespan is five to seven years [81].

Guinea pigs have been increasingly used in myopia research since they were first proposed as a potential model in 1995 [112]. Many laboratory rodents, such as mice and rats, are nocturnal. Guinea pigs, however, are crepuscular, meaning that they are most active during dusk and dawn [84, 155]. Like most rodents, guinea pigs rely primarily on their sense of smell, but guinea pigs do utilize their vision across a large, dynamic light intensity range [197].

Guinea pigs are known to respond to spatial form-deprivation stimuli with increased eye elongation, resulting in "form deprivation myopia"; they can also compensate for both myopic and hyperopic defocus by appropriately altering their eye growth [62, 63]. Similar to humans, guinea pigs have a rod-dominated retina [13]. Whereas humans have trichromatic

vision, supported by three different retinal cone photoreceptors, guinea pigs are dichromatic, with middle- and short-wavelength-sensitive cones [74]. In the human eye, except for the absence of short-wavelength-sensitive cones in the fovea, the cone types are evenly distributed throughout the retina. In the guinea pig, however, middle-wavelength-sensitive cones dominate the superior retina, whereas short-wavelength-sensitive cones dominate the inferior retina [154]. The transition zone between these two retinal regions contains both cone types and cells with both photopigments and corresponds to the visual streak [154]. Guinea pigs have a visual streak rather than a fovea [122], which provides a visual acuity that has been reported to range from 1.0 cycles/degree (cpd) to 2.7 cpd [133, 11]. This is in the same range as the tree shrew, another common animal model for refractive error research [140, 130]. Myopia can also be induced locally through manipulation of the input to local retinal areas [113].

In the following sections of this chapter, an anatomical comparison of the human eye and the guinea pig eye is provided, highlighting key features, along with advantages and disadvantages of using the guinea pig for refractive error research.

2.3 Comparative Anatomy of the Guinea Pig Eye

The guinea pig is an increasingly popular model for myopia because their eyes share several important characteristics with human eyes. A comparison of each of these ocular components is reviewed here.

The Tear Film

Guinea pigs have a very low blinking frequency (2-5 blinks over 20 mins), leaving the cornea quite exposed to environmental conditions [194, 15]. Humans, in contrast, blink nearly 20 times per minute on average [8]. Common tests for dry eye disease in humans, including the Schirmer test, tear break-up time, and phenol red thread test, have been performed in guinea pigs. Reported results from the Schirmer tear test I (designed to measure both basal and reflex tearing) ranges from 0.36mm [194] to 3mm [32] after 1 minute of wetting. Schirmer tear test II (designed to measure basal tear secretion, after administration of a local topical anesthetic) ranges from 0.43mm [194] to 4mm [32] after 1 minute. In human eyes, the normal range of results for Schirmer tear tests I and II are 10mm and 5mm, respectively, after 1 minute of wetting [87]. Under the phenol red thread test, another measure of tear production, guinea pigs produce 16 mm of wetting per 15 seconds [15]; for humans, a result greater than 30 mm in 15 seconds is considered normal [87]. These results support that human eyes have a larger tear reservoir and a higher rate of tear production compared to the guinea pig.

The tear break-up time, as measured using sodium fluorescein, is reported to be 4.95 seconds in the guinea pig [15], compared to 10 seconds in humans [87]. Punctate and linear superficial epithelial defects are common in guinea pigs [15], which is likely reflective of

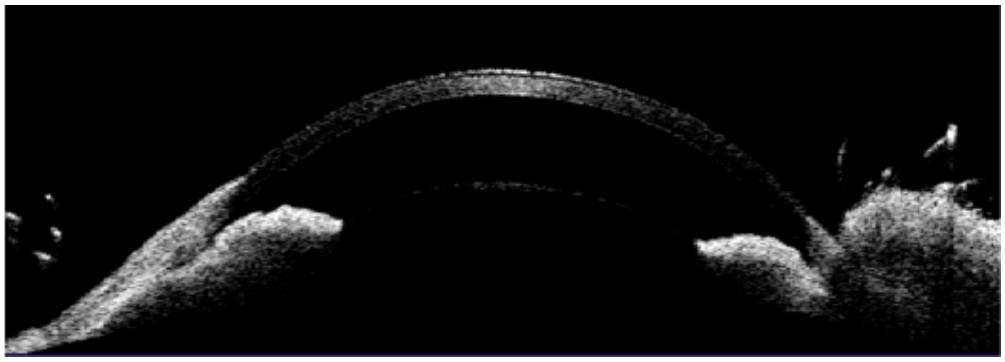

Figure 2.1: Anterior Segment OCT image of a guinea pig.

their dusty habitat. These results suggest that the guinea pig tear film is less stable than that of human eyes, however, this has not been our observation of guinea pigs in the lab, where we often observed a stable tear film for several minutes after the instillation of sodium fluorescein. Their very low blinking frequency also supports a more stable tear film than the referenced report.

Cornea

The cornea is the most anterior refracting element of the eye. It has smooth, curved boundaries and is an optically transparent tissue. In the guinea pig, it occupies 85-90% of the interpalpebral area [15], with the average adult guinea pig corneal diameter and thickness being approximately 6 mm and 225 um, respectively (measured by OCT, our lab). Figure 2.1 shows a representative anterior segment OCT image of the guinea pig. Unlike humans, the central and peripheral corneal thickness in the guinea pig is nearly identical [15]. The normal, adult human corneal is both much larger and thicker, with an average diameter ranging between 11.5-12.5 mm [158] and central corneal thickness between 518-558 um [54].

Like human corneas, the guinea pig cornea is composed of 5 distinct layers: epithelium (outermost), Bowmans layer, stroma, Descemets membrane, and endothelium (innermost). The composition of the guinea pig cornea is also similar to that of humans in terms of both cell types and relative thicknesses of the layers. The corneal epithelium contains superficial epithelial cells, basal cells, and wing cells and has a thickness of approximately 45 um or 20% of the total thickness of the cornea [15]. The corneal stroma is composed of specialized fibroblasts, known as keratocytes, embedded in a highly organized extracellular matrix, with a total thickness of approximately 163 um or 75-80% of the total thickness of the cornea [15]. The corneal stroma is innervated by the trigeminal nerve, with nerve endings penetrating Bowman's layer to reach the deeper corneal epithelial layers [70]. The innermost endothelial layer is the thinnest of the cellular layers, measuring approximately 5 um in thickness and comprising of a single layer of hexagonal shaped cells interconnected by tight junctions, with their outlines generating a honeycomb pattern [15].

The corneal limbus, which includes a vascular arcade, is continuous with the white sclera and overlying bulbar conjunctiva [15]. The limbus is identified histologically by the loss of Bowman's layer and loss of highly regular organization of collagen fibers seen in the corneal stroma [15]. Interestingly, pigmented guinea pigs have melanin-containing epithelial cells irregularly distributed circumferentially in the limbal region [15]. Albino guinea pigs do not share this characteristic [15].

Corneal sensitivity varies dramatically by location and individually in guinea pigs. The guinea pig cornea is most sensitive centrally, which is consistent with findings in many other animals, including humans [194]. However, even centrally, corneal sensitivity appears to be quite poor as evidenced by the results of one study in which five out of ten guinea pigs reportedly showed no blink response to the strongest applied pressure [194].

Iris

Guinea pigs typically have a heavily pigmented iris, with a central round and dynamic aperture known as the pupil, that regulates the amount of light entering the eye by constricting in response to light. Like humans, the iris muscle is composed primarily of smooth muscle fibers with muscarinic receptors on the pupillary sphincter and adrenergic receptors on the dilator [17]. The predominant muscarinic receptor subtype on both human and guinea pig iris sphincter muscles is the M3 subtype [17]. Because of these close parallels between the guinea pig and human eyes, pharmacologic strategies for manipulating pupil size in humans can also be applied to guinea pig pupils. Therefore, sympathomimetic drugs, such as phenylephrine, and muscarinic antagonists, such as atropine and cyclopentolate, can be used to dilate the pupils of guinea pigs, and pilocarpine can be used to stimulate pupillary constriction.

Guinea pigs have large pupils relative to the size of their eye and unlike human eyes, the guinea pig pupil increases in diameter over time, from approximately 4 mm at birth to approximately 6.5 mm by 100 days of age [61]. In comparison, the pupil size in children is approximately 8 mm, reaching 3-4 mm in the elderly [216]. This difference is important to keep in mind while investigating optical treatment strategies for myopia.

Ciliary Body

The ciliary body is responsible for the production and drainage of aqueous humor and it also facilitates accommodation [151]. The guinea pig ciliary muscle, like the human ciliary muscle, undergoes active development, with cells going through a phase of hyperplasia followed by hypertrophy to reach the adult size and shape [143, 142]. Muscarinic subtypes M1 to M5 have been identified in the guinea pig retina, choroid, sclera, iris, and ciliary body. Little else is known about the anatomy and development of the ciliary muscle and changes with induced myopia, despite speculation that ciliary muscle abnormalities may play a role in the underlying mechanism of myopia development in humans.

Lens

Guinea pigs have relatively large crystalline lenses compared to the length of their eyes and also compared to human eyes [61]. Their crystalline lenses also show a rapid increase in thickness over the first 5 weeks after birth, from 2.72mm to 3.62mm [233].

Interestingly, guinea pigs appear to be susceptible to lens opacities, e.g., cataracts. For example, in one study of the prevalence of ocular disease in a population of normal guinea pigs, nearly half of the animals examined (446 of 1000) had some ocular abnormality, with the majority of abnormalities being lens changes, including frank cataracts and nuclear sclerosis [215].

Accommodation

There are significant differences across species in the mechanisms and amount of accommodation [193], which dynamically regulates the dioptric power of the eye and may be indirectly involved in myopia development through its influence on retinal defocus. In many species, including both humans and guinea pigs, accommodation involves changes to the power of the crystalline lens, achieved by contraction of the ciliary muscle, whereas in other species, it is achieved by moving the lens [202].

Rodents appear to vary in their ability to accommodate. Experiments in rats and mice have consistently failed to demonstrate any accommodation responses [218, 2]. However, until recently, little was known about whether and how guinea pigs accommodate. An early study attempted to elicit accommodation in guinea pigs by presenting various near fixation targets (e.g., a pencil or a pair of scissors) [76]. While no significant refraction changes were observed, the salience of the stimuli must also be questioned. However, two more recent studies have reported that up to 5-6 D of accommodation can be elicited pharmacologically in juvenile guinea pigs [43, 135]. Both pharmacological studies involved topical pilocarpine, which decreased anterior chamber depth and increased lens thickness, suggesting an active accommodation mechanism.

Retina

Compared to the other ocular components of the guinea pig, its retina has been studied extensively. While the general retinal cellular organization and neural signaling circuitry are highly conserved among vertebrates [75, 223], there are important differences between the guinea pig and the human retinas. Both have specializations for high acuity involving high photoreceptor and ganglion cell densities, but humans have a single small spherical area (fovea), whereas guinea pigs have a horizontal visual streak. The latter central band has a ganglion cell density of 1500 cells/mm^2 [122] and a cone density of 20,000 cells/mm^2 [154, 227]. The visual streak is located in the central retina superior to the optic nerve and extends farther temporally than nasally. Noteworthy, the density of ganglion cells density is higher in the ventral than in the dorsal regions at equivalent distances from the visual

streak, suggesting that acuity in the upper visual field may also be higher than in the lower visual field [122], which may reflect an adaptation to their life in the wild as the prey of larger animals and birds. The estimated total ganglion cell count for the guinea pig retina is 159,000 ganglion cells [122], much lower than the estimated 1.5 million retinal ganglion cells in the human retina, although this is consistent with its much smaller surface area of 140 mm^2 compared to 1,094 mm^2. Calculations assume axial lengths of 8 mm and 22 mm in the guinea pig and human respectively, and that the retina occupies 72% of the globe in each case [86].

The guinea pig and human retinas also differ in the number of cone types and their distribution. The guinea pig retina contains only middle wavelength-sensitive (M) and short wavelength-sensitive (S) cones; the human retina also contains long wavelength-sensitive (L) cones, except in the case of genetically inherited color deficiencies. In normal human retinas, except for the absence of S cones in the fovea, all three cone types are randomly distributed throughout the retina. In contrast, in the guinea pig, the dorsal retina is reported to be dominated by M cones, whereas the ventral retina is dominated by S cones [154]. This may reflect an evolutionary adaptation to the different spectral backgrounds encountered by the dorsal retina (e.g., the ground) and ventral retina (e.g., the sky) [186]. Despite this bias in the distribution of cone subtypes, guinea pigs behave as dichromats [74]. Interestingly, the proportion of cones to rods in the retina is higher for guinea pigs than it is for humans. It is estimated that 8-17% of photoreceptors in the guinea pig retina are cones [74], but only 5-7% in human eyes [72, 73].

The electroretinogram (ERG) is a measure of light-evoked electrophysiologic retinal responses, which in its most basic forms makes use of flashes of light (so-called flash ERG), but may also involve more complex stimulus patterns (so-called pattern ERG). In both cases, they may be applied to evaluate retinal function. Because of these key retinal similarities, ERG recordings from guinea pigs are similar to those from humans and primates [156, 146, 91], leading to its use as a model for the study of human retinal electrophysiology.

In relation to retinal vasculature, there are substantial differences between humans and guinea pigs. The human retina has a well-developed retinal vasculature, which is responsible for supplying the inner retina with oxygen and nutrients, while the outer retina is dependent on the choroidal vasculature. In contrast, guinea pigs have only a primitive retinal vasculature, confined to the optic nerve head region; most of their retina is completely avascular, with the oxygen and nutrient needs of the entire retina being supplied only by the choroid [230]. This difference between human and guinea pig retinas reflects in part the relatively thinner guinea pig retina (150 um vs 200 um) [153], allowing the needs of even the inner retina to be met by diffusion from the choroid.

Choroid

The choroid is the vascular layer of the eye, located between the retinal pigment epithelium and the sclera. It extends from the anterior retinal boundary (ora serrata) to the optic nerve posteriorly. In addition to nourishing the retina and contributing to the regulation of

intraocular pressure, the choroid also appears to play an active role in eye growth regulation [214, 110, 126]. Specifically, through adjustments to choroidal thickness, the position of the retina relative to the optical focus plane of the eye can be modulated, adjusting for refractive error. In chickens, in which this mechanism was first described, the eye is able to rapidly change its refractive error in response to imposed myopic or hyperopic defocus by as much as 7 D [214]. Similar changes, albeit smaller in scale, have been observed in guinea pigs [63, 77].

Choroidal thickness modulation is now recognized as a key component of active emmetropization, with measurable changes to imposed defocus occurring within minutes to hours, depending on the species, and is now being investigated as a possible biomarker for altered eye growth. Consistent with this possibility, a recent study found that an Elm Hill strain of pigmented guinea pig, which proved to be minimally responsive to myopia-inducing form deprivation and defocus stimuli, had a naturally thicker and structurally more complicated choroid compared to a New Zealand strain which responds as expected to the same stimuli [47, 77]. As possible explanations for the insensitivity of the Elm Hill strain to myopia-inducing stimuli, it was hypothesized that their thicker choroids may serve as a mechanical buffer against scleral expansion, or as a more effective barrier to scleral-directed, myopia-generating molecules released from the retinal pigment epithelium (RPE). Noteworthy, the Elm Hill strain was also reported to have a more heavily pigmented choroid as compared to the New Zealand strain [77], and as ocular melanocytes have been suggested to play a role in eye growth regulation, the more heavily pigmented choroids could play a protective role against myopia in the Elm Hill strain.

Sclera

The sclera is the outermost, structural support layer of the eye, and its anatomy - dense, fibrous, viscoelastic connective tissue - is consistent with this role. Evidence from clinical and experimental studies indicates that the biomechanical properties of the sclera determine, at least in part, the shape and size of the globe and therefore the sclera has a major influence on the refractive error status of the eye [147].

The guinea pig sclera is very similar to human sclera both in structure and cellular composition. In both cases, the sclera comprises a dense and disorganized meshwork of collagen, supported by a sparse population of fibroblasts. Scleral fibroblasts also appear to have the capacity to convert into myofibroblasts, which have also been observed in the guinea pig sclera [4]. The guinea pig sclera thickens with age, beginning at approximately 125 um, and increasing to approximately 170 um when fully-grown [61], as opposed to human scleras, which range in thickness from 400-900 um depending on the location analyzed [132]. In humans, scleral thickness changes dramatically with axial length, with myopic scleras being significantly thinner, but age does not appear to change scleral thickness, at least in adults [196]. Bone morphogenetic proteins (BMPs), which are known to play important roles in eye development and tissue differentiation [219] and appear to also be tied to ocular

growth regulation [231], have also been found to be expressed in both guinea pig and human scleras [205].

Optic Nerve

A recent study characterized the optic nerve head in the guinea pig eye and found it to share many features, both in terms of structure and biochemical composition, with those of other higher order mammals, including humans [134]. In both human and guinea pig eyes, the lamina cribrosa is collagenous in nature and organized as a multilayered meshwork, with radially-oriented connective tissue bundles [134]. In contrast, the lamina cribrosa of lower-order rodents, e.g., mice and rats, are cellular in nature [119]. The exiting axons of retinal ganglion cells in the guinea pig and human eyes are organized into fascicles to pass through the lamina cribrosa, becoming myelinated as they emerge from the distal portion of the lanima cribrosa. As noted above, the guinea pig retina is largely free of blood vessels. However, their optic nerve head is vascularized [153, 134].

Visual Performance

Visual Acuity

The visual acuity of the guinea pig, as behaviorally measured, is quite poor. In one study, using an optokinetic nystagmus (OKN) response as an indicator of resolution, the visual acuity of juvenile guinea pigs was measured to be 2.7 cycles per degree [11], approximately 10-fold lower than normal human spatial vision (30-60 cycles per degree).

Color Vision

As noted previously, the guinea pig retina has both M- and S-cone types and is therefore equipped for dichromatic color vision, which has been confirmed behaviorally [74]. The peak sensitivities of their S- and M-cones are 429 nm and 529 nm respectively, similar to that of corresponding human photoreceptors [74, 138, 91].

2.4 The Guinea Pig in Refractive Error Research

For the advantages described in the previous section, guinea pigs are becoming an increasingly popular model for refractive error research. Previous studies have established that guinea pigs respond to commonly used myopia-inducing stimuli, including form deprivation with diffusers and facemasks, as well as to imposed hyperopic defocus using negative lenses by causing excessive eye elongation and myopia [62, 63]. Historically, form deprivation and negative lens-wear have been used interchangeably in studies of eye growth. However, the visual experience for the animals being tested are quite different with these two stimuli and

data from several animal models suggests that there may be important underlying mechanistic differences between the two induction methods. Form deprivation provides no visual feedback, commonly referred to as an open-loop system, while negative lenses constitute a closed-loop system, meaning that they do provide a target focal plane for eye growth.

In addition, the condition that we are attempting to study should be given consideration. Visual form deprivation does occur in humans in the presence of neonatal pathology such as ptosis, corneal opacity, congentital cataract, and eyelid hemangioma. However, these conditions are rare and do not represent the commonly encountered "school myopia" and may limit the translation of results of animal research to understanding human myopia. Despite this, most research utilizes form deprivation methodology [128, 117, 125, 166, 124], and although lens-induced models are increasing in popularity, there is no consistent protocol used for myopia induction (for a summary, see Table 2.1).

In total, all of the lens-induced myopia studies in guinea pigs demonstrate that when a negative lens is mounted in front of the eye, there is a consistent response to accelerate the rate of axial elongation to eliminate the refractive error (becoming more myopic in the treated eye). However, there is considerable variety in the stimulus used (e.g., power of lenses used to induce myopia), the age of the animals at the start of the study, as well as the duration of applied treatment. The average treatment duration is 2.9 weeks (SD 1.59, range 1-6 weeks). The average lens (goggle) power is -6.9 D (SD 3.00, range 2-12 D). The average age at the start of treatment is 2 weeks (SD 1.11, range 3 days to 4 weeks). Guinea pigs tend to complete the emmetropization process by 3 weeks of age, which has been suggested to limit the efficacy of the stimulus. Despite this, a multivariable linear regression shows that only the stimulus power has a statistically significant effect on the final magnitude of myopia induced ($p = 0.036$, 95% confidence interval 0.018-0.49). Although there appeared to be more myopia at the end of the experimental period the younger the guinea pig was at the start of treatment and the longer the treatment was administered, neither variable reached statistical significance. This suggests that for the most dramatic effects, researchers should use higher lens powers. The age of the animals and treatment duration may be less critical, and should be selected to best translate to the human condition.

2.5 Summary and Conclusion

The guinea pig has been utilized in vision research for more than 40 years. More recently, it has been adopted as an experimental model for studying eye growth regulation and refractive error development, contributing significantly to our understanding of underlying mechanisms and the role of visual feedback. The guinea pig provides the following advantages in vision research: (1) as a mammalian model, it shares many anatomical ocular features with humans; (2) it is easy to handle in administering treatments and collecting data; (3) it is amenable to optical and retinal imaging; and (4) it is relatively low cost to maintain. Disadvantages include: (1) relative to higher order mammals, vision is an under-developed sense compared to smell or hearing and (2) Genetic manipulation is often speculative.

Table 2.1: Summary of lens-induced myopia studies in guinea pigs. Myopia induced refers to the reported mean difference between the treated and fellow untreated eye. PD = peripheral defocus (-4 D periphery with 5mm optic zone plano center), F = Fresnel lens

Stimulus (goggle power)	Age at Start	Duration of Treatment	Myopia Induced	Reference
-10 D	2-3 weeks	5 weeks	not reported	Dong et al. 2019 [39]
-2 D	11 days	5 days	1.75 D	Jiang et al. 2019 [77]
-12 D	3-4 weeks	36 days	not reported	Dong et al. 2019 [38]
-10 D	3 weeks	6 weeks	6 D	Ding et al. 2018 [34]
-4 D	4 days	8 days	3.6 D	Wu et al. 2018 [220]
-4 D	not reported	3 weeks	5 D	Liu et al. 2017 [101]
-4 D	8 days	10 days	-4.4 D	Bowrey et al. 2017 [10]
-4 D / 0 PD			-3.5 D	
-10 D	2-3 weeks	2 weeks	not reported	Jiang et al. 2017 [78]
		2 weeks	5 D	
-10 D	3 weeks	4 weeks	5 D	Guoping et al. 2017 [55]
		6 weeks	5 D	
-10 D	3 weeks	4 weeks	not reported	Zhao et al. 2017 [232]
-10 D	14 days	6 weeks	5.5	Liu et al. 2016 [100]
-7 D	not reported	3 weeks	4.7 D	Cai et al. 2016 [16]
-4 D	3 weeks	3 weeks	2 D	Li et al. 2016 [94]
-10 D	3 days	4 weeks	6.5 D	Gao et al. 2015 [46]
-4 D	3 weeks	3 weeks	2.3 D	Li et al. 2015 [93]
		1 week	1.2 D	
not reported	3 weeks	2 weeks	4 D	Sha et al. 2015 [168]
		4 weeks	4.5 D	
-4 D	1 week	3 weeks	1.5 D - 2.5D	Li et al. 2014 [95]
-7 D	4 weeks	14 days	5.3 D	Xiao et al. 2014 [224]
-6 D	3 weeks	14 days	4.7 D	Wang et al. 2014 [206]
-5 D/0 D F			1.6	
-5 D/+5 D F	3 days	11 days	0.3 D	McFadden et al. 2014 [115]
-5 D			5.2 D	
-10 D	1 week	6 weeks	7 D	Li et al. 2013
		6 days	1.8 D	
-10 D	2 weeks	15 days	3.5 D	Chen et al. 2012 [23]
		30 days	5.75 D	
-4 D	3 weeks	11 days	3.64 D	Dong et al. 2011 [37]
-4 D or	2-3 days	10 days	3.7 D	Howlett 2009 [63]
-2 D			2.1 D	
-4 D	3 weeks	2-4 weeks	3 D	Lu et al. 2009 [106]

Chapter 3

The Optics of the Guinea Pig Eye

3.1 Introduction

The guinea pig has emerged as an important mammalian model for studies of refractive error development and myopia. Normal ocular development in the guinea pig, including the process of emmetropization, has been well-documented [61, 233]. As with other animal models used in such studies, visual input has been shown to be important for guiding early ocular growth in the guinea pig [63, 62, 105, 114]. They are known to accommodate, implying that the guinea pig has a visually (retina)-guided focusing mechanism [135]. Young guinea pigs also respond to lens-induced blur with compensatory adjustments to eye growth [63].

As a model for studying visually-guided eye growth regulation, knowledge of the retinal image quality of the developing guinea pig eye is important. Rodents are typically nocturnal with small eyes and relatively poor vision compared to other mammals, relying instead on highly developed senses of olfaction and hearing [60]. However, the guinea pig is one of a small number of exceptions, being a diurnal rodent, with relatively large eyes. While this difference in eye length offers the potential for greater resolving power, the visual acuity of the guinea pig, based on behavioral measures, is reported to be relatively poor, between 1.0 cycles per degree (cpd) [133] and 2.7 cpd [11], making it only slightly better than that of mice (0.5 cpd) [20], and much lower than that of chicks (6-8.6 cpd) [19] and humans (30-60 cpd). Interestingly, albino guinea pigs and pigmented guinea pigs were found to have very similar visual spatial resolution thresholds, despite the increased light scatter in albino eyes [133], raising the possibility that the optical quality of the guinea pig eye is inherently poor. Characterization of the high-order aberrations of the guinea pig eye can help to model image transfer in the guinea pig eye and inform the limits of its spatial resolution.

Additionally, and perhaps more importantly, animal models of myopia assume an ability of ocular growth regulatory mechanisms to respond to altered visual experience, including the effects of imposed defocus. The ability of the retina to detect such changes is determined in part by the nature and magnitude of naturally occurring optical aberrations, which in turn determine retinal image quality and the depth of focus of the eye. Therefore, information

about the high-order aberrations of guinea pig eyes would be informative, as the effects of focusing errors on eye growth will be very different for an eye that is diffraction-limited compared to a highly aberrated eye. At this time, relevant studies are limited to just one paper [139], which used laser ray tracing to quantify the optical aberrations of four pigmented guinea pigs (ages 30 - 40 days) over a 2 mm pupil.

The current study made use of a Shack-Hartmann wavefront sensor, which allows for rapid, accurate, and objective measurements of wave aberrations. Wave aberration data collected from one eye of each of 8 young guinea pigs were used to derive image quality metrics over a 4 mm pupil, which were compared with known wavefront error trends in humans.

3.2 Methods

Animals

Male and female pigmented English Short Hair guinea pigs (*cavia porcellus*) were generously provided by Prof. John Phillips (University of Auckland, NZ) and housed in breeding harems (1 male and a maximum of 3 females). These harems were placed in oval-shaped breeding tubs in the animal facilities of the University of California, Berkeley. Eight pigmented adolescent guinea pigs (6-11 weeks of age, offspring of this original line) were weaned at 7 days of age and transferred from the breeding facility to the Minor Hall housing facility, where they were housed in transparent plastic wire-top cages (16 inches wide by 20 inches long), in a room with a 12h/12h light/dark cycle. The animals were housed with their siblings (up to 3 guinea pigs per cage) until they reached a weight of 350g, after which point they were housed as single sex pairs. The cage floor was lined with low dust Aspen shavings. The animals had free access to water and vitamin C-supplemented food, and received fresh fruit and vegetable enrichment three times per week. Animals were given Timothy Hay on weekends and after experimental procedures.

All animal care and treatments conformed to the ARVO statement for the Use of Animals in Ophthalmic and Vision Research. Experimental protocols were approved by the Animal Care and Use Committee of the University of California, Berkeley.

Wave Aberrations

Ocular aberrations were measured with a custom-built Shack-Hartmann aberrometer, which is a widely accepted method for measuring monochromatic high-order aberrations of the eye [96]. The aberrometer used an 840 nm light source as the laser beacon, with a power of about 10 uW. Lenslets sampled the pupil in a rectilinear grid with 0.375 mm spacing. Each lenslet had a focal length of 7.6 mm. Custom software was used for image capture, image analysis, and for computing the weights on the Zernike polynomial coefficients used to describe the

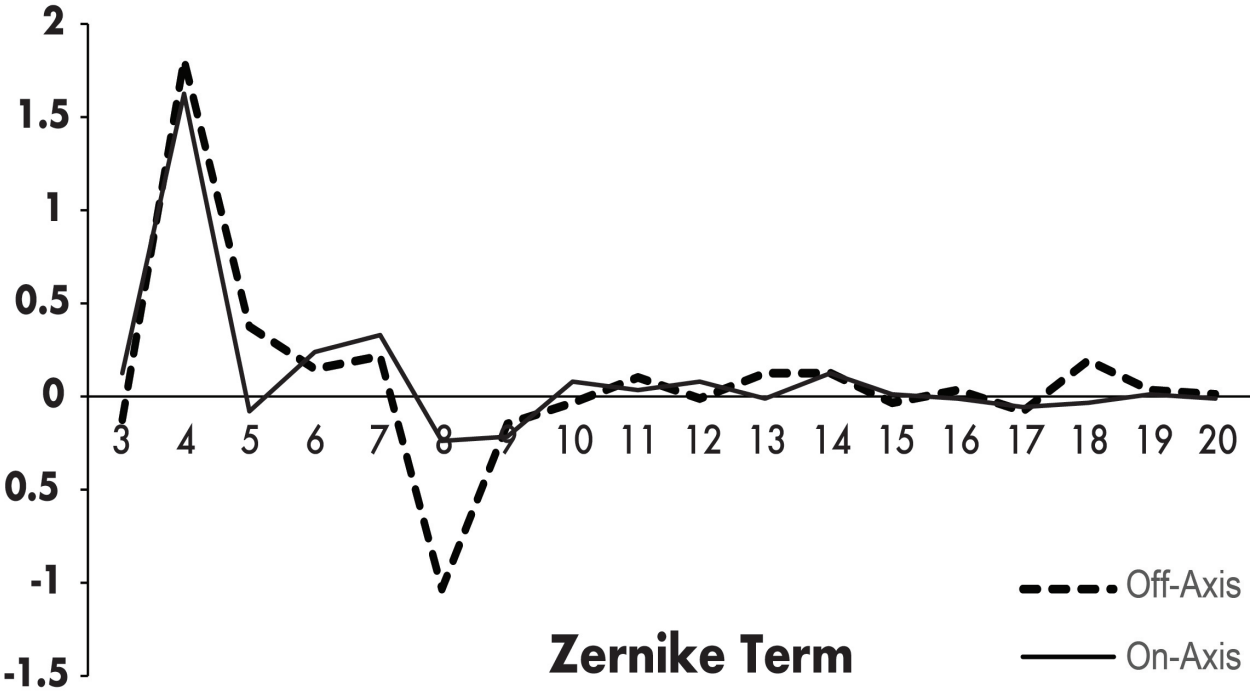

Figure 3.1: Mean Zernike coefficients for terms 3-20 for one representative guinea pig, measured on-axis (solid line) and off-axis (dashed line); profiles were similar except for a higher level of coma (8th term) in the latter case. Calculations used a 4 mm pupil and 550 nm wavelength.

wavefront [24]. Wavefront aberrations were fit with an OSA-standard Zernike polynomial function to the 10th order (65 terms) [188].

Measurements were limited to the left eyes of the guinea pigs, which were cyclopleged with topical 1% cyclopentolate, instilled 30 mins prior to imaging, and were otherwise untreated. Pupil sizes ranged from 4.10 to 5.56 mm across animals after cycloplegia. The guinea pigs were not anesthetized. Guinea pigs are known to have a superiorly tilted optical axis. When seated flat on the platform, measurements resulted in unusually high levels of coma (Z_3^1, Z_3^{-1}), as seen in Figure 3.1. Due to this superior tilt, the animals were held at a slight angle in order to image perpendicular to the pupil plane. The lack of excessive 3rd order terms was used as an indicator of valid (on-axis) alignment during measurement in accepting data for use in further analyses. Five to ten images were collected per eye.

All analyses were performed over a 4 mm pupil to accommodate the inter-animal variation in pupil size and allow for direct comparison of the optical properties of all eyes. Note that the raw images sometimes exhibited an elongated or dual spot pattern, consistent with reflections from both the inner retinal surface and a deeper retinal layer (presumably the photoreceptors) [159]. In these cases, care was taken during image analysis to choose spots originating from the deeper layer. Reported data represent averages derived from at least

five individual measurements (images). Data collected from seventeen young adult human subjects were also analyzed for comparison.

All wavefront analyses were performed using custom written software in MATLAB (MathWorks, Natick, MA). As per the OSA-standard Zernike polynomial, terms 3-5 are considered 2nd order aberrations and account for defocus and astigmatism, which are typically the largest ocular aberrations. Terms 6-9 (trefoil and coma), 10-14 (including spherical aberration) and 15-20 comprise the 3rd, 4th, and 5th orders respectively. The optical quality of the eyes was assessed in terms of these individual Zernike coefficients and further analyzed in terms of root-mean-square wavefront errors (RMSs) for these different orders [188]. Point-spread functions (PSFs) and optical modulation transfer functions (MTFs) were computed from the derived Zernike polynomials using a wavelength of 550 nm to generate metrics of image quality. The PSFs were used both qualitatively, by convolving the image with a letter E in order to assess legibility, and quantitatively, to generate Strehl ratios. The Strehl ratio is defined as the ratio of the peak aberrated image intensity of a point source compared to the maximum attainable intensity of a diffraction-limited system for the same pupil size. A higher Strehl ratio corresponds to improved image representation. The ocular Modulation Transfer Function (MTF) represents the optical contribution to the contrast sensitivity function, reflecting the extent to which details from objects in space are captured in the retinal image.

For every subject, a series of files were created to include the Zernike coefficients for a range of pupil sizes, from 1.5 mm to the maximum pupil size, in 0.5 mm increments. The tiff images of the spot patterns collected from each subject were also used in analyses. The depth of focus of the guinea pig eye was calculated from the Strehl ratios using the through-focus approach, in which the defocus term was computationally adjusted in 0.25 D steps from -5 D to +5 D. In this study, the depth of focus was computed as the width of the through-focus Strehl ratio at half of its maximum height.

3.3 Results

The spherical equivalent refractive errors (computed from the defocus terms) ranged from -0.84 to +4.23 D, with a mean refractive error of +2.54 ± 1.6 D (mean SD). Figure 3.2 shows a selected Shack-Hartmann image captured from each guinea pig, as well as the derived wavefront aberration maps, point spread functions, and mean Zernike coefficients. Only 2nd through 5th order terms (coefficients 3-20) are shown. One of the guinea pig subjects (#8), showed significantly increased aberrations relative the other subjects, and although its data are included in Table 3.1, they were otherwise excluded from further analysis. The increased aberrations were subsequently discovered to be due to a previously undetected cataract.

The high-order root-mean-square wavefront errors (RMS) for each order, derived for a 4 mm pupil size and averaged across the 8 guinea pig subjects, are shown in Figure 3.3. As a rule, the defocus state that gives the minimum RMS (optimal image quality based on all Zernike coefficients) is zero for all guinea pigs, as shown in Table 3.1. The maximum Strehl

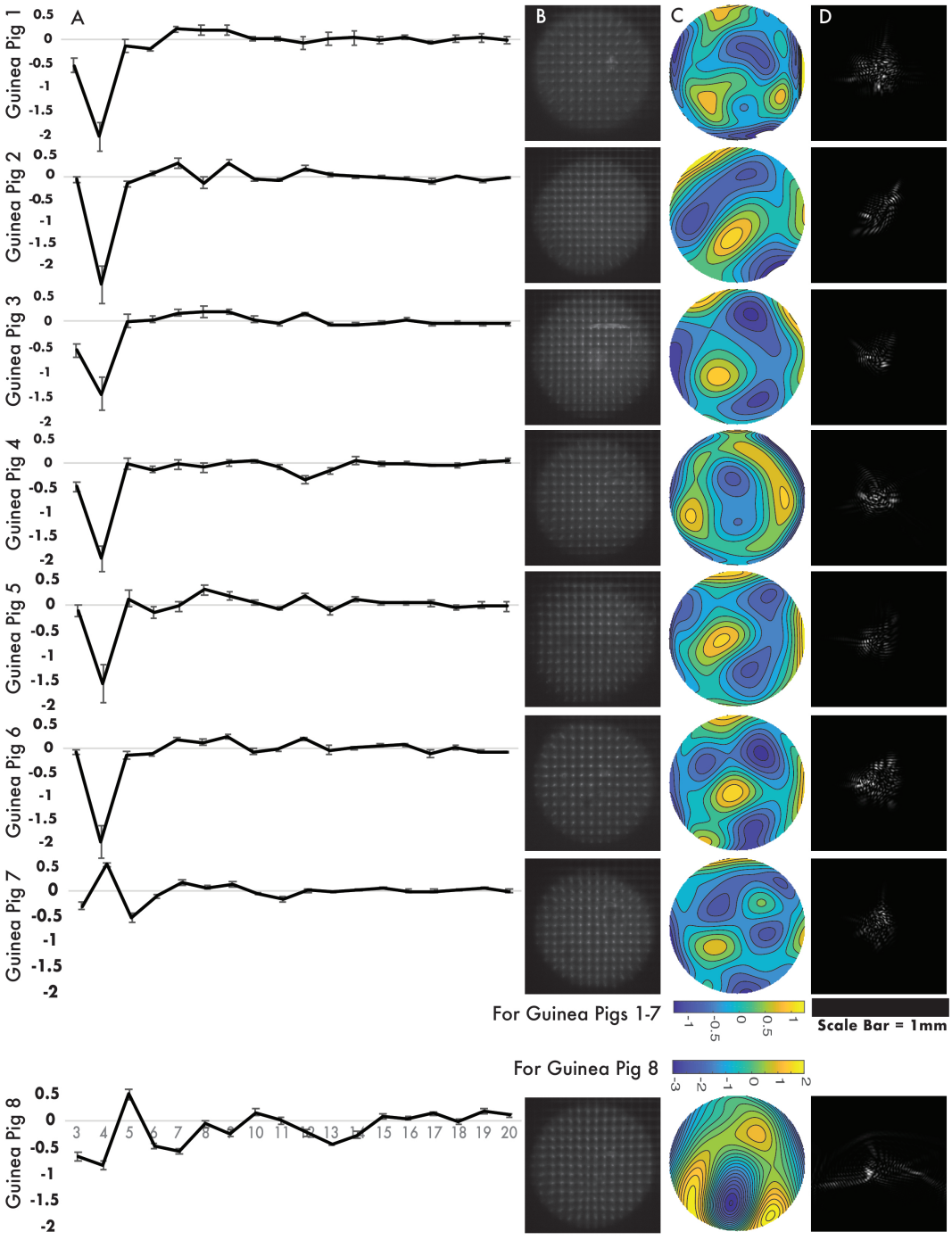

Figure 3.2: Column A shows mean Zernike coefficients for terms 3-20, derived from at least five images, for each of the 8 adolescent guinea pigs. Error bars represent the standard deviation. Column B shows the raw Shack-Hartmann wavefront sensor spot patterns, column C shows the derived wavefront aberration patterns (color scale in mm), and column D shows the point spread functions for each guinea pig measured.

Table 3.1: Minimum RMS wavefront error and corresponding maximum Strehl ratio for each of the 8 adolescent guinea pigs. The minimum RMS occurred at 0 D defocus for all guinea pigs, as did the peak Strehl ratio, except where noted in parentheses.

	1	2	3	4	5	6	7	8
RMS	0.56	0.56	0.39	0.45	0.50	0.60	0.37	1.06
Strehl	0.019 (-0.25D)	0.027 (-0.25D)	0.031	0.028 (-1.50D)	0.026 (-0.50D)	0.025 (-0.75D)	0.027	0.014 (-0.25D)

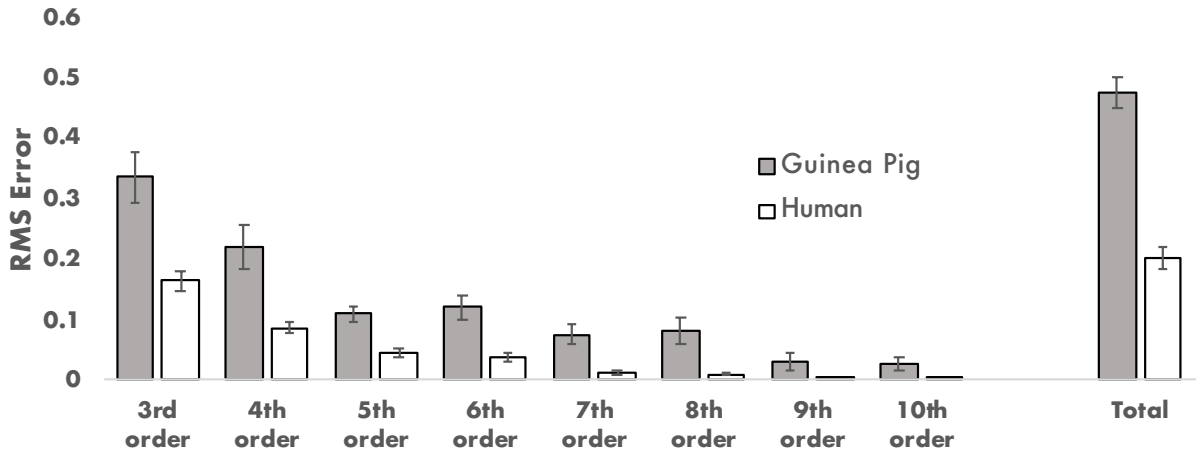

Figure 3.3: Mean RMSs plotted as a function of wavefront order for the eyes of 7 adolescent guinea pigs (gray bars) and 17 young adult humans (white bars). Error bars represent standard error of the mean. Calculations used a 4 mm pupil and 550 nm wavelength.

(optimal image quality based on PSF), however, does not necessarily match the defocus state with the minimum RMS and was a small but non-zero value for most of the guinea pigs. There is generally good agreement for both of these image quality metrics, however, the RMS is influenced by all Zernike coefficients, without weighting the relative importance of their impact on vision, leading to some differences in judgment of the optimal image quality [187]. Table 3.1 summarizes the high order RMS wavefront errors for each of the guinea pig subjects along with the corresponding peak Strehl ratios. The RMS wavefront error as a function of radial order is plotted on Figure 3.3 with equivalent data from human eyes included for comparison. For both guinea pig and human eyes, the high-order RMS decreases with increasing order. However, RMS values were consistently larger for the guinea pig eye, by 2-3 times (0.475 vs. 0.20 for the guinea pigs and humans, respectively). Guinea pig 8, which was found to have cataracts, had the largest RMS and smallest peak Strehl ratio, 1.06 and 0.014, respectively, consistent with poor optical and image quality respectively. Of the remaining 7 guinea pigs, the minimum RMSs ranged from 0.37 to 0.56, and the corresponding peak Strehl ratios ranged from 0.019 to 0.031.

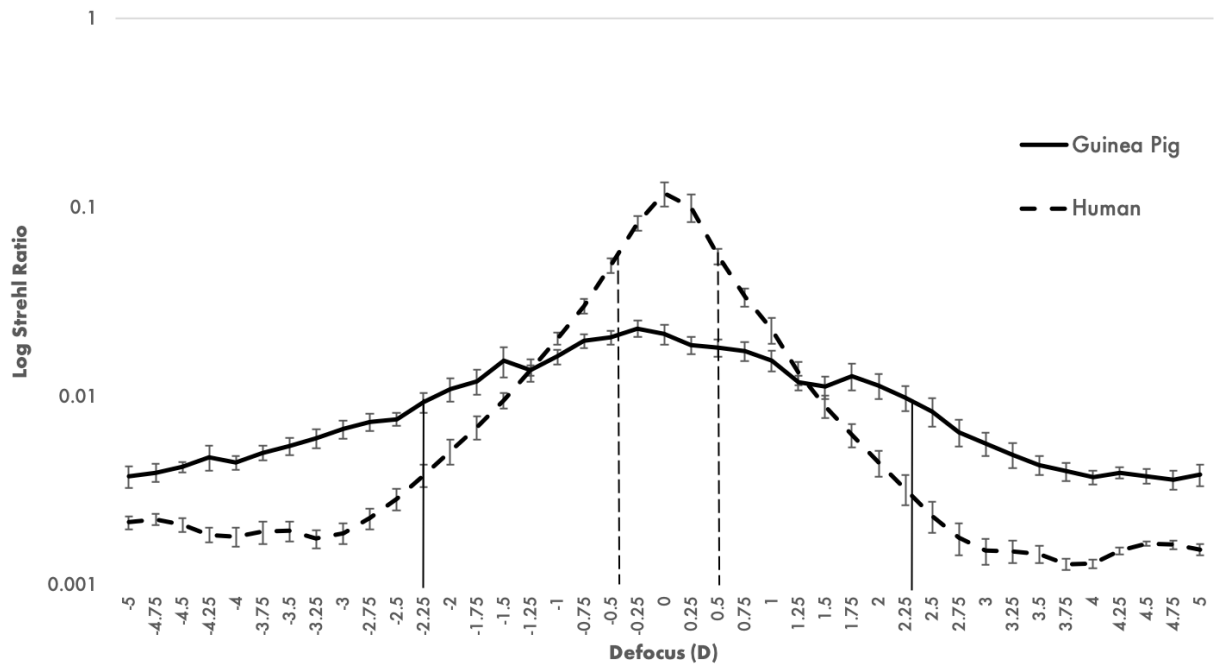

Figure 3.4: Through-focus estimation of depth-of-focus (DOF) derived from Strehl ratios. The DOF estimated for 7 guinea pig eyes is 3.75 D (-2.25 to 1.5 D), which is much larger than the estimated DOF for 17 human eyes, 0.875 D (-0.375 to 0.50 D). Error bars represent the standard error of the mean. Calculations used a 4 mm pupil and 550 nm wavelength.

Strehl ratio data for a 4 mm pupil size and various levels of defocus are shown plotted against defocus in Figure 3.4, for both guinea pig and human eyes. The depth of focus was estimated from these plots for both eyes using through-focus technique (full width at half max Strehl ratio). Consistent with the comparatively larger RMS errors across all orders for the guinea pig eye, the average depth of focus of the guinea pig eye is also larger, by approximately 4 times (3.75 versus 0.875 D).

The radial average best focus MTFs for both guinea pig and human eyes are shown in Figure 3.5, corrected for best focus (maximum Strehl ratio) over a 4 mm pupil. Both human and guinea pig eyes perform well at very low spatial frequencies. However, the guinea pig eye shows a much steeper decline with increasing spatial frequency, dropping below 0.3 at 9 cpd; this drop-off is not reached until 34 cpd for the human eye.

The impact of pupil size on both RMS errors at best focus and the radial average best focus MTF of the guinea pig eye is shown graphically in Figure 3.6A and B respectively. For pupils ranging in size from 1.5 to 4 mm in diameter, the mean RMS increases rapidly with increasing pupil size, from a mean value of 0.167 um for a 2 mm pupil size. The radial average best focus MTF curves shown in Figure 3.6B are based on data from one representative guinea pig. While the ability of a diffraction-limited optical system to transfer contrast of an object to an image increases with increasing pupil size, the opposite is true for the guinea pig

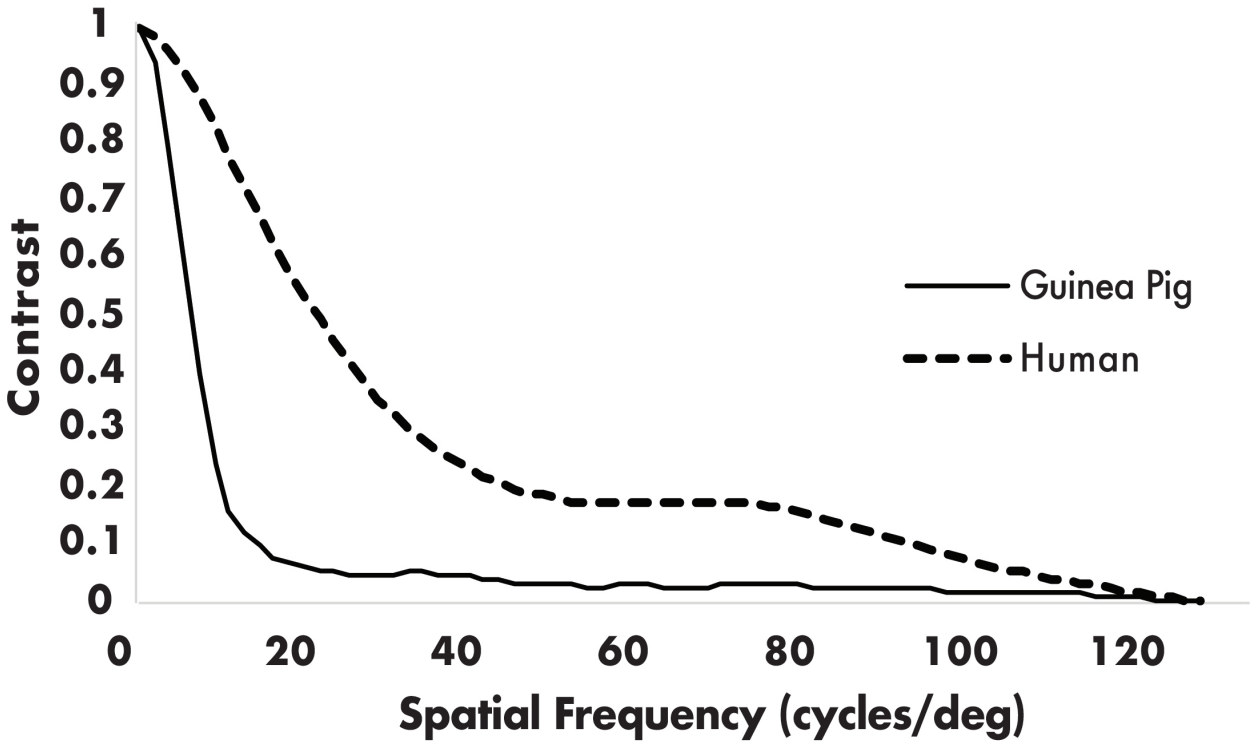

Figure 3.5: The radial average MTFs for guinea pig and human eyes. Human eyes are superior to guinea pig eyes in preserving contrast across most spatial frequencies. Calculations used a 4 mm pupil and 550 nm wavelength.

eye, which represents an aberrated optical system. Specifically, the decline with increasing spatial frequency becomes steeper with increasing pupil size. On the other hand, the high spatial frequency cutoff decreases proportionally with decreasing pupil size, meaning that eyes with smaller pupils are less sensitive to higher spatial frequencies.

The area under an MTF curve is a way of characterizing the modulation properties of an imaging system, which captures both spatial contrast and resolution information. These data for representative guinea pig and human eyes are summarized in Table 3.2. For both human and guinea pig eyes, the area under the MTF is largest for the smallest pupil size, decreasing thereafter. These results suggest that, overall, the smallest pupil size will yield the best image quality. These trends are also opposite to that just described for the cut-off frequency, which decreased with decreasing pupil size for the guinea pig eye.

3.4 Discussion

The study reported here made use of a Shack-Hartmann aberrometer to optically profile the eyes of young adolescent guinea pigs. The power of this approach is that its ability to capture all optical aberrations, including 2nd order Zernike terms, which are the limit of information

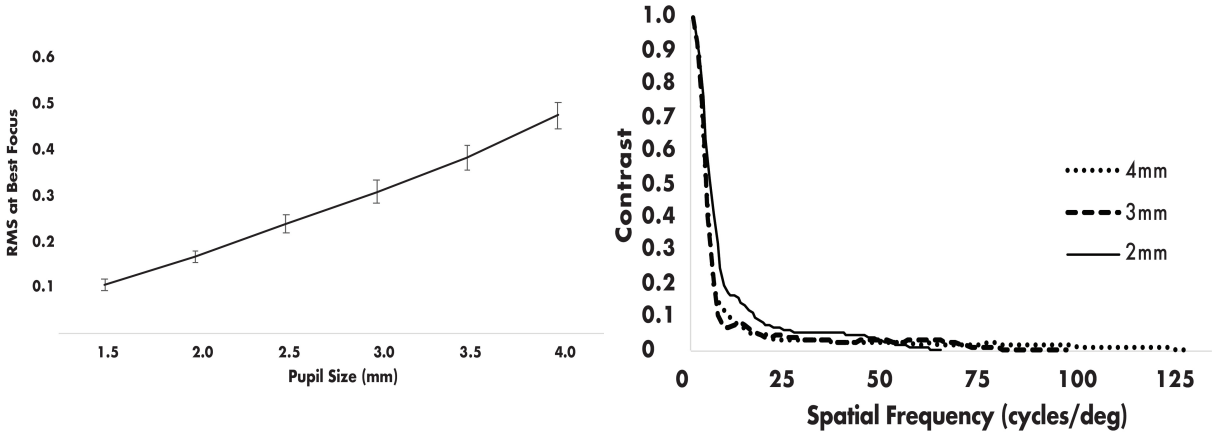

Figure 3.6: (A) Mean RMS wavefront error plotted as a function of pupil size for guinea pig eyes (n = 7). RMS increases with increasing pupil size. Error bars represent the standard error of the mean. (B) Radial average MTFs for a representative guinea pig eye and 2 - 4 mm pupil sizes. With decreasing pupil size, contrast is better preserved, up to 50 cycles per degree. Calculations used 550 nm wavelength.

Table 3.2: Calculated areas under the radial average MTF curve for representative young adult human and adolescent guinea pig eyes that correspond to the maximum Strehl value.

Pupil size (mm)	2	3	4	5	6
Human	20.58	17.95	17.68	15.85	12.84
Guinea Pig	7.94	6.14	6.62	n/a	n/a

collected with traditional refractometry methods. Our adolescent guinea pigs proved to be slightly hyperopic (2.54 ± 1.6 D), as reported in a previous study for similarly-aged animals using retinoscopy [61, 233]. While some have attributed the common finding of hyperopia to a small eye artifact, arising from the reflections in measurements arising from the inner retina, our method allows us to rule out this explanation. Furthermore, the majority of spot-pattern images that were analyzed for this study did not exhibit a dual spot pattern, which is commonly found in mice [50]. Likewise, Howlett and McFadden previously ruled out a small eye artifact as the origin of the hyperopia recorded in their guinea pigs [61].

Active emmetropization, the process by which early eye growth is actively regulated to reduce and/or eliminate neonatal refractive errors, is a developmental phenomenon shared by a wide range of animals, as well as humans. This regulatory mechanism appears to be able to decode and respond to the sign of defocus, with the retina playing a key role in the process [191, 212]. It is still unknown what optical information the eye is using to generate growth modulatory signals. The measurement of the optical aberrations of the guinea pig eye represents an important step forward, in allowing the nature of the defocus stimuli and their effects on retinal image quality to be better understood for this mammalian model.

Comparison of the wave aberration contour plots derived from our 8 guinea pigs suggests a

degree of randomness with respect to interanimal differences, based on the Zernike coefficients computed over a 4 mm pupil. However, it is also noteworthy that, after the exclusion of the data for the animal with cataracts, the derived group averages of individual Zernike coefficients were mostly close to zero. We know that for human eyes, variations in aberrations also appear to be to some extent random, albeit small in size. When Salmon et al. compiled statistics from 2560 human eyes, of high order aberration terms, only spherical aberration was found to be non-zero [160]. The small positive value reported for spherical aberration in the aforementioned study is similar to our finding for the guinea pig eye (0.0481 ± 0.077); although it did not reach statistical significance, this may reflect the small number of guinea pig eyes included in the current study. A previous study found that the crystalline lens of the guinea pig exhibits significant negative spherical aberration [135], implying that the cornea contribution to the overall spherical aberration is opposite in sign (positive) which is also consistent with the finding for human eyes [1].

Of the mammalian models used in myopia research today, rodent models have become increasingly popular, with mice and guinea pigs emerging as the two most common. The fact that the visual acuity of guinea pigs is slightly better than that of mice raises the question of how much this is attributable to differences in the optical quality of their eyes. One approach is to compare the root-mean-square wavefront error (RMS) of different terms. As our model is intended to make predictions about human ocular development, we undertook such a comparison between the guinea pig and human eyes. We excluded second order aberrations (defocus and astigmatism) from our comparison, which are most deleterious to vision, and also correctable by standard optical means. For both guinea pig and human eyes, RMS errors decreased with increasing order, although they were consistently larger for the guinea pig eye. Nonetheless, RMS errors for the guinea pig eyes were only 2-3 times the estimates for our human eyes (Figure 3.3). The relatively high optical quality of the guinea pig eye contrasts with their relatively poor visual acuity, which presumably has a neuroanatomical origin.

Among other animal models commonly used in myopia research, ocular monochromatic aberration profiles have been published for the rhesus monkey [148], marmoset [31], chicken [85, 18], and mouse [19, 50] and tree shrew [159], in all cases measured using traditional Hartmann-Shack aberrometry. A comprehensive comparison of these animal models is warranted, particularly in order to investigate animal models, like the guinea pig, in which optical quality and visual performance are dramatically different.

Pupil size plays an important role in optical quality. Compared to both humans and also young chicks, guinea pigs have naturally large pupils. This is reflected in our choice of a 4 mm pupil size for follow-up analyses that aimed to characterize the visual experience under laboratory lighting conditions. In contrast, the earlier guinea pig study that made use of laser ray tracing (LRT) limited data acquisition and analysis to 2 mm pupil size [139]. They report average RMS values of 0.10 um, as measured by LRT, and 0.18 um, from an OCT-based simulation. The average RMS estimated for our adolescent guinea pigs and a 2 mm pupil size is 0.167 um, which falls within the latter range (slightly higher than the LRT measurement, but lower than the OCT simulation). However, as described previously, RMS

Figure 3.7: Five arcmin letter E shown alongside point spread functions (PSFs) and convolved images for a representative human eye (top row) and guinea pig eye (bottom row). Calculations used a 4 mm pupil size and 550 nm wavelength.

errors increase rapidly with increasing pupil size (Figure 3.6A).

As an alternative and commonly used approach for measuring and comparing the optical quality of eyes, we also derived Strehl ratios for both our guinea pig and human subjects. Although the recorded ranges for these populations overlapped, overall the values representing guinea pig eyes (0.031 to 0.019) were much lower than those for human eyes (0.137 to 0.0204) (see summary in Table 3.1). As another way of illustrating this difference in the optical quality of the guinea pig and human eyes, we show in Figure 3.7, a 5 arc min (20/20) letter E convolved with a PSF from representative human and guinea pig subjects. The difference in retinal image quality between them is quite apparent; the blur is greater and the contrast is reduced for the guinea pig simulation, as is expected given the lower Strehl ratio and higher magnitude of high-order aberrations. Nonetheless, the 20/20 letter is still legible, even though the letter is far smaller than the threshold of the visual acuity of the guinea pig, as measured behaviorally.

In the context of eye growth regulation, it is apparent that the guinea pig eye can decode the sign of defocus imposed artificially with lenses. The related question arising from the optical aberration data reported here is how these aberrations impact the depth of focus of

the guinea pig eye. Depth of focus is generally defined as the variation in defocus that can be tolerated by the eye without causing any notable change in sharpness of the retinal image. Here we derived depth of focuses for both guinea pig and human eyes from Strehl ratios, which correlate reasonably well with perceived image quality [109]. Using a 50% threshold to estimate depth of focus yielded a depth of focus for the guinea pig eye of 4 D, which is over 4 times larger than the depth of focus for the human eye. Curiously, even younger guinea pigs, such as those 2-3 days of age, have been shown to respond with ocular growth changes to smaller amounts of imposed optical defocus (2 D) [63]. It is likely that their depth of focus would be larger than that of the adolescent guinea pigs used in the current study, and this disparity suggests that other factors, such as chromatic aberration, may contribute to the decoding of defocus by the retina.

How does the physical size of the PSFs for the guinea pig and human eye compare? To address this question, PSFs were converted to linear units, as shown in Figure 3.8. Although the guinea pig eye is more aberrated than the human eye, as measured by RMS errors, the extent of the PSF on the retina is smaller due to its shorter focal length. To further understand how this difference in eye length affected retinal image processing, the radial average MTFs were also replotted in cycles/mm (linear units) (Figure 3.8). If we use the maximum measured ganglion cell packing density of 3000 cells/mm^2 for the guinea pig visual streak [122], this corresponds to a sampling resolution of 29 cycles/mm as given by the formula:

$$\text{sampling resolution} = \frac{1}{2}\sqrt{\frac{2}{\sqrt{3}}\text{x sampling density}}$$

Given that 1 degree of visual angle corresponds to an 82 um across the retina in a guinea pig, then 29 cycles/mm would suggest a visual acuity of 2.4 cycles/deg. For human eyes, the average cone density in the fovea is 163,000 cones/mm^2 [207], which corresponds to a sampling resolution of 215 cycles/mm. The same calculations in the human eye lead to 62.5 cycles/deg. While optics limit human spatial vision, ganglion cell tiling appears to limit the visual acuity of the guinea pig, as 2.4 cycles/deg correlates well with behavioral acuity estimates.

With the linear transformation (cycles/mm), the high frequency cutoff for the guinea pig eye becomes larger than for the human eye and has a contrast advantage for low spatial frequencies, where the peak sensitivity lies. It remains unknown which of these factors carry more weight in terms of eye growth regulation, but the different analyses (spatial vs. angular) offer very different perspectives.

3.5 Summary and Conclusion

While visual acuity is much poorer in the guinea pig compared to the human eye, high order aberrations are not major sources of optical quality degradation. As in humans, second order aberrations are most deleterious for vision, while higher order aberrations have much less of

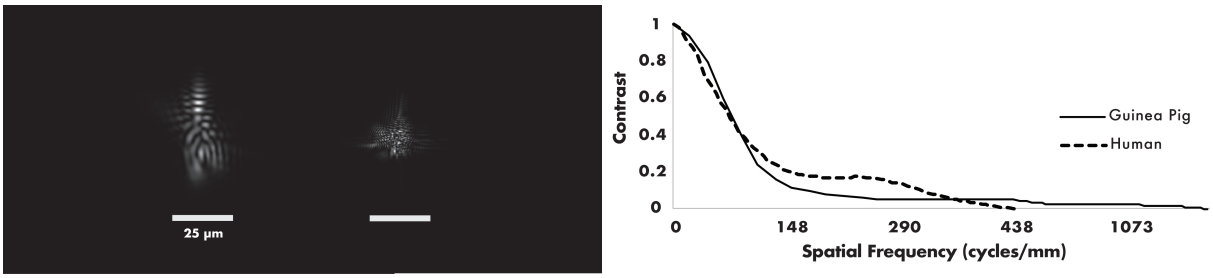

Figure 3.8: On the left are PSFs of representative human (left) and guinea pig (right) eyes, shown in linear units. While the guinea pig eye suffers from more high-order aberrations than the human eye, the physical size of its PSF is smaller, due to its shorter focal length. On the right are the radial average MTFs in cycles/mm for guinea pig (solid line) and human (dashed line) eyes. Calculations used a 4 mm pupil size and 550 nm wavelength.

an influence on vision. Future studies may involve comparing these different species used in models of eye growth regulation, particularly to study the function of optics that are far superior to visual acuity. Importantly, the data reported here on the optical quality of the guinea pig eye cover the normally encountered pupil size for the guinea pig and thus represent an important resource for future studies into optical defocus regulation of eye growth using this model. The comparative data derived from spatial versus angular analyses of optical quality offer an additional new perspective on how optical aberrations impact on vision.

Chapter 4

Development of a Lens-Induced Myopia Model Using Gas-Permeable Contact Lenses in Guinea Pigs

4.1 Introduction

It is now well-established that early disruption to the visual experience can disrupt emmetropization, leading to abnormal eye growth and refractive errors. In humans, congenital cataracts (if they are not removed promptly), ptosis, and hemangioma of the lid have been shown to cause excessive axial elongation of the visually-deprived eye and significant myopia [145, 64]. Similarly, in young animals, experimentally applied form deprivation treatments can accelerate eye growth, resulting in myopia. Myopia can also be induced in a growing eye by imposing optical defocus with negative lenses. When hyperopic defocus is applied by using a negative lens, the eye elongates at a faster rate until the compensation of the imposed defocus is achieved so that emmetropia is restored with the lens in place. Myopia is observed when the lens is removed. Conversely, imposing myopic defocus using a positive lens causes a decrease in the rate of eye growth, resulting in hyperopia after the lens is removed.

There are several advantages to studying ocular development in the guinea pig. Firstly, eye growth in the guinea pig is rapid [114], and the guinea pig is born with a well-developed visual system. While all rodents, including the guinea pig, have rod-dominated retinas, most other rodents have few cones, which are limited to one ultraviolet-sensitive cone type, consistent with their nocturnal lifestyle [74]. Guinea pigs, on the other hand, are crepuscular, with both short- and medium-wavelength-sensitive cones, allowing for dichromatic vision [74]. Guinea pigs also have an area of higher cone density, referred to as a visual streak, which serves a similar function to the area centralis of primates [66, 152].

Guinea pigs have other advantages as an animal model. Guinea pig breeding colonies reproduce an average of one pup per female per month [104], providing a relatively large and steady supply of animals available for testing. This feature along with their precocial

nature, relative ease of handling and husbandry, and standard cage housing needs have positive practical implications for studies requiring animals to be raised under controlled visual conditions, such as in studies of eye growth regulation and myopia control treatments. As a result, the guinea pig has become the most popular mammalian model for such studies.

Guinea pigs, like other animal models, respond to both positive and negative lens-induced defocus, with sign-dependent (opposite), compensating changes to the rate of axial elongation [63]. Historically, spectacle-mounted lenses or diffusers (such as the ones shown in Figure 4.1) are used to induce myopia in guinea pigs. The lenses (or diffusers) are typically mounted on Velcro ring supports. To attach the lens to the guinea pigs, segments of opposing loop Velcro, prepared from rings of the same Velcro, are glued to the hair surrounding the guinea pig's eyes under light general anesthesia. However, these protocols require very frequent monitoring of the animals, and as necessary, reattachment of semi-detached or completely detached diffusers and lenses, and/or reapplication of Velcro supports in addition to the daily cleaning routines for spectacle lenses. Full-time wear of diffusers has also been associated with an increased risk of corneal infections (unpublished observation), perhaps reflecting induced adverse changes in the anterior surface environment, such as increases in temperature and/or humidity under the diffusers, which are not removed as regularly as spectacle lenses.

Figure 4.1: A guinea pig fitted with a Velcro-mounted diffuser (left) and a Velcro-mounted spectacle lens (right).

In the study reported here, rigid gas permeable (RGP) contact lenses were explored as an alternative method for inducing myopia in guinea pigs, with potential practical and bio-compatibility benefits for long-term experiments. This approach carries the additional advantage of allowing the testing of multifocal myopia control contact lens designs in an animal model, when testing has been limited to spectacle lenses to-date. It was hoped that the contact lenses would also be compatible with simultaneous use of topical pharmaceutical agents of interest in relation to myopia control.

4.2 Materials and Methods

Animals

New Zealand pigmented guinea pigs (*Cavia porcellus*) were used in this study. This line was established from male and female English Short Hair breeders obtained from the University of Auckland, New Zealand. Animals used in this study are descendants of this original line. Pups were weaned at 7 days of age and housed as single sex pairs in transparent plastic wire-top cages (16 inches x 20 inches) in a room with illumination following a 12h/12h light/dark cycle. Low-dust aspen shavings were used on the floor of the cages to absorb animal waste and spilled water. While animals were wearing contact lenses, the shavings were covered with a single layer of cardboard in order to further minimize dust and to easily locate the contact lenses when dislodged from the eye, either through blinking or scratching.

The guinea pigs had free access to vitamin-C supplemented food and water, and received daily fresh fruit and vegetable enrichment Monday through Friday. They were also given Timothy Hay on weekends and after any experimental procedures as a reward. Animal care and treatments in this study conformed to the ARVO statement for the Use of Animals in Ophthalmic and Vision Research. Experimental protocols were approved by the Animal Care and Use Committee of the University of California, Berkeley.

Contact Lens Design

Designing suitable contact lenses involved first characterizing the corneal shape of the guinea pig, examining the fit of prototype lenses, and then investigating the feasibility of longer-term wear. Finally, negatively powered lenses were tested for their ability to induce myopia.

Characterizing the Corneal Shape

To design rigid contact lenses for the eyes of young, rapidly growing animals, it is essential to understand their corneal topography and how it changes over the anticipated lens wearing period. In this respect, available corneal curvature data from a previous study by Howlett and McFadden [61], is not sufficiently comprehensive, as it describes only the central 40% of the cornea. Specifically, as our contact lenses were designed to cover approximately 90% of the corneal surface, characterization of the shape profile of the peripheral cornea was also necessary.

The relatively steep corneas of young guinea pigs also ruled out the use of standard topographers without modification. Instead, high resolution images of the anterior segment were captured with a Visante Anterior Segment OCT (Zeiss Meditec, Dublin, CA) (see example, Figure 4.2) and used to derive corneal curvature profiles. Developmental profiles were derived from anterior segment images collected from three guinea pigs, imaged twice per week over the course of three weeks starting at three weeks of age.

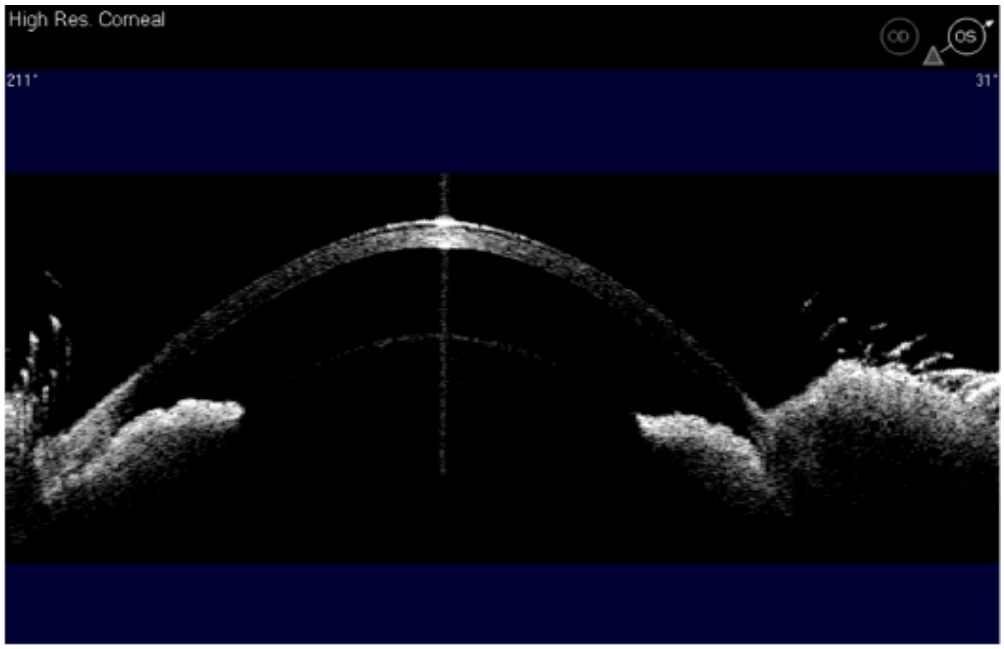

Figure 4.2: A typical Visante image acquired and used for curvature analysis. The bright vertical band intersecting the apex of the cornea is an indicator of image quality.

Corneal curvature profiles were then derived from the images using custom MATLAB software (MathWorks, Natick, MA; written by Ethan Bessinger). In brief, after first identifying the corneal (limbus) margins, the apex of the cornea was located and used as a reference to radially segment the cornea in 15-degree increments (Figure 4.3). This process allowed selection of corresponding corneal points for comparison across the guinea pigs tested. For analysis, three points including the central apical point and points 75 degrees to its left and right were selected. These points were chosen to correspond to the approximate location of corneal touch for an ideal fitting rigid gas permeable contact lens, with minimal apical clearance. The radius of curvature of the cornea was estimated as the radius of the circle drawn through these points (Figure 4.4). This method can also be applied to derive the curvature of the posterior cornea, although this was not undertaken for the current study.

The anterior corneal radius of curvature can be converted into diopters using the formula:

$$\text{corneal curvature in diopters} = \frac{337.5}{\text{radius of curvature in mm}}$$

In addition to the corneal curvature data, corneal diameter data were also extracted from images acquired by the Anterior Segment OCT using the built-in segmentation software. An example is shown in Figure 4.5.

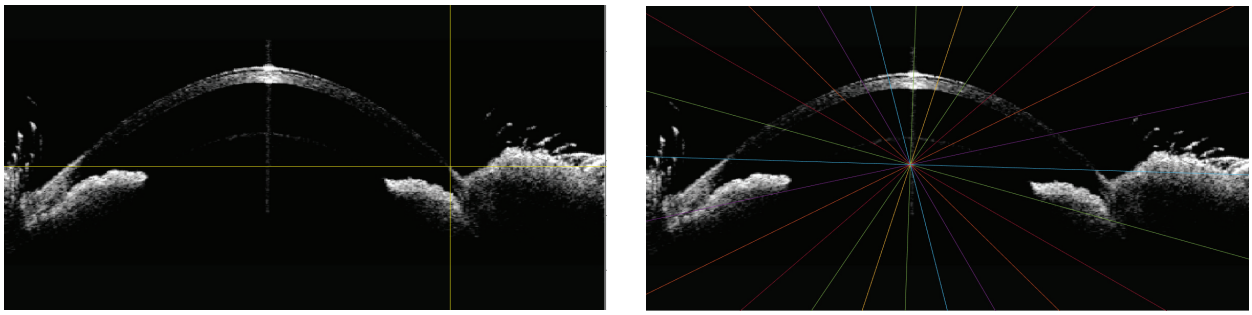

Figure 4.3: Using the same exported image, the image on the left shows the marking of the left limbal point (at the cross of the two yellow lines). Once the right limbal point is also marked, the software plots radial lines in 15-degree increments as shown in the image on the right, allowing us to locate the corneal apex.

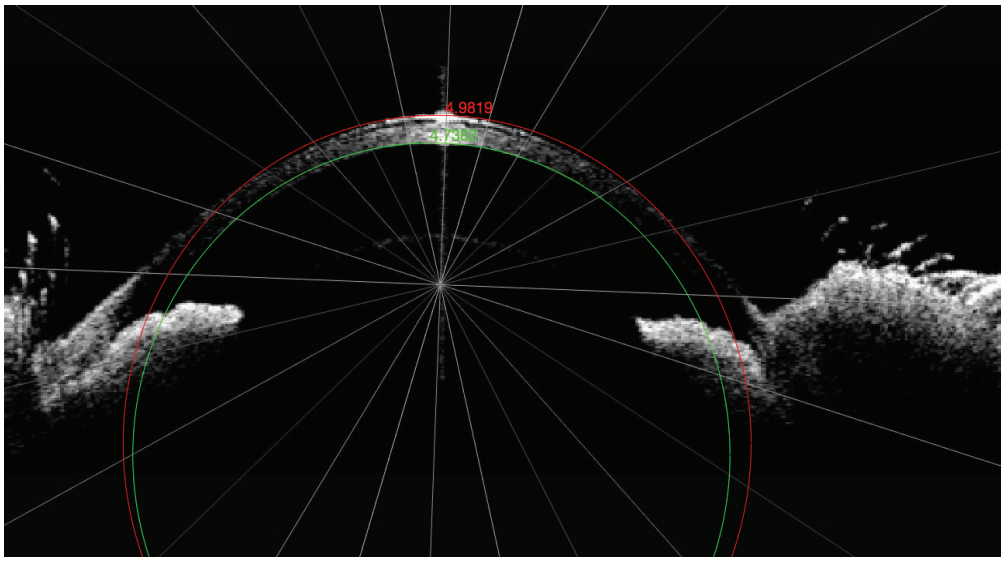

Figure 4.4: Using the radial lines generated in Figure 4.3, we can then select points on the anterior surface of the cornea to generate an estimate of the radius of curvature (measured in mm). The red circle represents the peripheral anterior radius of curvature (made by selecting points 75 degrees from the apex on both the nasal and temporal sides. The green circle represents the posterior peripheral radius of curvature (made by selecting points 75 degrees from the line bisecting the apex of the cornea on both the nasal and temporal sides.

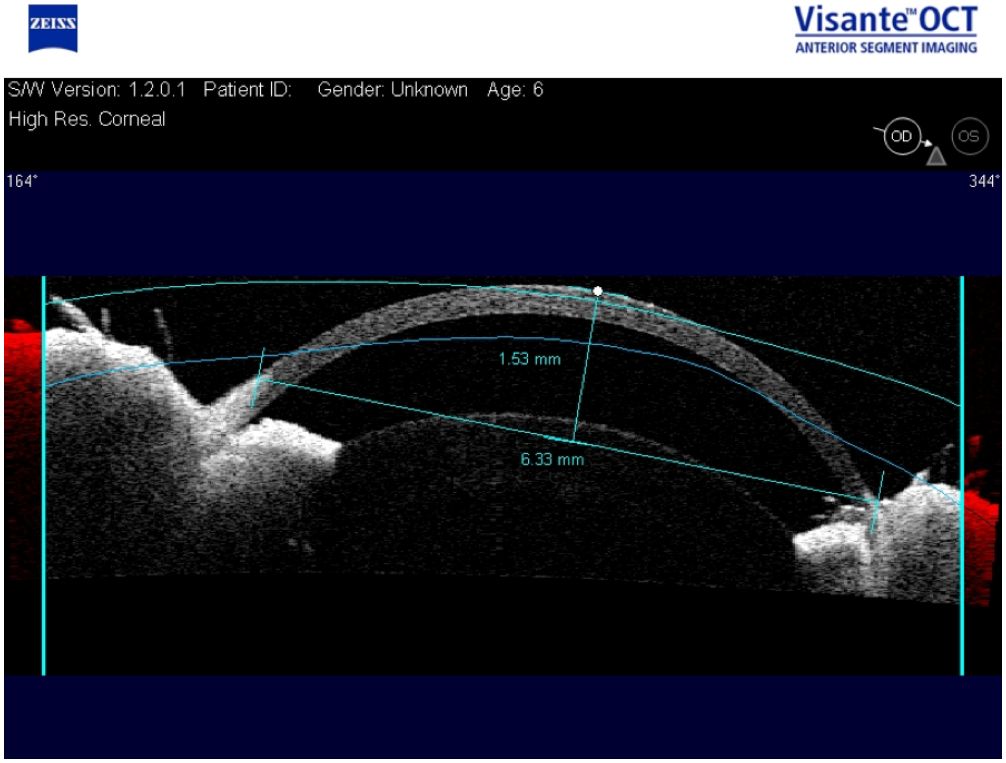

Figure 4.5: This is another representative anterior segment OCT image that was captured. The blue lines are automatically generated by the software in an attempt to outline the cornea. However, the guinea pig cornea is much steeper than a human cornea, so the outline is irrelevant. The limbal points are visible by the transition from the bright white sclera to the more grainy cornea. Corneal Diameter was measured limbus to limbus using the calipers built in to the Zeiss Visante software (6.33 in this example). The sagittal depth from the corneal apex to the limbus is also marked (1.53 in this example).

Using Contact Lenses to Induce Myopia

Beginning at 10 days of age, another group of four guinea pigs had their right eyes fitted with single-vision -10 D rigid gas permeable contact lenses. The fellow left eyes served as untreated controls. The lenses were worn for 24 days. Animals were monitored hourly during the 12-hour light cycle to ensure that the lenses remained in place and to check for any adverse events. The lenses were removed daily and replaced with a clean lens. The previously worn lens was soaked in Boston Simplus (Boston, Bausch and Lomb, Rochester, NY), and a protein remover was used as needed during the period of lens wear.

At baseline, measurements including optical biometry, anterior segment OCT imaging, and refraction were measured, immediately prior to the start of lens wear. Refractive errors, axial lengths, and corneal curvatures were collected over the experimental period. For some of the measurement procedures, alert animals were simply swaddled with an absorbent pad

in order to keep them comfortable, still, and in proper alignment with the measuring device (Figure 4.6). Guinea pigs were acclimated to being wrapped in the absorbent pad with positive reinforcement including food rewards such as hay and fresh vegetables, and positive interaction such as petting. This positive reinforcement increased in 5-minute increments per day until reaching 15 minutes.

Figure 4.6: Setup for Lenstar measurements. Guinea pigs were swaddled with an absorbent pad and seated comfortably on the platform for measurements.

Refractive errors were measured on days 0 (baseline), 7, 14, 21, and 24 of the experiment, in all cases using streak retinoscopy on awake animals 30 minutes after instillation of two drops of 1% cyclopentolate hydrochloride (Bausch and Lomb, Rochester, NY), spaced 5 minutes apart. Refractive errors were recorded along the two principal meridians. Spherical equivalent refractive errors (SERs), i.e., the average of the results for the two principal meridians, are reported.

Axial length data were collected at the same time points listed above, using the Lenstar (Haag-Streit, Kniz, Switzerland), a partial coherence interferometry-based ophthalmic device designed for measuring the ocular biometry of human eyes. The instrument measures central corneal thickness (CCT), anterior chamber depth (AD), lens thickness (LT), and axial length (AL). For this study, which involved contact lens wearing animals, this instrument offered a significant advantage over commonly used high-frequency ultrasound-based biometry techniques. With the Lenstar, there is no physical contact between the instrument and the animal's eye, which eliminates the need for gels and anesthesia of any kind. Each Lenstar measurement comprised of an average of at least five recordings. Measurements were conducted at the same time of day in order to avoid any possible confounding effects of circadian rhythms of eye growth [127].

The Lenstar output, when used to measure human eyes, includes peaks corresponding to the anterior and posterior corneal surfaces, anterior and posterior crystalline lens surfaces, vitreous/retina interface, retina/choroid interface, choroid/sclera interface, and back of the

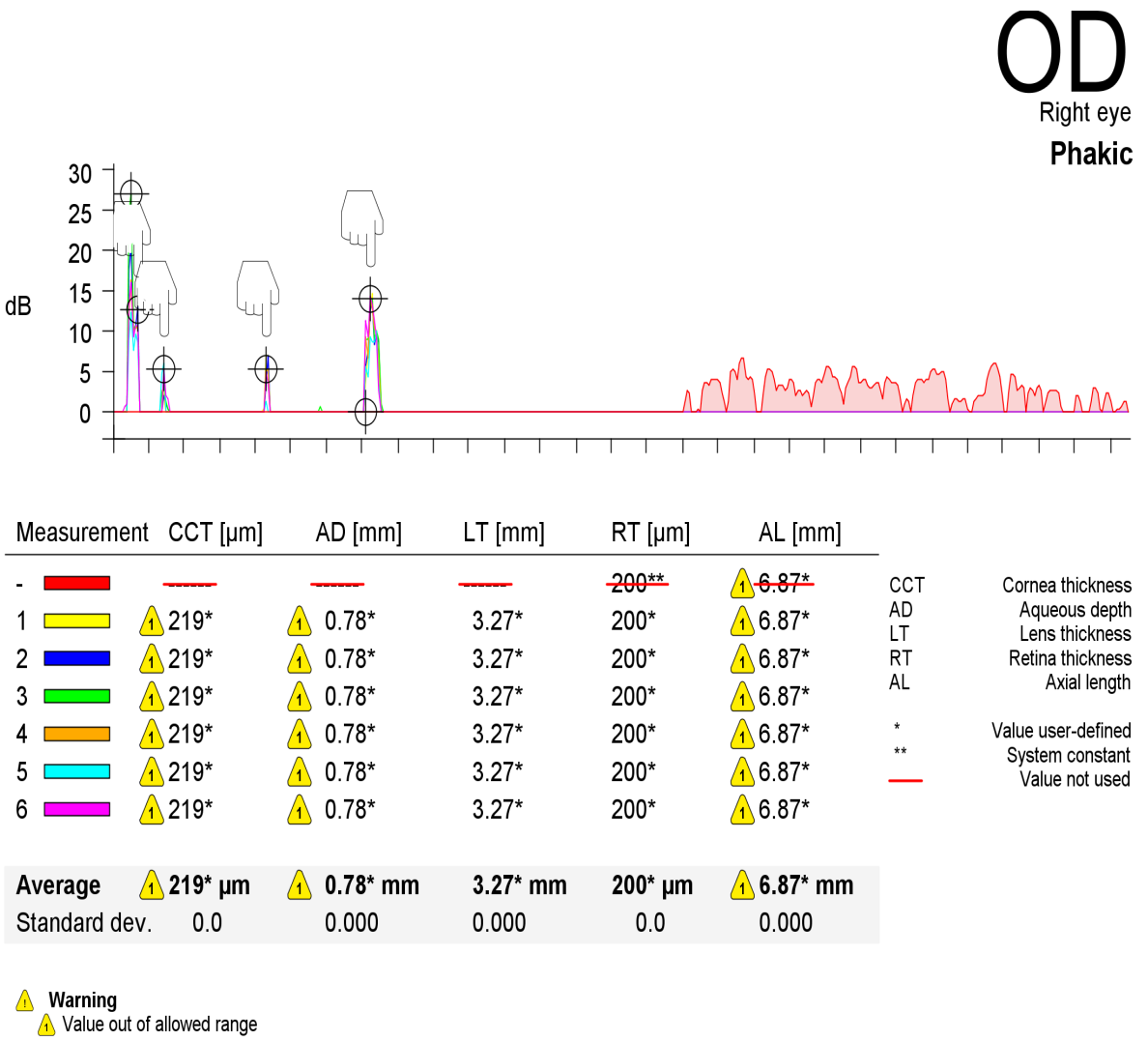

Figure 4.7: An example of a good Lenstar tracing showing reliable peaks for the anterior and posterior corneal surfaces, anterior and posterior lens, and retina.

sclera. When used to measure guinea pig eyes, reliable peaks representing the anterior and posterior corneal surfaces, anterior and posterior crystalline lens surfaces, and vitreous/retina interface can be obtained (Figure 4.7), although an error message is encountered with each recording because the axial length is outside the expected measurement range.

Finally, the measured lengths assume the contents of a human eye. To convert into true guinea pig axial lengths, we can use the indices of refraction for 30 day old guinea pigs measured by Howlett and McFadden [61] as shown in Table 4.1.

Table 4.1: Refractive indices of the human and guinea pig eye [61]

	Human	Guinea Pig
Cornea	1.376	1.376
Aqueous	1.333	1.335
Lens	1.42	1.539
Vitreous	1.335	1.335

Statistical Analyses and Data Representation

All data were recorded and visualized using Excel 2013 (Redmond, WA) and statistical analyses made use of Stata version 14 (College Station, TX). Data are reported as mean interocular differences (treated eye minus control eye) or changes over time, referenced to the baseline values, along with the standard error of the mean. Differences between treated and contralateral (fellow) eyes for all measured parameters were statistically compared using paired t-tests.

4.3 Results

Contact Lens Design

Characterizing the Corneal Shape

The corneal curvature data are summarized in Table 4.2. Each value represents the average curvature derived from at least three images captured for the same guinea pig during the same measurement session. The average values for the horizontal curvatures are also plotted over time in Figure 4.8. There is a small but statistically insignificant flattening of the corneal curvature over time. The median corneal curvature, derived from data from all animals and time points, is 98.4 D (range 87.4 - 104.88). The latter value was selected as the initial back optic radius for the trial contact lens in the interest of efficiency in contact lens fitting.

In addition to corneal curvatures, corneal diameters were also tracked as the guinea pigs grew. The mean corneal diameter, derived from all animals and time points, was 5.97 mm ($\pm$0.30). Corneal diameters are plotted against age in Figure 4.9. There was a significant increase in corneal diameter on day 19, with reference to the baseline.

Based on derived corneal curvature and diameter parameters, 12 trial contact lenses, ranging in power from 0 D to -10 D were ordered. Table 4.3 summarizes the parameters of these lenses. Lenses were designed to have an aspheric edge lift of 0.15, axial edge lift, and finished edges. The contact lenses were custom-made from fluorosilicone acrylate (Optimum Comfort, Contamac, Ltd., Saffron Walden, UK, contamac.com), a commonly used human rigid gas permeable contact lens material. This material has high oxygen permeability (65%) and good wetting angle (6). The optical powers of ordered contact lenses were verified prior to their use.

Table 4.2: Horizontal (H) and Vertical (V) corneal curvature values calculated from the Zeiss Visante images using custom MATLAB software. All values represent the average of at least three measurements with the exception of Subject 2, Day 1 (in bold), for which we were only able to collect one image (due to poor cooperation of the subject).

Subject			1		2		3	
Day			OD	OS	OD	OS	OD	OS
	H	Avg	97.95	96.09	**100.03**	98.94	97.95	96.09
1		SD	0.39	0.31		1.20	0.39	0.31
	V	Avg	102.4	100.3	**103.3**	103.1	102.4	100.3
		SD	1.13	0.26		1.06	1.13	0.26
	H	Avg	96.85	95.30	100.3	99.18	96.85	95.30
4		SD	0.22	1.66	0.29	1.55	0.22	1.66
	V	Avg	101.1	100.3	104.8	102.9	101.1	100.3
		SD	0.18	0.57	0.58	0.63	0.18	0.57
	H	Avg	87.40	92.72	98.05	96.18	96.61	94.20
7		SD	2.96	1.32	0.87	2.45	4.59	0.74
	V	Avg	98.43	98.75	101.7	100.3	100.0	100.4
		SD	2.52	1.00	1.70	1.35	1.07	0.75
	H	Avg	97.64	96.57	97.15	98.64	96.17	95.56
11		SD	0.54	1.00	0.81	0.79	3.58	3.41
	V	Avg	98.47	98.83	102.6	101.0	100.5	99.44
		SD	0.34	2.63	2.18	0.75	2.47	1.68
	H	Avg	94.06	94.58	98.90	96.78	102.1	95.79
15		SD	3.24	1.40	1.61	1.54	4.01	1.58
	V	Avg	96.68	97.90	99.86	99.15	104.6	97.31
		SD	1.84	1.34	1.84	1.20	4.14	0.69
	H	Avg	95.60	95.28	97.41	94.39	94.10	96.45
19		SD	0.93	1.21	0.90	2.16	0.18	1.59
	V	Avg	96.93	96.66	98.04	98.10	95.55	98.46
		SD	1.29	1.19	0.82	0.84	0.38	2.07

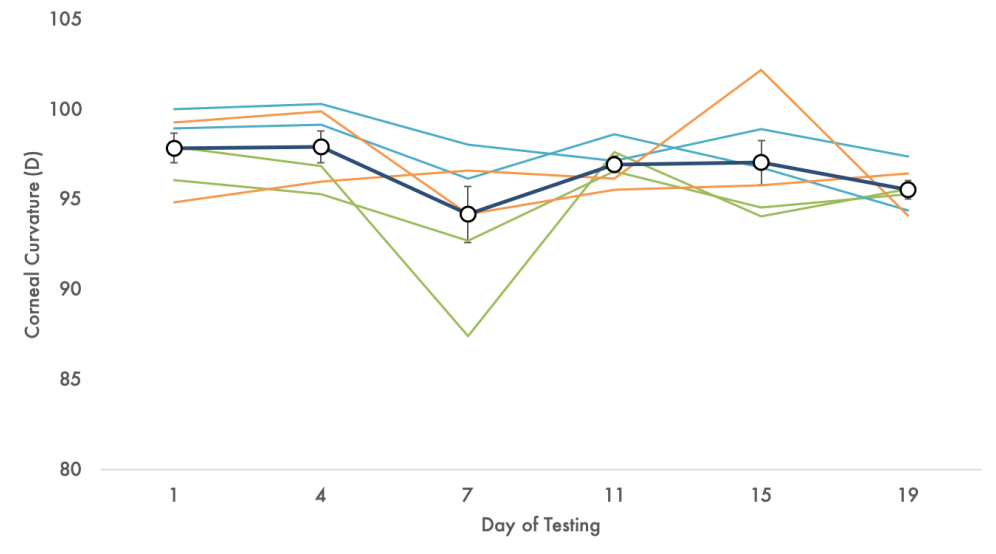

Figure 4.8: Average corneal curvature over time. There was no significant difference in corneal curvature relative to day 1 (paired t-test). Each color represents the average horizontal curvature value for one guinea pig (acquired from at least three images) and the average change for all three guinea pigs is plotted. Error bars represent the standard error of the mean.

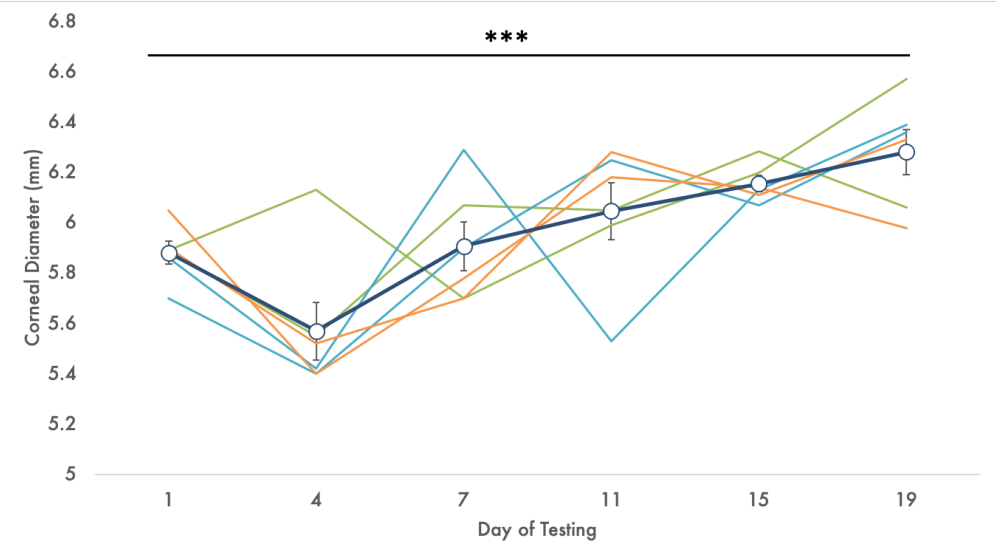

Figure 4.9: Average corneal diameter over time. There was a significant increase in corneal diameter on day 19 (referencing day 1) ($p = 0.001$, paired t-test). Each color represents the average values for one guinea pig (acquired from at least three images) and the average change for all three guinea pigs is plotted. Error bars represent the standard error of the mean.

Table 4.3: Trial Contact Lenses Ordered

Lens	Base Curve (mm)	Lens Power (D)	Diameter (mm)
1	3.53	0.00	6.00
2	3.50	0.00	6.00
3	3.46	0.00	6.00
4	3.44	-5.00	5.50
5	3.44	-10.00	6.00
6	3.43	-5.00	5.50
7	3.43	-5.00	6.00
8	3.41	-10.00	5.50
9	3.41	-10.00	6.00
10	3.39	0.00	5.50
11	3.38	-5.00	5.50
12	3.34	-10.00	5.50

Testing and Confirming the Fit

Guinea pigs were observed for at least five minutes after their first experience of a contact lens in the eye, to watch for signs of discomfort (such as scratching or excessive blinking). To insert the lenses, the animals were placed on a lab bench, the lower lid was gently pulled down and upper lid lifted up to widen the palpebral aperture, and then the lens was placed directly on the cornea and the lids were released.

For each animal subject, the fit of the contact lenses were first evaluated under white light, and then under cobalt blue light following the instillation of sodium fluorescein (Figures 4.10 and 4.11). The same criteria as applied for a human minimal apical clearance fit was used to judge an appropriate overall fitting pattern in the guinea pigs. A fit was determined to be appropriate when there was no visible apical touch, fluorescein easily entered into the post-lens tear film, and a minimal amount of fluorescein was visible under the edge of the lens. Central clearance was also verified with OCT imaging (Figure 4.12).

The optimal lens design was determined to have a base curve of 3.38 mm (99.85 D) and 6.0 mm diameter. While the smaller 5.5 mm diameter lenses represented a true interpalpebral fit, they were too easily blinked off when the anterior lens surface became a little dry. Lenses were easily inserted and removed. Rarely did it take 2-3 attempts as opposed to just one attempt to remove a lens from the eye of a guinea pig. Similar to human contact lens wear, the process was facilitated by the insertion of a non-preserved artificial tear prior to removal of the contact lens.

Over the lens wearing period, the behavior of the guinea pigs were very carefully observed and recorded. The guinea pigs were able to tolerate the contact lenses very well. Behaviorally, no excessive blinking or scratching was observed following lens insertion, and their corneas did not show any epithelial disruption, as detectable by sodium fluorescein staining after lens removal. In fact, the non-lens wearing eye often showed some evidence of superficial corneal

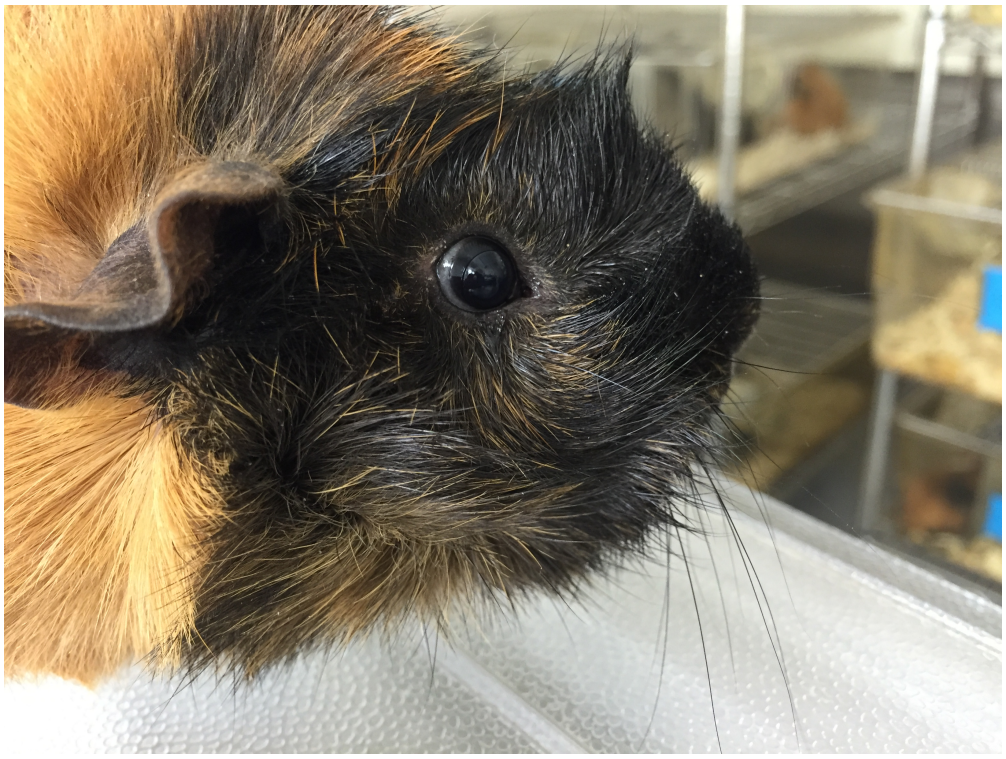

Figure 4.10: Appropriate positioning of the RGP on the right eye of a guinea pig. This was a 5.5 mm diameter lens.

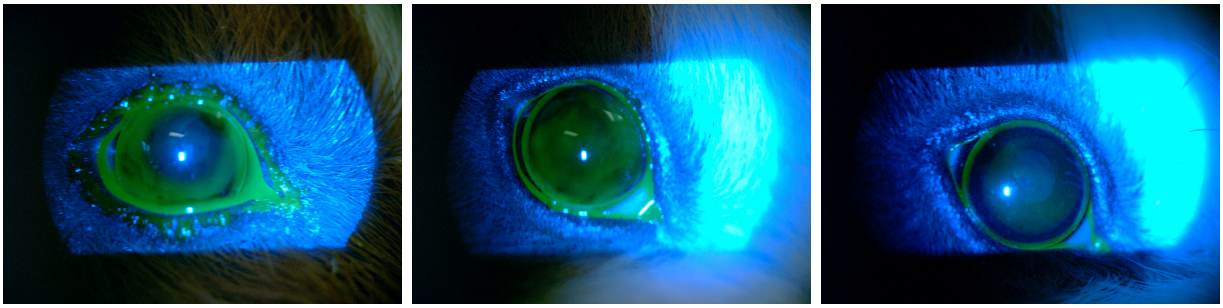

(a) Too Flat (b) Too Steep (c) Ideal Fit

Figure 4.11: Sodium fluorescein evaluation of trial contact lenses. The lens in panel A is too flat, as evidenced by the absence of fluorescein in the central part of the lens and excessive fluorescein in the periphery. The lens in panel B is too steep, with excessive fluorescein underneath the lens and minimal edge lift. The lens in panel C is an example of an ideal fitting lens, with minimal apical clearance and appropriate edge lift.

epithelial defects, from which the cornea of the lens-wearing eye appeared to be protected.

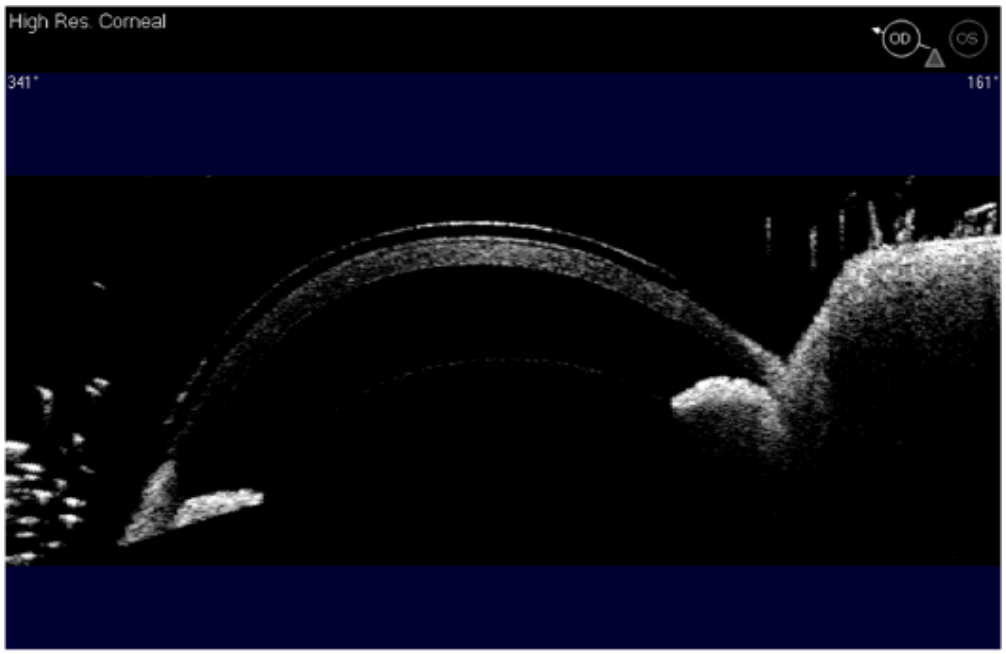

Figure 4.12: Anterior Segment OCT image collected while a guinea pig was wearing a contact lens to confirm appropriate fit. Anterior to the corneal surface, the front and back surface of the contact lens is visible as two thin, bright bands with a completely dark space between them. there is a thin dark space between the posterior surface of the contact lens and the anterior surface of the cornea, confirming an appropriate lens fit.

Using Contact Lenses to Induce Myopia

Myopia was successfully induced in all four of the guinea pigs tested with contact lenses (Figure 4.13). In the untreated (control) eyes, refractive errors changed from +4.68 D (±0.71) at baseline to +2.75 D (±0.20) at 24 days. The greatest change occurred over the first 7 days of lens wear, with progressively smaller changes over the remaining time. As expected, the refractive errors of the treated (lens wearing) eyes were no different from their fellows at baseline +5.94 D (±0.53) ($p = 0.86$), but exhibited low myopia by day 24, -0.68 D (±1.05). The greatest change for treated eyes also occurred between the baseline and day 7 time points, although there was substantial myopia progression across the day 7 to day 14 period, after which there was a steady but slower progression of myopia. The interocular difference (treated eye - control eye) at day 14 was -1.94 D ($p = 0.05$), reaching borderline statistical significance. By day 24, the difference had further increased to -3.44 D ($p = 0.03$).

In contrast to the trends just described for refractive errors, where the greatest changes occurred within the first week, the axial length increases in lens-wearing eyes developed more steadily over the experimental period, at an average rate of 0.25 mm/week. Nonetheless, for these eyes, the greatest increase in axial length occurred over the first week of treatment (0.35 mm), followed by 0.26 mm in week 2 and 0.18 mm in week 3. Overall, axial lengths

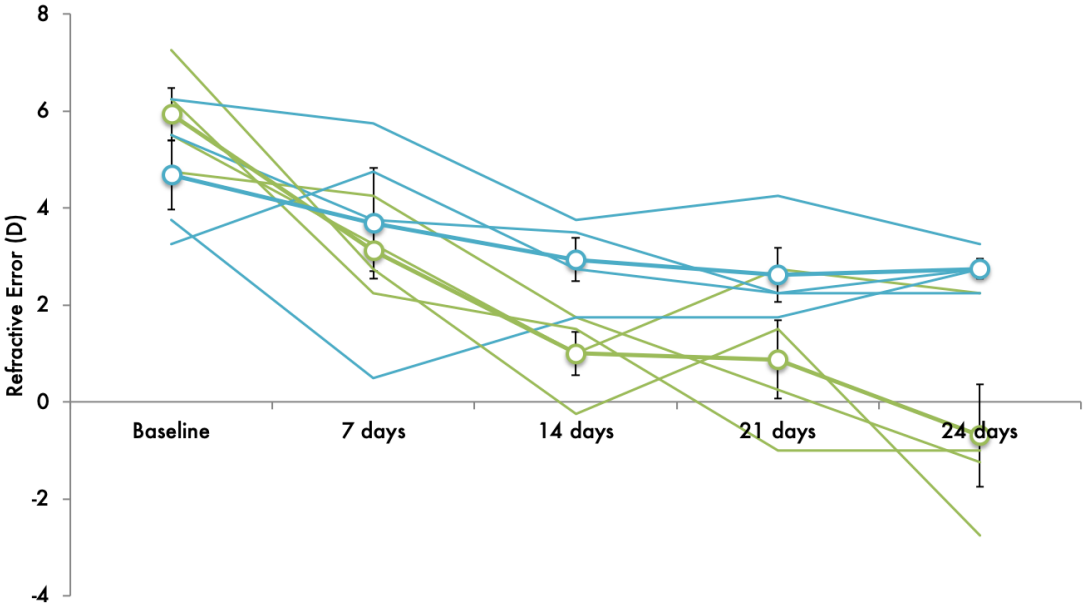

Figure 4.13: Change in refraction over the experimental period. The green lines show the treated eye and blue lines show the untreated, contralateral control eye. Error bars represent the standard error of the mean.

increased from 6.59mm (±0.072) at baseline to 7.50 mm (±0.043) by day 24. In the untreated (control) eyes, axial length increased from 6.58 mm (±0.068) at baseline to 7.40 mm (±0.052) at 24 days. A statistically significant interocular difference in axial length was achieved by day 7 (difference of 0.089 mm, $p = 0.02$) and was maintained for the duration of the 24-day experimental period. By day 24, this difference had further increased to 0.10 mm ($p = 0.01$). Individual animal and mean differences are shown in Figure 4.14.

Corneas became flatter over the course of the experimental period. The mean corneal curvatures for treated and untreated eyes at the beginning of the treatment period were 3.63 mm (±0.086) and 3.58 mm (±0.16), respectively, while comparable values at the end of the treatment period were 4.99 mm (±0.17) and 4.55 mm(±0.17). There was also a statistically significant difference between treated and untreated eyes on day 21, when the corneas of non-lens-wearing eyes appeared to have steepened slightly, while the corneas of lens-wearing eyes continued to flatten at a steady rate. Differences between the treated eyes and their fellows were not significant at any other time point.

Corneal thickness increased significantly in the treated eyes and minimally in the untreated eyes over the experimental period. For the treated group, the mean central corneal thickness increased from 203 um (±5.2) to 243 um (±3.7), while for the non-lens-wearing eyes, the mean central corneal thickness increased from 194 um (±6.5) to 219 um (±3.22) over the same time period. The interocular difference reached statistical significance on day 7 ($p = 0.02$) and remained significant throughout the remainder of the experimental period.

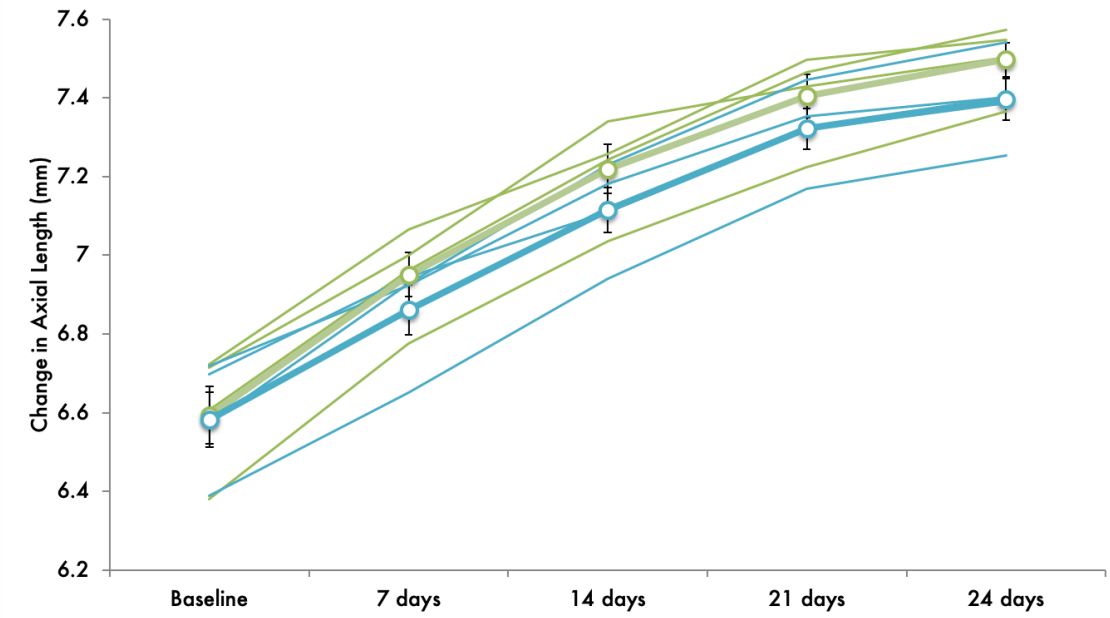

Figure 4.14: Change in axial length over the experimental period. The green lines show the treated eye and the blue lines show the untreated, contralateral control eye. Error bars represent the standard error of the mean.

Both lens-wearing eyes and their fellows showed small increases in anterior chamber depth over the experimental period. For treated eyes, mean values increased from 0.78 mm (±0.03) to 0.97 mm (±0.01), and fellow eyes showed a similar increase from 0.78 mm (±0.03) to 0.91 mm (±0.02). By day 14, these changes represented significant increases from baseline values, and they were sustained throughout the remaining experimental period. There was no significant difference between lens-wearing eyes and their fellows at any time point.

Finally, there was a small increase in lens thickness in both lens-wearing eyes and their fellows, increasing from 3.21 mm (±0.054) to 3.68 mm (±0.017) in the former and from 3.21 mm (±0.053) to 3.67 mm (±0.027) in the latter. However, there was no significant difference between the lens-wearing eyes and their fellows at any time point.

4.4 Discussion

The contact lens protocol described in this chapter represents a novel method for inducing myopia in an animal model, and the method of measuring axial length is also a relatively new approach for guinea pig-based myopia research.

The Use of Contact Lenses

Rigid gas permeable contact lenses have great potential as an alternative method for defocus-induced myopia induction to spectacle-mounted lenses. Because of the novelty of this approach, the behaviors of the guinea pigs while wearing the contact lenses were very carefully observed. No abnormal behavior (including blinking, scratching, or fear of the experimenter), or signs (including corneal irritation or infection, redness in or around the eye, or weight loss) were noted. Therefore, this approach is not only less invasive than the spectacle lens-based approach, it also appeared to be less stressful for the guinea pigs.

In relation to unintentional discontinuation of the defocus treatment, the contact lenses provided more reliable treatment than spectacle lenses as they very rarely accidentally came out of the eye. This had the practical advantage of allowing for less frequent monitoring of the animals undergoing treatment. Previous studies have found that myopic ocular growth responses, such as those induced by lens-imposed hyperopic defocus or diffuser treatments, are easily disrupted. Even very brief periods of interruption to treatments can be sufficient to slow axial elongation. In form-deprived monkeys [177] and negative-lens treated tree shrews [169], just one hour of normal vision is effective in preventing myopia development. In the guinea pig, just 36 minutes of normal (uninterrupted) vision is enough to prevent the expected responses to myopia-inducing treatments [92]. Therefore, having a method of inducing myopia that is both more reliable and tolerable for the animals and experimenters, such as this contact lens-based approach, is very beneficial, particularly when researching treatments that must be applied for extended duration.

Experimental Myopia

In this study, guinea pigs developed a significant amount of myopia over the 24-day treatment period. At the end of the experimental period, there was a mean interocular difference for the group of nearly 3.50 D, with the contact lens-treated eyes being more myopic. Comparing the changes across the treatment period, we found that the contact lens-wearing eyes of the guinea pigs developed up to 6.50 D of myopia relative to their baseline value, while their control (untreated) eyes changed by only 2.00 D over the same 24-day experimental period. There are two other research groups who have thoroughly characterized normal developmental refractive error changes in guinea pigs. Zhou et al. found moderate hyperopia in three week-old guinea pigs (+3.27 D), with a continued decline in hyperopia but at a much slower rate beyond this time point [233]. On the other hand, Howlett and McFadden reported a more rapid decline in neonatal hyperopia, from an average of +4.40 D at birth to +0.70 D at 30 days of age [61]. Our data lie between these two estimates, with a mean value of +2.75 D at 34 days of age (experimental day 24).

Eyes wearing -10 D contact lenses had significantly longer axial lengths than the fellow eyes, with most of the axial elongation occurring during the first week of treatment. Compared to the changes reported in a previous study using -4 D spectacle lenses [63], the magnitude of the induced interocular difference in axial length is nearly double, consistent

with a dose-dependent response, reflecting the higher lens power used for myopia induction (-10 D) in the current study. However, it is possible that the greater reliability of the contact lens treatment, as discussed above, may also be a contributing factor.

To our knowledge, only one other group [79] has used the Lenstar to measure ocular dimensions in the guinea pig. Although their approach was similar overall, Jnawali et al. performed the procedure under general anesthesia [79]. They also confirmed the accuracy of measurements made with the Lenstar against measurements made using A-scan ultrasonography, as well as with a ruler following enucleation. They found that all three approaches yield comparable results. The Lenstar has also been used on tree shrews [49, 48], which have comparable eye sizes to guinea pigs. In the current study, we were able to obtain at least five traces that contained all four refractive surfaces for all animals measured, which showed excellent consistency. The guinea pigs were also sufficiently cooperative for this non-invasive procedure so that general anesthesia could be avoided, an additional advantage when working with young animals that require frequent measurements. One disadvantage of the Lenstar is that retinal thickness is fixed at 200 um. However, given that this distance is fixed for all measurements, the relative changes can still be compared.

While it is generally accepted that myopia development is primarily or completely a result of vitreous chamber elongation, some investigators have reported corneal steepening occurring in school myopia. For example, in one longitudinal study including children between the ages of 3 and 14 years of age, a paradoxical corneal steepening was found in 10 out of 25 myopes, while this was only observed in 14 out of 62 non-myopes [181]. In contrast, the corneas of the guinea pigs flattened over time, and actually flattened at an accelerated rate in the lens-wearing eyes compared to the untreated control eyes. Howlett and McFadden also observed corneal flattening in their guinea pigs from 3.1 mm at 2 days of age to 4.4 mm at 300 days of age, with an average rate of flattening of 4.3 um/day [61]. Nevertheless, the rate of corneal flattening in our guinea pigs is substantially higher than that observed by Howlett and McFadden. This difference could be a result of different measurement techniques (anterior segment OCT in our case, compared to videokeratometry in their study). The cornea is an aspheric surface, with the central cornea being steeper than the peripheral cornea. As our OCT measurement technique gave more weight to the peripheral cornea, accounting for nearly 90% of the corneal surface, while the videokeratometry data represent the central 40% of the corneal surface, logically, this difference predicts flatter corneal curvatures with the former technique.

As previously mentioned, there was a significant difference in corneal curvature between lens-wearing eyes and their fellows on day 21 but not at any other time point. On day 21, it appears that the corneas of the untreated eyes steepen slightly, while the corneas of treated eyes continue to flatten at a steady rate. Although this may represent a random variation, given the small number of animals involved, interestingly, Zhou et al. reported a similar pattern [233]. Specifically, they reported the corneal radius of curvature to decline significantly in the first week of life followed by a "rebound" increase for one week, and then another slow decline thereafter. Such patterns of change have also been reported in tree shrews [130] and primates [12]. Although the time points in our study do not match well

with those of Zhou et al. (our "rebound" occurred between weeks 2 and 3 of the experiment, corresponding to 3.5 and 4.5 weeks of age), the trend is interesting. In addition, we did not see this "rebound" in the contact lens-wearing eyes.

Another interesting finding in the current study was the increase in corneal thickness in eyes wearing contact lenses. Most likely this is an effect of corneal edema as a result of extended (continuous) contact lens wear [57], rather than an effect of the myopia treatment. This change is unlikely to be problematic in comparative studies in which all treatment groups wore contact lenses, and thus the effect of lens wear will be the same for all treatment groups. However, a follow-up study involving plano contact lenses would help to rule out a side-effect of myopia-induction as an alternative explanation for the corneal thickening observed in the contact-lens wearing eyes.

It has been reported that lens defocus-induced changes to axial length are primarily due to induced changes in the depth of the vitreous chamber, which is sensitive to both the sign and power of the lenses worn [63]. Generally, lens thickness and anterior chamber depth are not significantly affected by myopia inducing treatments, at least in guinea pigs [62, 63]. However, one exception was previously noted in that guinea pigs treated with -4 D spectacle lenses had significantly thicker crystalline lenses compared to fellow eyes. The magnitude of this effect was very small (a difference of 0.01 mm), albeit statistically significant. In our study, we found that the crystalline lens increased in thickness during the experimental period, but there was not a significant difference between the treated and untreated eyes, despite using a higher lens power for myopia induction. Nonetheless, our study was not powered to detect such small differences, and the clinical significance of such differences is questionable.

Strengths and Limitations

A great strength of this study was its longitudinal design with frequent measurements, allowing us to closely track changes in ocular parameters over time. Another strength of this study was that the guinea pigs did not require general or topical anesthesia at any time, which would have precluded frequent measurements. Anesthesia is known to cause alterations in blood flow and intraocular pressure, both of which can influence recorded biometric data, giving strength to our findings.

A limitation of this study was the use of an anterior segment OCT to measure corneal curvature, which was designed for human use. In that application, the positioning of a person's head against a forehead rest allows standardization of the distance, which was not as easily controlled in imaging the eyes of our guinea pigs. Nonetheless, we were able to visualize a built-in image quality indicator for good alignment (the presence of a bright streak at the corneal apex) in the majority of images collected. In addition, we captured multiple images at each time point, with the same experienced examiners in order to minimize any measurement error.

We used the same lens power (-10 D) in all animals to induce myopia. However, there is a natural variation in the hyperopic defocus exposure of individual animals due to variations

in their baseline refractive errors, as well as in the magnitude of the positive tear lens that is created between the back surface of the contact lens and the anterior corneal surface. To ensure that the guinea pigs were experiencing hyperopic defocus, we confirmed the presence of "with motion" with retinoscopy while the guinea pigs were wearing their contact lenses. Nevertheless, in studies requiring consistency in the magnitude of imposed hyperopic defocus across subjects, the lens power would need to be adjusted on a per animal basis to account for the baseline differences in corneal curvature and the ocular refractive error status throughout the experimental period.

4.5 Summary and Conclusions

New Zealand pigmented guinea pigs developed a significant amount of myopia over the 24-day treatment period, with the majority of the growth occurring during the first week of treatment. We have established that the Lenstar is a reliable method to measure ocular biometry in guinea pigs and has the advantage of not requiring anesthesia for measurements. Rigid gas permeable contact lenses are well-tolerated in guinea pigs and can be used in place of spectacle-mounted lenses and diffusers for myopia induction as well as for testing of myopia treatments.

Chapter 5

Topical Atropine Prevents Myopia in Guinea Pigs

5.1 Introduction

Myopia is the most common ocular disorder in the world, and progressive childhood myopia is a major public health concern. East Asia currently bears the burden of this condition, with up to 96.5% of Korean military conscripts [80], and 94.9% of university students in China [185] reported to have myopia. However, the prevalence of myopia is increasing at an alarming rate worldwide, and it is predicted that half of the world population will be myopic by the year 2050, with as much as 10% being highly myopic [58, 157]. High myopia carries an increased risk of associated ocular pathologies, many of which are vision-threatening [44].

Myopia is not only increasing in prevalence, but the onset of myopia is occurring earlier in life. Historically, the prevalence of myopia is low in children younger than 6 years of age [56, 41, 52, 35, 88, 222, 228, 204, 208]. However, more recently, Fan et al. reported the prevalence of myopia in preschoolers in Hong Kong to have more than doubled over ten years [40]. A strong correlation between the intensity of education and myopia onset has been established and is being explored as a possible cause [118, 108, 117].

Topical ophthalmic atropine drops have been generally accepted as either an effective approved product or off-label treatment, depending on the country of practice. Atropine is a nonselective muscarinic antagonist that has been used for myopia control since the 1960s [6, 7, 14, 51]. As the only topical pharmacological treatment available, low-concentration topical atropine drops are now considered one of the most effective myopia controlling treatments. Topical atropine has a well-established safety record, it's low in cost, it's easy to use (when compared to contact lens treatments, especially in places where contact lens hygiene and sanitation are concerns), and it appears to be effective in controlling myopia progression [90, 30, 42, 27, 25].

Despite atropine's favorable profile, the exact mechanism of atropine's anti-myopia effect remains unresolved, and the dosing regimen for myopia control is not evidence-based [179].

As treatments to slow myopia progression are generally initiated in early childhood (between the ages of 6 to 12), with the necessary duration of treatment not readily predicted, it is important not to unnecessarily expose children to high doses of the drug. Therefore, it is important to establish the minimum effective dose of atropine needed to control myopia progression. There is also a large body of evidence from both experimental and clinical studies that demonstrate that long-term use of topical ophthalmic formulations can cause significant adverse ocular surface changes [5]. In particular, benzalkonium chloride (BAK), a commonly used preservative in eye drops, may have harmful consequences to the tear film, cornea, conjunctiva, and even trabecular meshwork [5]. Reduced exposure, for example, with less frequent dosing, is likely to lessen related adverse events, providing another argument for establishing a minimum effective dosing regimen for topical atropine as a myopia control therapy.

In the United States, low concentrations of topical atropine are not FDA-approved for any treatment. Instead, atropine is being compounded for off-label use in myopia control. Because compounded drugs are not subject to the same tight regulations as FDA-approved products, potential unintended variations in concentrations and pH may occur, and choices of preservatives may also vary between products. It is also not uncommon to hear of parents choosing to dilute atropine on their own, which is a very unsafe practice. The risks of adverse corneal effects and other toxicity issues over the treatment period for an individual patient are not insignificant and are also unpredictable, leading to many issues with topical atropine therapy being more widely adopted by practitioners.

A good starting point in our search for an optimal atropine dosing regimen for myopia control in humans is to establish an animal model for topical dosing of atropine. The ability of atropine to prevent the development of myopia is a fairly consistent finding in animal studies. However, important exceptions have been noted. Raviola and Wiesel found that chronic atropine administration prevented the development of form-deprivation myopia in stumptail Macaque monkeys [149], but did not in Rhesus monkeys. In addition, while intravitreal injection of atropine blocked myopia in tree shrews [111, 116] and chicks [184, 3, 107, 33, 167, 124, 166, 98, 203], topical atropine did not block myopia in either animal model [130, 183, 111]. Key findings from previous animal studies are summarized in Table 5.1.

To our knowledge, topical atropine has not been tested as a myopia control therapy in guinea pigs. The guinea pig is an increasingly popular model for myopia, in part due to its cooperative nature and large pupils, both of which make it amenable to ocular measurements [164]. For studies involving atropine in particular, guinea pigs share several relevant characteristics with human eyes. Muscarinic receptors are present throughout the ocular tissues, including the iris and ciliary body [144, 99]. Second, unlike chicks, another popular model, the ciliary muscle, which mediates accommodation, is made up of smooth muscle with muscarinic receptors in the guinea pig as in humans [135, 43]. These shared properties mean that in response to topical atropine therapy, guinea pigs may demonstrate changes that are translatable to those seen in human patients.

In the study described here, we tested the hypothesis that topical atropine sulfate can

Table 5.1: Summary of previous atropine research in animal models. **FDM** = Form Deprivation Myopia, **LIM** = Lens-Induced Myopia, **IV** = Intravitreal Injection, **IP** = Intraperitoneal Injection, **CGL** = Ciliary Ganglion Lesioning, **NV** = Near Viewing Restriction

Animal Model	**Myopia Stimulus**	**Treatment**	**Findings**	**Reference**
Chicks	FDM	Topical	no effect	Stone 1991 [183]
	FDM	Topical	no effect	McBrien 1993 [111]
	FDM	IV	protective	McBrien 1993 [111]
	FDM	IV	protective	Ashby 2007 [3]
	FDM	IV	protective	Luft 2003 [107]
	FDM	IV	protective	Diether 2007 [33]
	LIM	IV	protective	Diether 2007 [33]
	FDM	IP	no effect	Diether 2007 [33]
	LIM	IP	no effect	Diether 2007 [33]
	FDM	IV	protective	Schwahn 2000 [167]
	FDM	CGL	protective	Nickla 2012 [124]
	LIM	CGL	no effect	Nickla 2012 [124]
	LIM	IV	protective	Schmid 2004 [166]
	FDM	IV	protective	Schmid 2004 [166]
Rhesus macaques	FDM	Topical	protective	Tigges 1999 [189]
	lid suture	Topical	no effect	Raviola 1985 [149]
Stumptail macaques	lid suture	Topical	protective	Raviola 1985 [149]
Tree shrews	lid suture	IV	protective	McKanna 1981
	lid suture	Topical	no effect	Norton 1991
Guinea pigs	FDM	IV	protective	Zou 2014
Mice	LIM	Topical	protective	Jiang 2018
Old world monkeys *Macaca nemestrina*	NV	Topical	protective	Young 1965 [229]

inhibit progression of myopia in guinea pigs, measured both in terms of refractive error and axial elongation. In a pilot study, we also compared the effects of varied dosing strategies for topical atropine using the guinea pig.

5.2 Materials and Methods

Animals

Twenty-one pigmented English Short Hair guinea pigs (*Cavia porcellus*) were used in this study. They represent a line established from breeders obtained from the University of Auckland, New Zealand, and housed in breeding harems (1 male and a maximum of 3 females). These harems reside in oval-shaped breeding tubs in the animal facilities of the University of California, Berkeley. Pups were weaned at 7 days of age and transferred from the breeding facility to the Minor Hall research facility, where they were housed in transparent plastic wire-top cages, with room lighting set to a 12h/12h light/dark cycle. The animals were housed with their siblings (up to 3 guinea pigs per cage) until they reached a weight of 350 g, after which point they were housed as single sex pairs. The animals had free access to water and vitamin C-supplemented food, and received fresh fruit and vegetable enrichment three times per week. All experimental protocols were approved by the Animal Care and Use Committee at the University of California, Berkeley and met the ARVO resolution for care and use of laboratory animals.

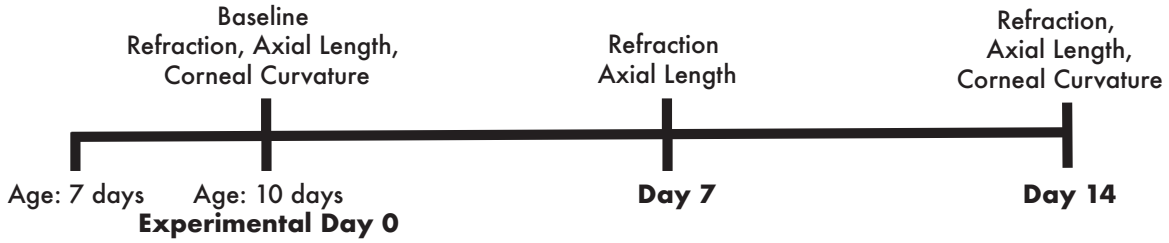

Figure 5.1: A schematic of the experimental period. Experiments began at 10 days of age for all guinea pigs and continued for 14 days. Refraction and axial length were measured at baseline and at the end of week 1 and week 2. Corneal curvature was measured at baseline and at the end of week 2.

Experimental Protocol

Guinea pigs were slowly adapted to being hand-held from 7 days of age to 10 days of age as described in Chapter 4. At 10 days of age, baseline measurements including optical biometry and refraction were undertaken. Beginning at 10 days of age, all guinea pigs wore -10 D rigid gas permeable contact lenses in one eye (the chosen eye was randomly selected) to induce myopia as also described in Chapter 4. The fellow eye served as an untreated control. A schematic of the experimental design of studies described in this chapter is shown in Figure 5.3.

Guinea pigs were randomly assigned to one of three groups:

- Daily atropine (n = 8)
- Weekly atropine (n = 5)
- No atropine, Placebo (n = 7)

Animals in the atropine groups received 1% topical atropine sulfate (Bausch and Lomb, Rochester, NY) in their contact lens-wearing eye. Animals in the placebo group received a drop of non-preserved artificial tears in their contact lens-wearing eye.

Contact Lenses

Contact lenses were manufactured according to the protocol described in Chapter 4. All treatments were monocular, with fellow untreated eyes serving as contralateral controls. Lenses were inserted into the selected eye immediately following the baseline measurements. The appropriateness of lens fits were confirmed with a sodium fluorescein evaluation.

The lenses were worn continuously and checked every hour for the first 5 days of treatment and then every 4 hours during the light cycle for the subsequent duration of the 14-day trial. Lenses were removed and replaced with a clean lens once per day. While not in use, lenses were soaked for 24 hours in a combination of Boston protein remover and Boston Simplus solution (Bauch and Lomb, Rochester, NY). Lenses were rinsed thoroughly with Opti-Free soft contact lens solution (Alcon, Fort Worth, TX) prior to re-insertion.

Measurements

All measurements on both the right and left eyes were performed by the same two examiners under the same lighting conditions. Guinea pigs were alert and hand-held for all measurements.

Refractive error and axial length measurements were made 3 times over the 14-day experimental period (Figure 5.1). Refractive errors were measured using streak retinoscopy following cycloplegia with 1% cyclopentolate, instilled 30 mins prior to measurement. Both the sphere and cylindrical components were recorded and spherical equivalent refractive errors derived.

Table 5.2: Measurement range and resolution for the Lenstar 900.

	Range	Resolution	Repeatability (1 SD)
Central Corneal Thickness	300-800um	1um	2.3um
Anterior Chamber Depth	1.5-6mm	0.01mm	0.04mm
Lens Thickness	0.5-6.5mm	0.01mm	0.08mm
Axial Length	14-32mm	0.01mm	0.035mm

The Lenstar optical biometer (Haag-Streit, Kniz, Switzerland) was used for biometry measurements. Each measurement comprised an average of at least five recordings. Measurements on individual animals were performed at the same time of day to prevent any possible confounding effects of circadian rhythms in eye growth [127]. The measurement range and resolution for the measured variables of the Lenstar 900 is listed in Table 5.2. The Lenstar outputs peaks representing the anterior and posterior corneal surface, the front of the lens, back of the lens, vitreous/retina interface, and retina/choroid interface. Optical axial length refers to the distance from the anterior surface of the cornea to the posterior surface of the retina (the retina/choroid interface).

Finally, corneal curvature data were obtained using custom MATLAB software (MathWorks, Natick, MA) applied to high resolution images from the Visante OCT (Zeiss Meditec, Dublin, CA) (See Chapter 4 for further details).

Data and Statistical Analysis

All data were recorded and visualized using Excel 2013 (Redmond, WA) and statistical analyses made use of Stata version 14 (College Station, TX). Mean values of results for treated eyes and/or interocular differences (treated eye - control eye) recorded over the 14-day treatment period are reported. For all three treatment groups, differences between treated and contralateral (fellow) eyes for all measured parameters were statistically compared using paired t-tests. Mean differences between treatment groups were compared using unpaired t-tests.

5.3 Results

Baseline parameters are summarized in Table 5.3 as means and standard deviations. There were no significant differences between the “treated” and fellow “untreated” eyes at baseline, although inter-ocular and inter-animal variability are evident in the associated standard error of the mean. Box plots representing the baseline values for central corneal thickness, anterior chamber depth, lens thickness, and axial length are also included to demonstrate this natural variability noted in the baseline parameters (Figure 5.2).

The changes for all measured ocular biometric parameters over the treatment period are summarized in Table 5.3. Significant treatment-induced changes are largely limited to axial

Table 5.3: Baseline Refractive Error and Biometric Parameters

			n	Mean (± SD)	p-value
Central Corneal Thickness (mm)	Control	Treated	7	221(27)	0.65
		Untreated	7	216(10)	
	Daily Atropine	Treated	8	211 (7.9)	0.47
		Untreated	8	213(5.4)	
	Weekly Atropine	Treated	5	197 (2.7)	0.47
		Untreated	5	201(5.4)	
Anterior Chamber Depth (mm)	Control	Treated	7	0.82(0.079)	0.35
		Untreated	7	0.78(0.060)	
	Daily Atropine	Treated	8	0.75 (0.087)	0.21
		Untreated	8	0.77(0.060)	
	Weekly Atropine	Treated	5	0.77 (0.045)	0.64
		Untreated	5	0.78(0.014)	
Lens Thickness (mm)	Control	Treated	7	3.3(0.10)	0.86
		Untreated	7	3.3(0.10)	
	Daily Atropine	Treated	8	3.3 (0.074)	0.29
		Untreated	8	3.3(0.099)	
	Weekly Atropine	Treated	5	3.2 (0.065)	0.75
		Untreated	5	3.2(0.070)	
Axial Length (mm)	Control	Treated	7	6.8(0.28)	0.82
		Untreated	7	6.8(0.22)	
	Daily Atropine	Treated	8	6.8 (0.20)	0.91
		Untreated	8	6.8(0.19)	
	Weekly Atropine	Treated	5	6.8 (0.11)	0.88
		Untreated	5	6.8(0.13)	

length changes, which are described first.

Change in axial length was the primary outcome measure used to evaluate and compare treatment efficacy. As expected, the contact lens-wearing eyes elongated significantly more than the contralateral control eyes over the 14-day experimental period. The contact lens-wearing eyes of the placebo group (no atropine) increased by an average of 0.33 mm (± 0.034) in week 1 and 0.57 mm (± 0.039) in week 2 compared to 0.24 mm (± 0.027) in week 1 and 0.42 mm (± 0.030) in week 2 in their fellow control eyes ($p = 0.04$ and 0.003, respectively). These values correspond to mean axial length differences of 0.11 mm and 0.18 mm in weeks 1 and 2 respectively.

In the group treated with daily atropine, there was no significant difference in the axial length change of treated eyes and their contralateral control eyes at either the week 1 or week 2 evaluations. The treated eyes increased by an average of 0.31mm (± 0.027) over week 1 and 0.49 mm (± 0.030) over week 2 compared to 0.24 mm ± 0.020) over week 1 and

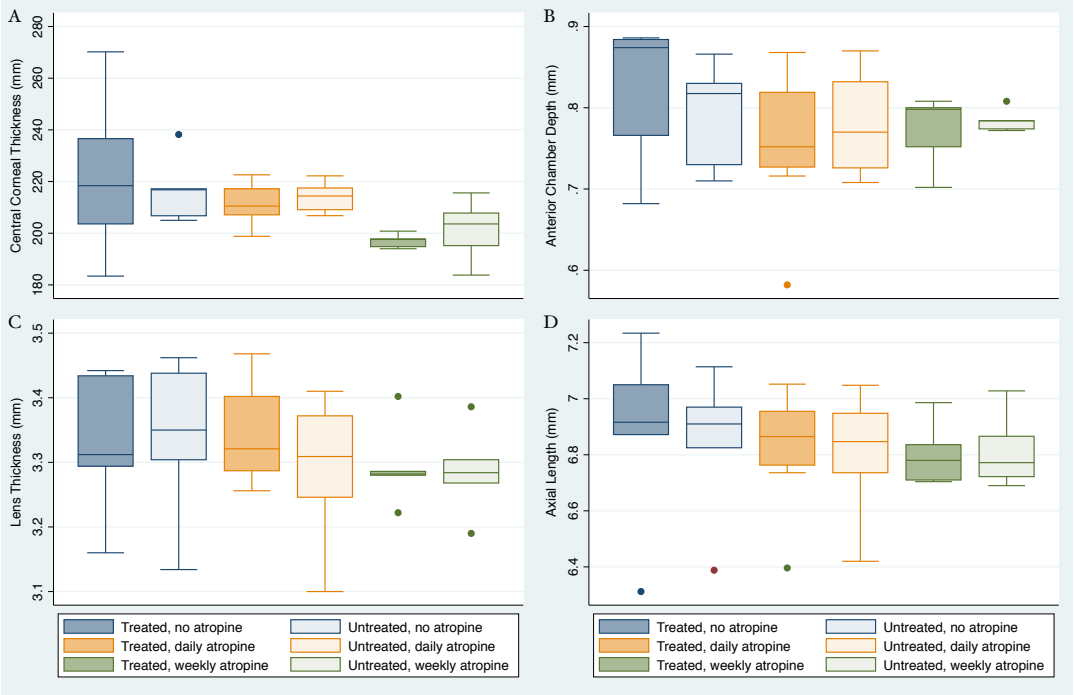

Figure 5.2: Baseline (A) central corneal thickness (CCT), (B) anterior chamber depth (AD), (C) lens thickness (LT), and (D) axial length for experimental animals.

0.44 mm (± 0.022) over week 2 (p = 0.06 and 0.19, respectively).

In contrast to the results for the above group, the group treated with atropine weekly experienced significant differences between treated eyes and their contralateral control eyes at both the week 1 and week 2 evaluations. The treated eyes increased by an average of 0.31 mm (± 0.031) over week 1 and 0.54 mm (± 0.022) over week 2 compared to 0.17 mm (± 0.017) over week 1 and 0.39 mm (± 0.016) over week 2 (p = 0.01 and 0.0005, respectively). The changes for all measured ocular biometric parameters are summarized in Table 5.4. Comparison of the axial length changes in the three treatment groups to one another over the treatment period revealed several important trends. As shown in Figure 5.3, guinea pigs treated with atropine daily showed significantly less axial elongation over the two-week treatment period compared to placebo-treated groups (p = 0.04). However, there was no significant difference between the daily atropine and weekly atropine groups (p = 0.34) or between the weekly atropine and placebo-treated groups (p = 0.21).

Analysis of changes in other ocular dimensions is limited to the 14-day treatment period. For the other anterior segment components, which includes the central corneal thickness, anterior chamber depth, and lens thickness, there were no statistically significant differences between the treated and control eyes for any component. The changes in these components for contact lens-wearing eyes and their fellows over the treatment period are represented in

Table 5.4: Ocular component changes over the treatment period

Biometry Value	Treatment Period	Change in Treated Eye Mean ± SEM	Change in Untreated Eye Mean ± SEM	p-value
Control Group (no atropine)				
CCT	Week 1	25.02 (12.1)	0.55 (6.4)	0.0137
	Week 2	26.00 (11.5)	-0.62 (7.6)	0.0049
AD	Week 1	0.0457 (0.019)	0.0615 (0.012)	0.4646
	Week 2	0.109 (0.020)	0.0955 (0.013)	0.0378
LT	Week 1	0.1205 (0.016)	0.1014 (0.019)	0.4439
	Week 2	0.2028 (0.014)	0.1814 (0.015)	0.0287
AL	Week 1	0.3331 (0.034)	0.2495 (0.027)	0.0485
	Week 2	0.5719 (0.039)	0.4215 (0.030)	0.003
Daily Atropine Group				
CCT	Week 1	45.77 (9.6)	8.47 (2.6)	0.0082
	Week 2	33.65 (8.6)	13.22 (4.1)	0.1063
AD	Week 1	0.0885 (0.0094)	0.0502 (0.016)	0.4968
	Week 2	0.1187 (0.018)	0.078 (0.012)	0.3397
LT	Week 1	0.0715 (0.017)	0.1205 (0.019)	0.9052
	Week 2	0.1667 (0.020)	0.2122 (0.016)	0.8866
AL	Week 1	0.3117 (0.027)	0.2412 (0.020)	0.0678
	Week 2	0.498 (0.030)	0.4497 (0.022)	0.1949
Weekly Atropine Group				
CCT	Week 1	27.32 (7.6)	-1.040 (6.4)	0.0413
	Week 2	40.64 (3.4)	3.399 (3.3)	0.0015
AD	Week 1	0.1012 (0.0089)	0.0548 (0.0064)	0.0601
	Week 2	0.1456 (0.017)	0.0784 (0.0075)	0.0152
LT	Week 1	0.828 (0.0190)	0.1092 (0.010)	0.3312
	Week 2	0.2144 (0.027)	0.2152 (0.019)	0.5964
AL	Week 1	0.3136 (0.031)	0.1743 (0.017)	0.0165
	Week 2	0.5403 (0.022)	0.392 (0.016)	0.0005

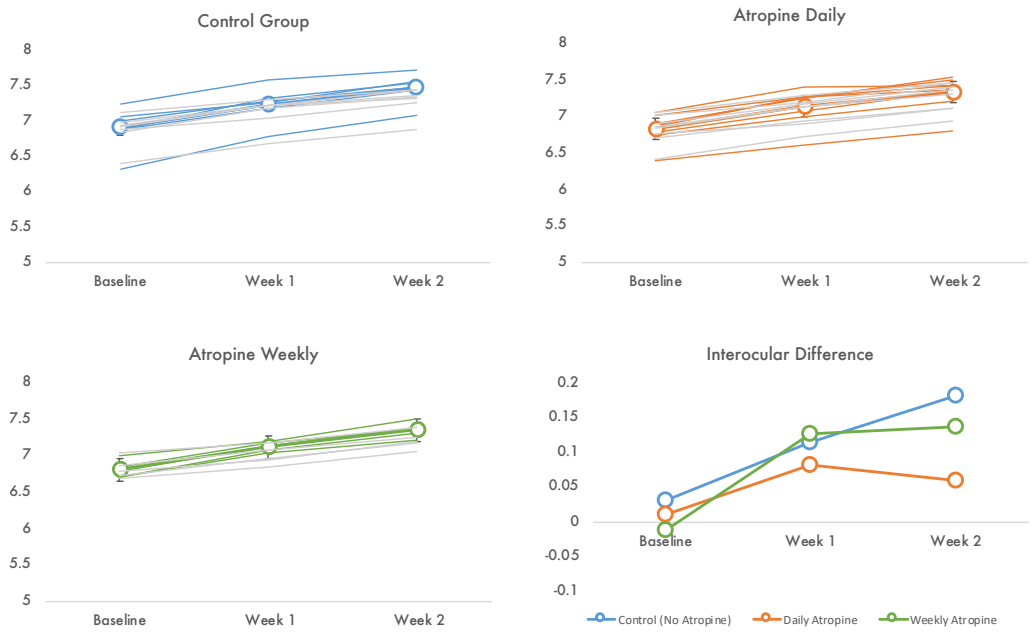

Figure 5.3: Change in axial length over the experimental period. Lines in panels A-C represent individual animals. Colored lines are treated eyes and grey lines are control eyes. The average for each treatment group is shown. Error bars represent the standard error of the mean. The interocular differences for each group are compared in panel D.

Figures 5.4, 5.5, and 5.6, respectively.

Refractive error trends mirrored those of the axial lengths with the control group (no atropine) showing a steady increase in myopia from +4.8 D (± 2.0) of hyperopia at baseline to +2.5 D (± 2.2) to -0.75 D (± 4.0) in weeks 1 and 2, respectively. The group treated with daily atropine showed less of a decline in hyperopia, from +4.36 D (± 0.55) at baseline to +1.94 D (± 2.8) to +2.11 D (± 2.0) in weeks 1 and 2. The difference in the mean refractive error for the treated eyes achieved a statistically significant and meaningful difference at week 2. The group treated with daily atropine was never statistically different from the control group and changed from +6.0 D (± 0.35) at baseline to +4.5 D (± 1.7) to -0.75 D (± 0.35) in weeks 1 and 2. The interocular difference over time is plotted in Figure 5.7.

5.4 Discussion

The experiment described in this chapter was designed to establish whether atropine is effective in slowing or stopping progression of contact lens-induced myopia in guinea pigs, and thus, whether guinea pigs can serve as an animal myopia model for atropine testing. We were also interested in learning how sensitive the myopia controlling effect of atropine was

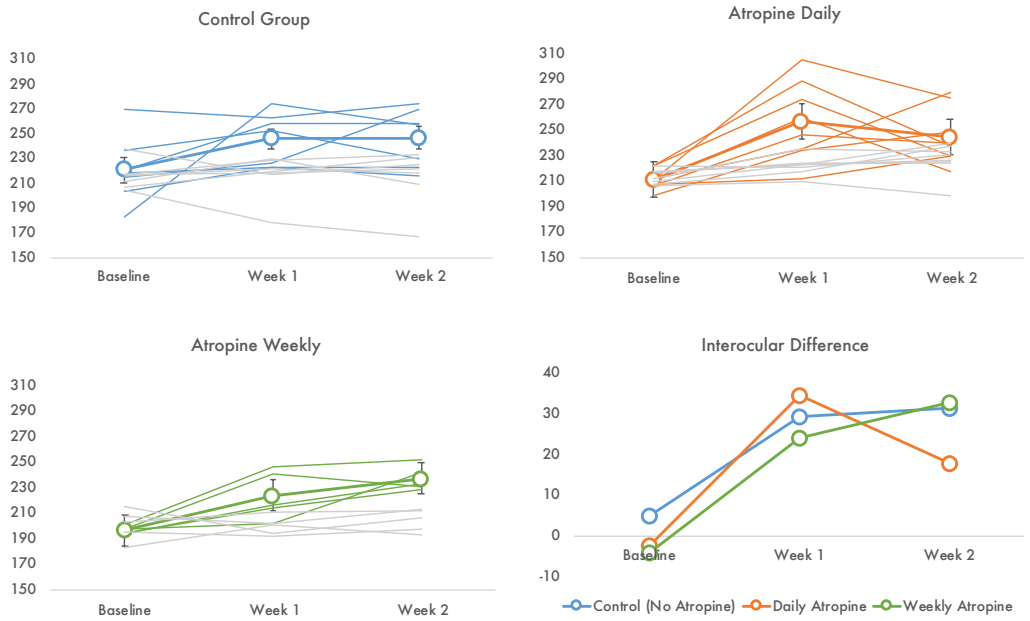

Figure 5.4: Change in central corneal thickness over the experimental period.

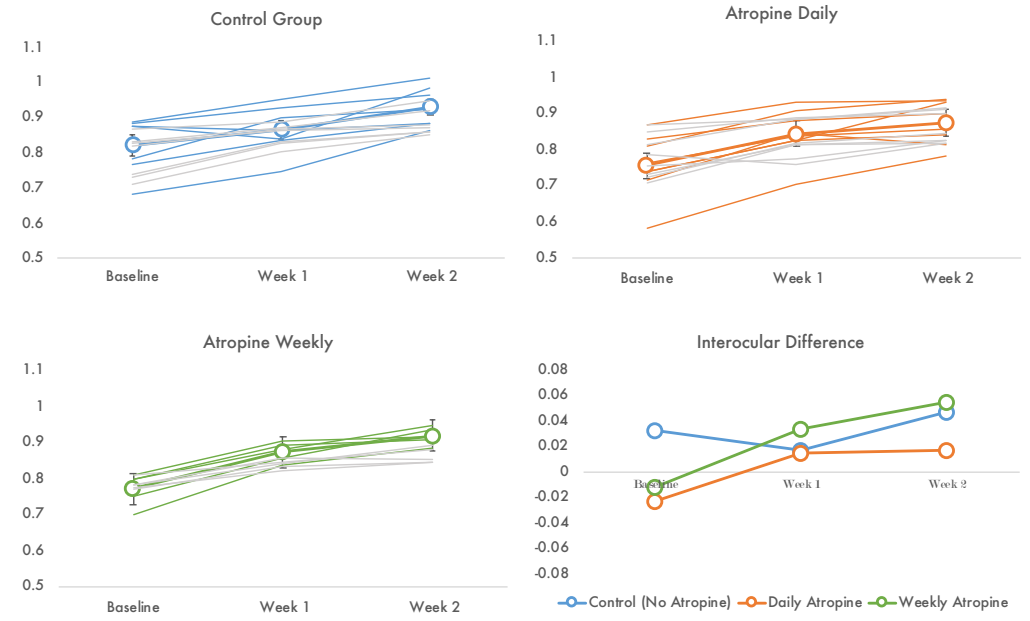

Figure 5.5: Change in anterior chamber depth over the experimental period.

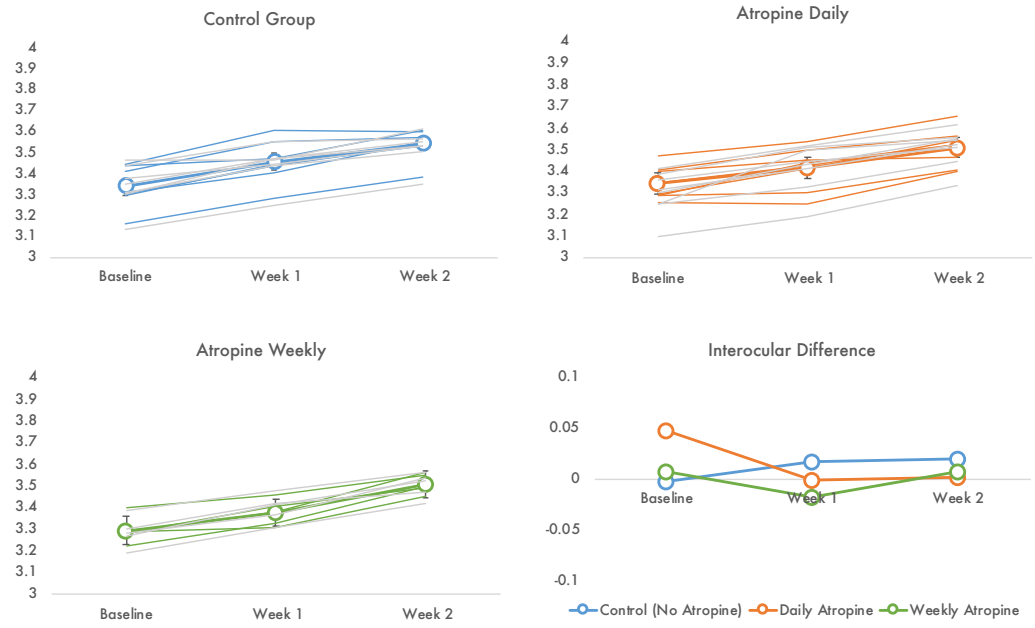

Figure 5.6: Change in lens thickness over the experimental period.

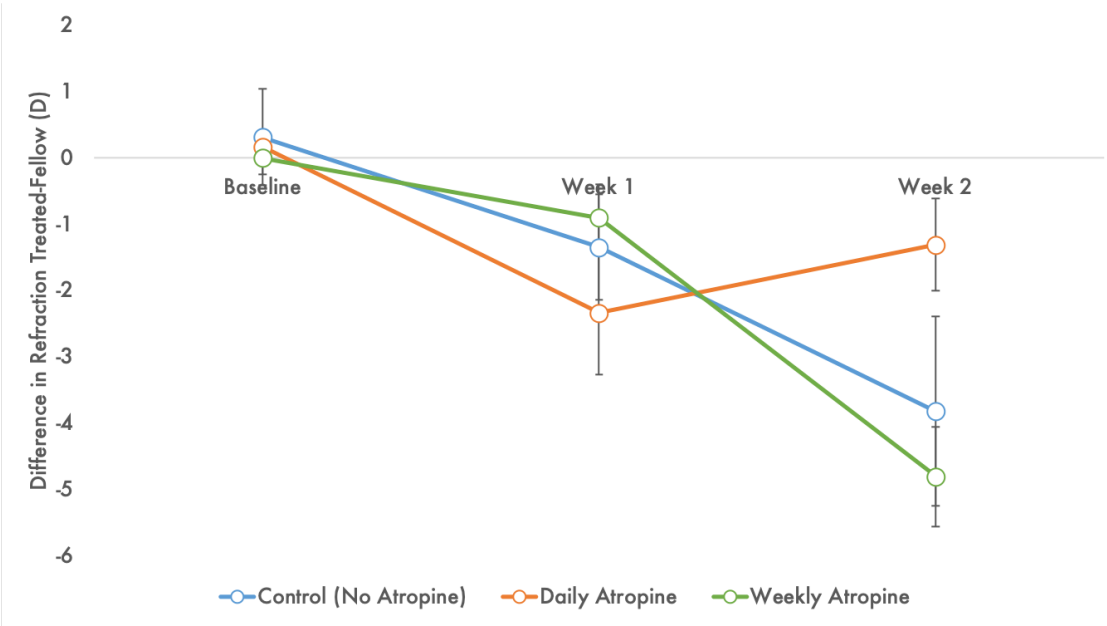

Figure 5.7: Mean interocular difference (treated eye - fellow eye) in refraction over the experimental period. There was a significantly lower refractive error (less myopic) in the group treated with atropine daily compared to both the weekly atropine and control groups ($p = 0.02$, unpaired t-test). Error bars represent the standard error of the mean.

to dosing frequency and specifically whether the treatment effect could be maintained with a reduced dosing frequency.

As noted in the introduction, atropine is a nonspecific, irreversible muscarinic antagonist [51], and while its efficacy as a myopia control treatment is well established, it remains unclear where and how atropine acts to inhibit myopia progression [163]. While initially it was thought that inhibition of accommodation was important, subsequent studies established that atropine can inhibit myopia without effects on accommodation, i.e., through a non-accommodative mechanism. The most convincing evidence is provided by a study of chickens in which atropine prevented myopia progression despite the fact that atropine has no effect on their accommodation, which is mediated by nicotinic receptors and striated muscle [111].

Daily administration of 1% topical atropine was successful in slowing myopia progression in guinea pigs, with a larger effect noted in the second week of treatment. While the finding that atropine almost completely prevented the development of lens-induced myopia is not new, this is the first study to demonstrate this effect in the guinea pig model using topical atropine sulfate solution.

Despite the fact that atropine is an irreversible muscarinic antagonist, and therefore is expected to have an enduring effect, weekly dosing of atropine did not have a significant effect on myopia progression in this study. However, daily atropine also appeared to attenuate eye growth more over the second week compared to the first week of treatment. The underlying mechanism is unclear, although it is possible that atropine accumulated in the eye over this period and bound to melanin, thereby creating a local intra-ocular depot from which it was subsequently released to maintain maximum receptor blockage, despite receptor turnover. This being the case, similar depot effects may be achieved with weekly dosing over a longer period. This possibility warrants investigation.

Other ocular dimensional changes showing interesting trends includes central corneal thickness, which increased significantly in eyes wearing the contact lenses (all treatment groups). This is also reported and discussed in Chapter 4. Most likely this reflects corneal edema in response to continuous contact lens wear [57], rather than an effect of the atropine or placebo drop treatment.

Although there is a trend of increasing anterior chamber depth over the experimental period, the differences did not reach statistical significance at any time point. Zhou et al. studied changes in ocular components of normal guinea pigs starting at birth until 11 weeks of age and found that anterior segment length decreased during the first week, increased in the following two weeks, and then remained constant [233]. Given that we followed guinea pigs beginning at nearly two weeks of age, our results appear consistent with their findings. However, as atropine is a potent cycloplegic agent, it was surprising that the change in anterior chamber depth was insignificant as the crystalline lens became thinner.

Previous studies have found a rapid increase in crystalline lens thickness during the first 5 weeks, followed by a slow increase until 11 weeks of age [233]. There was a small, although statistically insignificant decrease in lens thickness relative to that of the untreated eyes in both atropine dosing groups. In the case of the group receiving daily atropine, this effect likely reflects the cycloplegic action of atropine, resulting in a relative thinning of the lens.

As the anterior segment of the eye, including the iris and ciliary body, is also exposed to the highest drug levels with topical dosing, it is possible that even weekly dosing results in some cycloplegia and a relative thinning of the lens.

Strengths and Limitations

Two advantages of this study were its longitudinal design and the fact that measurements were taken in alert guinea pigs. Avoiding the use of general anesthesia also allowed for more regular tracking of ocular components over time. To our knowledge, this is the first study to evaluate the use of topical atropine in guinea pigs. Simultaneously tracking corneal curvature, axial length, and refractive errors allowed for comprehensive ocular profiles to be developed for our guinea pigs, against which treatment effects could be evaluated.

Another strength was the use of a contralateral (fellow-eye) control eye. It is still debated whether comparing absolute changes in eye growth or relative eye growth is more appropriate. This design allowed us to make both comparisons in our study.

A major limitation of this work was the relatively short treatment period. As normal eye growth appears to stabilize by 24 days of age, as reported in previous studies [233, 61], lens defocus-induced growth changes may be easier to detect with more prolonged treatments, which might also offer additional insights into the apparent increase in treatment efficacy with daily atropine after week 1.

Additionally, as previously described in Chapter 4, we used the same contact lens power (-10 D) for all guinea pigs. While we confirmed that all guinea pigs were experiencing hyperopic defocus through the contact lens using retinoscopy, the magnitude of the lens power experienced varied in individuals depending on the natural refractive state. The same issues were also encountered with our adaptation of the Lenstar for the guinea pigs, requiring manual adjustment of the locations for each peak.

Finally, while there have been many studies assessing atropine as an intervention for myopia control, the site and mechanism of action of this effect of atropine remains unresolved. Until consensus is reached on the ocular tissue to be targeted, advances in drug delivery cannot be fully exploited [213].

5.5 Summary and Future Directions

Topical atropine sulfate was effective in reducing progression of myopia in guinea pigs. In this study, there was not a statistically significant difference between the effects of daily atropine and weekly atropine on axial length, although qualitative differences were observed. These results suggest that the dosing frequency may be reduced from the daily dosing regimen that has become the standard for myopia control in clinical practice, with potential benefits in terms of efficacy, side effects, and economics. This study supports exploration of alternative dosing frequencies in humans.

Considering that no single intervention is likely to be totally effective in inhibiting myopia progression, it would be useful to test topical atropine in combination with other optical treatments as an approach to improve treatment efficacy. Given that contact lenses were successfully used to induce myopia in this study, the testing of a multifocal version of the same lens in combination with topical atropine is a potential future direction of study. In addition, given that atropine is the only potential prophylactic treatment for pre-myopic children (most optical treatments require that the child already has myopia), it would be interesting to investigate whether early atropine treatment can prevent or delay myopia onset.

Chapter 6

Summary and Future Directions

6.1 Dissertation Summary

The studies described in this dissertation more comprehensively characterize the optics of the guinea pig eye and present a novel contact lens method of inducing myopia in guinea pigs. As a background to these studies, Chapter 2 described the known characteristics of the guinea pig eye and compares its relevant anatomy and physiology with the human eye as relevant to ocular research. Experimental models have established that visual feedback is critical for normal eye growth and refractive error development. Studies involving the guinea pig, which has been utilized in vision research for more than 40 years, have helped to develop a more complete understanding of the mechanisms underlying emmetropization. Advantages of the guinea pig as a model for myopia studies include: (1) as a mammalian model, it shares key anatomical ocular features with humans; (2) from a research funding perspective, it is relatively inexpensive and also easy to handle; (3) it is amenable to advanced ophthalmic optical imaging, including retinal imaging. Among the main disadvantages are that genetic manipulation, which can be advantageous in mechanistic studies, is limited and often speculative, especially when compared to the mouse. Additionally, vision is a relatively under-developed sense compared to smell or hearing when compared to primates including humans.

Chapter 3 presented data on the optical aberrations of guinea pig eyes. While visual acuity is much poorer in the guinea pig compared to humans, high order aberrations proved not to be a major source of optical quality degradation. Specifically, second order aberrations tend to have more deleterious effects on vision compared to higher order aberrations. The comparative data derived from spatial versus angular analyses of optical quality offer an additional new perspective on how optical aberrations impact vision. Future studies may involve comparing these different species used in models of eye growth regulation, to compare the quality of their eyes' optics in the context of their visual needs and neural resolution limits.

Chapter 4 described a novel method for inducing myopia in the guinea pig using rigid gas

permeable contact lenses. Rigid gas permeable contact lenses proved to be well-tolerated by young guinea pigs and represent a potentially more practical alternative to velcro-mounted lenses for myopia induction, for use in testing myopia treatments. The New Zealand strain of pigmented guinea pigs used in this study developed a significant amount of myopia over a 24-day treatment period, with the majority of the increased axial growth occurring during the first week of treatment. This study also established that the Lenstar to be a reliable method for measuring ocular dimensions in guinea pigs, with the advantage of not requiring general or topical anesthesia for measurements.

Lastly, Chapter 5 established that myopic guinea pigs respond to atropine therapy similarly to human myopes. Specifically, topical atropine was effective in reducing progression of myopia in guinea pigs. This study also compared the efficacy of daily versus weekly atropine. Their myopia control effects (when comparing axial lengths) were not significantly different, raising the possibility that a less frequent dosing schedule than daily dosing, as is the current clinical practice, might also be effective in humans. This result warrants follow-up, with alternate dosing frequency studies in humans.

Considering that no single intervention has proved to-date to be effective in totally inhibiting myopia progression, it would be useful to test topical atropine in combination with other treatments as a potential avenue for improving treatment efficacy. The studies reported in this dissertation would support the use of the guinea pig in such studies. The guinea pig would also seem a suitable model to investigate whether prophylactic intervention with topical atropine can prevent or delay myopia onset.

Appendix A

A Randomized Crossover Trial Comparing Spherical CRT Lenses to Dual Axis CRT Lenses

A.1 Introduction

Myopia is a leading cause of preventable visual impairment and has reached epidemic proportions in many parts of the world [9, 71, 136, 58]. The prevalence of myopia continues to increase and is projected to affect over 50% of the world population by the year 2050 [58]. In addition to the economic burden this carries, as the degree of myopia increases, the risk of sight-threatening complications increases at an exponential rate, making myopia a serious public health concern [44]. Therefore, efforts are shifting from simply correcting the refractive error to controlling the disease in its early stages with the aim of reducing the risks of blinding complications. Treatment options for slowing myopia progression include daily use of multifocal contact lenses and overnight use of Orthokeratology (ortho-k) lenses. As a myopia control treatment, ortho-k lenses are being increasingly used in pediatric eye care globally, given their consistent efficacy in reducing myopia progression compared to single vision spectacles and contact lenses [21, 22, 28, 29, 82, 162, 161, 198, 172], the unique ability to provide complete freedom from other optical corrections during the day, as well as their low rate of adverse events [102]. In general, these lenses are well-accepted by parents and children and have been especially appealing for younger children as parents can assist with lens insertion, removal, and cleaning, and not have to worry about the use of contact lenses at school without sufficient (or proper) monitoring.

Ortho-k lenses are reverse-geometry rigid gas-permeable lenses that are usually worn overnight and induce a temporary, reversible corneal reshaping for the correction of myopia. The lenses cause a flattening of the central cornea, which temporarily corrects myopia, with a corresponding steepening of the mid-peripheral cornea. Like any gas-permeable contact lens, the successful fitting of an ortho-k lens depends on mimicking the shape of the peripheral

LENS PARAMETERS AVAILABLE (See drawing)

Overall Diameter (D)	9.5 to 12.0 mm
Central Base Curve Radius	6.50 to 10.50 mm
Optical Zone Semi Chord (OZ)	2.50 to 3.50 mm
Return Zone Width (w)	0.75 to 1.5 mm
Return Zone Depth (Δ)	to 1.0 mm
Landing Zone Radius	to infinity
Landing Zone Angle (ϕ)	-25° to –50°
Landing Zone Width (LZW)	0.5 to 2.75 mm
Edge Terminus Width (P)	0.04 mm to LZW
Dioptric Powers	-2.00 to +2.00 Diopters

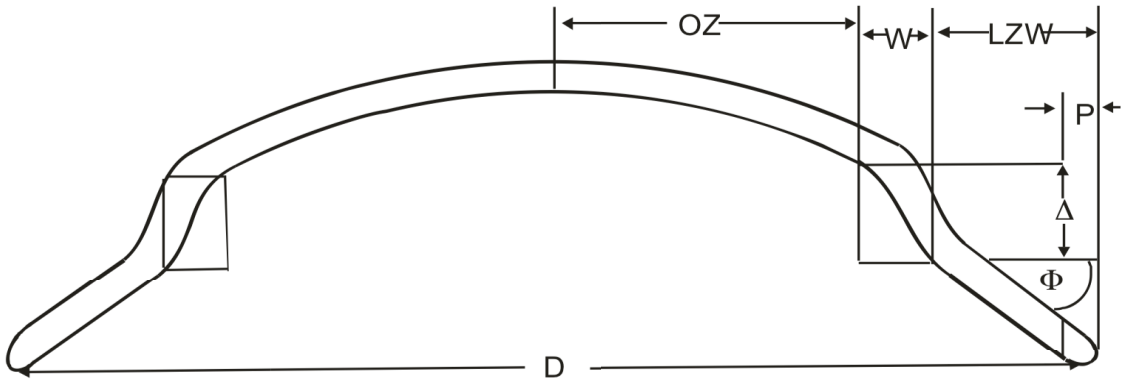

Figure A.1: CRT lens parameters available, according to the manufacturers fitting guide. Dual Axis lenses may have two different Return Zone Depths, two different Landing Zone Angles, or both.

cornea. This promotes lens comfort and reduces mechanical effects of the lens on the cornea that may lead to adverse events. The standard Corneal Refractive Therapy (CRT) design has a 6mm treatment zone surrounded by a 1mm return zone width. The landing zone makes up the remaining 1.25mm for the standard lens design with a 10.5mm total diameter, as shown in Figure A.1. The elevation difference in the corneal periphery plays a critical role in lens weight-bearing dynamics in the landing zone. Research has shown that peripheral corneal elevation differences are not necessarily correlated with central corneal astigmatism [150]. Even for patients with minimal corneal toricity in the central 8mm region, there may be elevation differences in the corneal periphery, making it impossible for the lens to reach the cornea's circumference in the landing zone. This creates an uneven weight distribution between the flat and steep meridians and may lead to poor centration and reduced efficacy.

Paragon CRT Dual Axis (DA) lenses allow for independent modulation of the sagittal depth of the return zone depth (RZD), and landing zone angle (LZA), while keeping the base curve constant, providing the practitioner the opportunity to compensate for peripheral corneal elevation differences of an eye. For example, a typical CRT lens may have the parameters BC 8.6mm RZD 550um LZA -33deg. A DA lens could have a deeper return

zone depth (e.g., 8.6mm RZD 550um/600um LZA -33deg), a steeper landing zone angle (e.g., 8.6mm RZD 550um LZA -33deg/-34 deg) or both (e.g., 8.6mm RZD 550um/600um LZA -33deg/-34deg) in the orthogonal meridian compared to the flatter meridian. These lenses are now suggested as the initial lenses for patients who (1) have a moderate amount of corneal toricity, especially if the corneal toricity extends beyond the central 8mm based on the baseline axial power map, or (2) have a more dramatic elevation difference (greater than 30um difference measured by placido-based topographers) in the corneal periphery based on the baseline elevation map.

The author's experiences from the UC Berkeley Myopia Control Clinic have demonstrated that, for some patients with little to no corneal toricity, the trialed CRT spherical lenses frequently present with superior decentration. This is likely due to the lower specific gravity of Paragon HDS 100 material compared to other commonly used materials for overnight ortho-k such as Boston XO or Equalens II and the tangent landing design, which results in stronger upper lid traction of the lenses. In those cases, the design of the CRT DA lenses was advantageous because it allowed for improved centration and created a stronger compressing force, resulting in improved treatment effect. In the Myopia Control Clinic at UC Berkeley, the DA design is now used more frequently than the standard design due to the faster and more stable treatment observed clinically. The present study prospectively aims to confirm these findings using the DA design compared to standard CRT lenses on patients with minimal with-the-rule corneal astigmatism and minimal elevation differences.

A.2 Materials and Methods

This study was a subject-masked, prospective randomized crossover study. The study was conducted in accordance with the tenets of the Declaration of Helsinki and received approval from the Biomedical Institutional Review Board at the University of California at Berkeley. Informed written consent was obtained from each subject.

Twenty-four subjects who met the eligibility criteria were enrolled between December 2016 and February 2017. Eligibility criteria included (1) age between 12-35 years at the initial visit; (2) myopia up to -6.00 D with less than 0.75 D refractive with-the-rule astigmatism, as measured by autorefraction; (3) best-corrected visual acuity better than or equal to 20/20 in each eye; (4) no manifest binocular vision issues; (5) no ocular conditions that would contraindicate contact lens wear; (6) no prior use of Orthokeratology lenses. The study took place at the UC Berkeley School of Optometry, with subjects recruited from the School of Optometry and the surrounding community.

The study was a two-stage crossover trial. Each subject was instructed to wear a DA CRT lens in one eye and a spherical CRT lens in the other eye for one week, the eye chosen for each lens being random. Subjects were masked to their treatment. All subjects underwent ocular exminations at baseline, after one day, and after one week. These examinations included a slit lamp examination, manifest refraction, autorefraction, pupillometry, and corneal topography. Follow-up visits were scheduled to fall between 7AM and 12PM to minimize confounding from

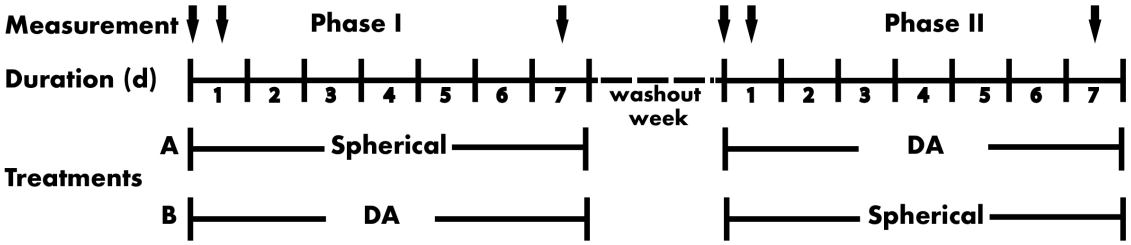

Figure A.2: Schematic of the trial design. Subjects were randomly assigned to wear either the spherical lens or the DA lens in their right or left eye (Phase 1). After a washout period of at least one week, they were switched to the alternate lens in each eye (Phase 2). Measurements were acquired at baseline, one day follow-up, and one week follow-up, as indicated by the arrowheads.

daytime regression of treatment [123]. Autorefraction was performed with the Grand Seiko WR-5100K binocular autorefractor/keratometer (Grand Seiko Co., Fukuyama, Hiroshima, Japan), pupil sizes were measured and recorded using the NeurOptics VIP-300 pupillometer (NeurOptics, Irvine, CA), and corneal topography was measured using the Medmont E300 Corneal topographer (Medmont International, Nunawading, Australia). After one week of lens wear, subjects underwent a washout period of at least one week (up to two weeks) to ensure a complete recovery of the corneal shape back to baseline, at which point they were switched to the alternate lens design in each eye. Follow ups occurred at one day and one week after lens wear for each set of lenses, as indicated by the arrowheads in Figure A.2.

Paragon CRT lenses, or CRT, and Paragon CRT Dual Axis lenses, or DA CRT, (Paragon Vision Sciences, Mesa, AZ) were used with the standard diameter of 10.5mm. Lens parameters were selected based on the subject's flat K reading as measured by the Grand-Seiko open field autorefractor and the Paragon slide rule calculator, per the manufacturers fitting guide. The DA CRT lenses selected were identical to the sphere, with a 50um difference in the return zone depth. For example, if the slide rule predicted the lens 86-525-33, then the DA lens that was selected was 86-525/575-33. The initial fitting was considered successful if visual acuity was within 1 line of the subjects habitual visual correction with the lens on, the lenses were reasonably centered over the pupil, and a bulls eye fluorescein pattern was observed. In addition, we confirmed that no remarkable corneal and/or conjunctival findings were noted at the one day follow-up. Complementary solutions (Boston SIMPLUS multi-action solution, Bausch and Lomb, Rochester, NY; Boston Rewetting Drops, Bausch and Lomb) and a DMV plunger (for lens removal) were prescribed to all subjects. Subjects were instructed to insert the lenses 20-30 mins before sleeping and to get a minimum of 7 hours of sleep each night.

Topographical analysis was performed using the tangential power difference maps generated by the Medmont software. An example image from this tangential difference map is shown in Figure A.3. Two trained observers marked and measured five locations: the center of the treatment zone and the points at which the highest power was induced in the

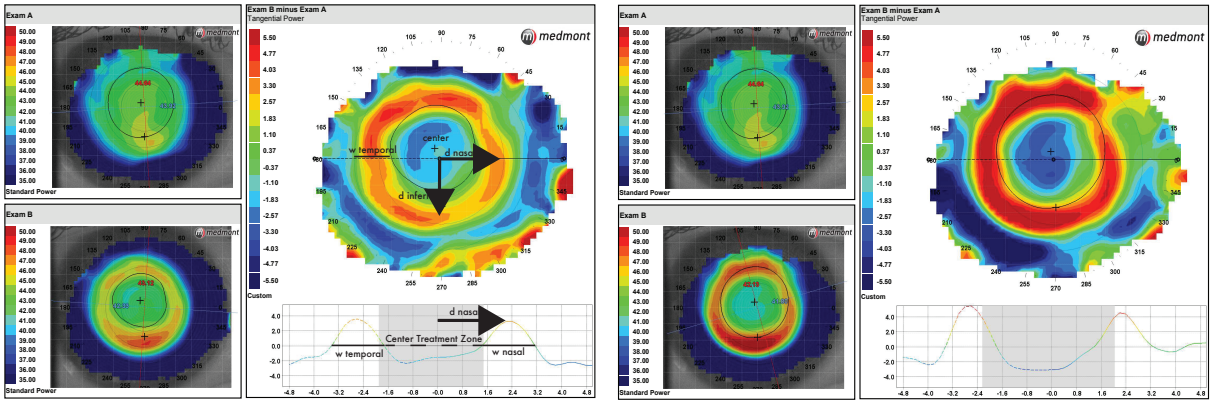

Figure A.3: Examples from one subjects right eye is shown. This subject wore the standard (sphere) lens in the right eye for phase 2 (left) and the dual axis lens in the same eye for phase 1 (right). The tangential difference map is annotated to demonstrate the analysis points. Looking at the magnitude of the induced power in the periphery in the horizontal meridian, the temporal side reaches a peak value of 5.56 D for the DA lens and 3.67 D for the spherical lens.

paracentral steepening ring at the nasal (n), temporal (t), superior (s), and inferior (i) locations, as indicated in Figure 3. The center point was used to quantify the magnitude and direction of the lens decentration (measured in mm) with overnight wear. The location to the steepest point (measured in mm) and the magnitude of the induced power (measured in diopters) were recorded for each subject. Then, the width of the paracentral steepening ring was recorded in the same four locations by measuring the distance (in mm) between the points in which there was no change to the corneal power (induced power = 0 D). One of the advantages of using a crossover trial design is that the participant's subjective impression of their experience with each lens type could be compared. Participants were asked to describe their visual experience and comfort for each pair of lenses worn. The survey used is available in Appendix B.

Statistical Analysis

Our minimum sample size was calculated to be 16 (alpha criterion 0.05, beta criterion 0.20) for the primary outcome measure of detecting a 1.00D difference in induced corneal power in the paracentral steepening region. Differences in power in the central and mid-peripheral points were compared for the two lenses using a paired t-test. There were no significant differences between the right and left eyes, therefore only data from the right eyes were used for analysis and expressed as mean standard deviation unless otherwise noted. Statistical analyses were performed using Stata (College Station, Texas) version 14.

Table A.1: Participant Characteristics

	Subjects that completed trial (n = 21)	Enrolled subjects (n = 24)
Male/Female (n)	3/18	4/20
Age (years)	25.7 (±2.7)	25.7 (±2.6)
Refractive Error (D) Sphere	-3.60 (±1.40)	-3.65 (±1.40)
Refractive Error (D) Cyl	-0.15 (±0.265)	-0.17 (±0.26)
Flat K (D)	43.3 (±1.34)	43.3 (±1.28)
Steep K (D)	44.3 (±1.45)	44.3 (±1.41)
Elevation Difference (e value) Flat	0.58 (±0.14)	0.57 (±0.14)
Elevation Difference (e value) Steep	0.40 (±0.18)	0.38 (±0.18)

A.3 Results

Demographic Characteristics of Subjects

Participant characteristics for the enrolled subjects are presented in Table A.1. Of the 24 subjects recruited for this study, 20 (80%) were female and 18 (72%) were Asian, with an average age of 25.7 years (± 2.56). The subjects had on average -3.65 D (± 1.4) myopia with -0.17 D (± 0.26) with-the-rule astigmatism and e-values of 0.57 (± 0.14) for the flat meridian and 0.38 (± 0.18) for the steep meridian. Pupil sizes were 5.42 mm (± 0.77) under mesopic conditions (typical laboratory lighting) and 3.15 mm (± 0.53) under photopic conditions. Two subjects did not complete the study. One subject had persistent hyperemia after lens wear with no other associated ocular findings and discontinued due to cosmetic reasons. The second had persistent temporal decentration of both lenses, leading to unacceptable visual performance. One subject completed the study but was excluded from analysis because of his cornea's poor response to treatment, and it was subsequently discovered that the subject had a systemic collagen disorder. Three additional subjects were excluded from topography analysis because the images collected could not provide all of the data that was necessary for this study (e.g., width of mid-peripheral steepening ring in one meridian). Appendix C shows the topography images obtained at the one week follow-up for each lens worn. Those excluded from analysis are indicated. There were no statistically or clinically meaningful differences between those initially enrolled (n = 24) and those who completed the study and whose data were analyzed (n = 21).

Refractive Correction

Initial lens parameters were selected for subjects based on the slide rule tool provided by the manufacturer. For all but one subject, the initial lenses selected were dispensed for the duration of the study. One subject required a base curve adjustment for the right eye

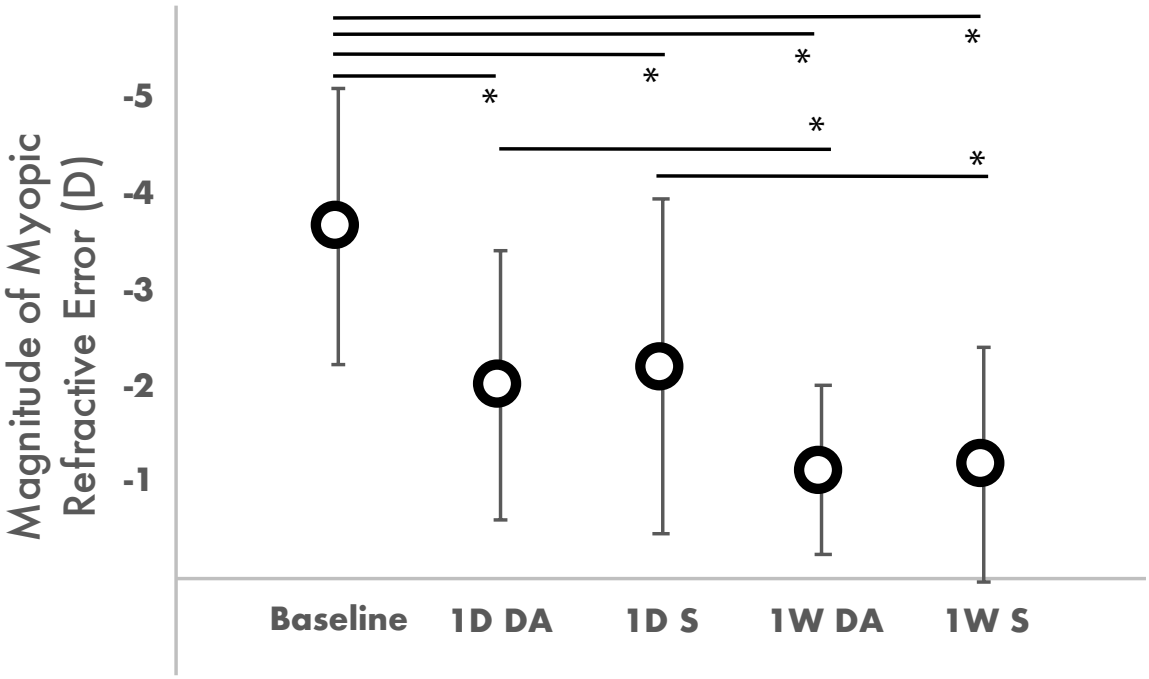

Figure A.4: The average spherical equivalent refractive error for the subjects' right eyes, as measured by autorefraction, are plotted at baseline, one day and one week follow-up for DA lenses (1D DA and 1W DA), and spherical lenses (1D S and 1W S), respectively. Error bars represent 1 standard deviation. Asterisks indicate significance $P<0.05$.

because they did not achieve a plus over-refraction through the initial lens selected. In that case, the base curve was adjusted for both the spherical lens as well as the dual axis lens.

For those subjects who completed the study, who averaged -3.60 D (± 1.40) myopia at baseline, all experienced a significant reduction of myopia both at one day and one week, as shown in Figure A.4. Subjects experienced a small but statistically insignificant increased treatment effect while wearing the DA design both at one day (post-treatment autorefraction of -1.58 D (± 1.66) vs. -1.66 D (± 1.60), respectively, p = 0.68) and at one week (-0.63 D ± 0.82 vs. -0.80 D ± 0.86, respectively, p = 0.061). Comparing the percent change in myopia reduction, the eyes wearing DA design experienced a 51% (± 27%) reduction in myopia vs a 46% (± 33%) reduction with spherical CRT treatment at one day. At one week, the two groups were similar, with a 72% reduction (±16% and ± 27% for DA and spherical CRT treatment, respectively) in myopia for both lens types, measured by non-cycloplegic autorefraction.

Visual performance was similar between the two groups throughout the study as shown in Figure A.5. Unaided visual acuity was similar between the two types of lenses both at the one day follow-up visit (LogMAR 0.41 ± 0.35 vs 0.43 ± 0.39 for DA and spherical CRT,

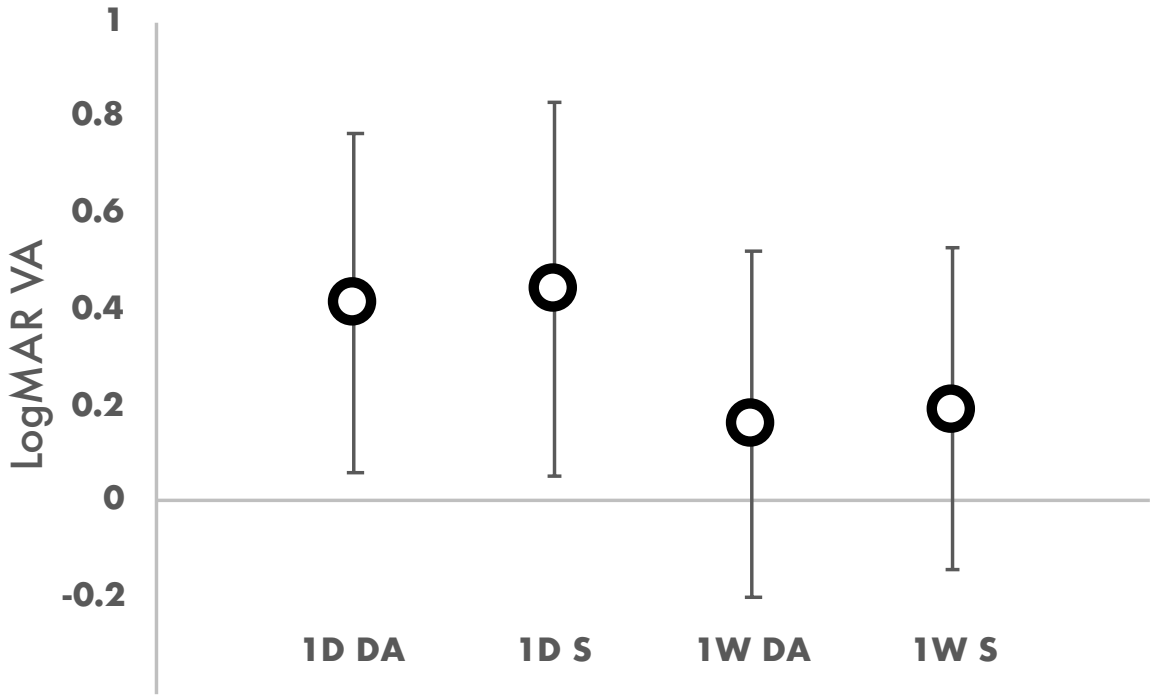

Figure A.5: The average unaided LogMAR visual acuity for the subjects' right eyes is shown for each lens type at one day and one week follow-up for DA lenses (1D DA and 1W DA), and spherical lenses (1D S and 1W S) respectively. Error bars represent one standard deviation.

respectively, p = 0.28) and the one week follow-up visit (LogMAR 0.16 ± 0.36 vs 0.19 ± 0.33 for DA and spherical CRT respectively, p = 0.57).

Topographical Analysis

In this cohort, the average elevation difference between the horizontal and vertical meridians at baseline was 16.5 (±2.3) at the 8mm chord. Both the DA design and the spherical CRT lenses centered well with less than 1mm decentration for both lens designs. The width of the center treatment zone was not significantly different between the two lens designs, as listed in Table A.2. The magnitude of paracentral corneal steepening induced was significantly different between the spherical and DA lenses in the superior, inferior, and temporal locations, with the DA lenses inducing more paracentral steepening, also shown in Table A.2 and Figure A.6. The location of this peak power, measured from the corneal apex to the point with the most induced curvature change (d in Figure A.3), was not different between the two lens designs. The width of the paracentral steepening ring was similar across each region for each lens type.

Table A.2: Differences between DA lenses and spherical CRT lenses. Analysis was conducted for the distance to the steepest point, the width of the induced peripheral steepening ring, the magnitude of induced corneal refractive change, and the width of the treated area. Only the magnitude of the induced paracentral corneal steepening carried a difference between the two lens designs.

	DA	Sphere	p-value
Distance to steepest point (d) measured in mm			
Temporal	2.93 (±0.08)	2.85 (±0.08)	0.15
Nasal	2.42 (±0.07)	2.33 (±0.06)	0.18
Superior	2.57 (±0.07)	2.56 (±0.06)	0.77
Inferior	2.43 (±0.12)	2.35 (±0.10)	0.19
Width of peripheral steepening ring (w) measured in mm			
Temporal	1.91 (±0.089)	1.93 (±0.11)	0.80
Nasal	1.73 (±0.05)	1.74 (±0.058)	0.68
Superior	1.66 (±0.071)	1.66 (±0.088)	1.0
Inferior	1.79 (±0.18)	1.51 (±0.098)	0.21
Magnitude of induced corneal power change measured in Diopters (D)			
Temporal	**4.73** (±0.50)	**3.80** (±0.40)	**0.0014**
Nasal	**4.93** (±0.44)	**4.22** (±0.46)	**0.019**
Superior	5.70 (±0.59)	4.74 (±0.43)	0.15
Inferior	**5.32** (±0.68)	**3.38** (±0.44)	**0.0005**
Average	**5.17** (±0.43)	**4.03** (±0.34)	0.0035
Treatment zone width measured in mm			
Horizontal	3.32 (±0.12)	3.27 (±0.13)	0.61
Vertical	3.09 (±0.17)	3.08 (±0.14)	0.91

Symptoms and Adverse Events

No serious adverse events occurred during the course of the study. Adverse events that were observed included grade 1 central staining (two subjects), grade 1 peripheral or mid-peripheral staining (two subjects), and hyperemia (one subject). There was no observed correlation with lens type. Of note, there was no increase in lens binding with DA lenses compared to the spherical CRT lenses, however, two participants reported slightly increased difficulty removing the DA lenses in the morning. Subjects reported symptoms of lens awareness/discomfort, blur, variable vision, dryness/scratchiness, haloes, and ghosting, all of which were worse after the first day than at the one week follow-up. Additionally, all symptoms reduced in frequency and severity with the second pair of lenses, regardless of which lenses were initially assigned to the subject.

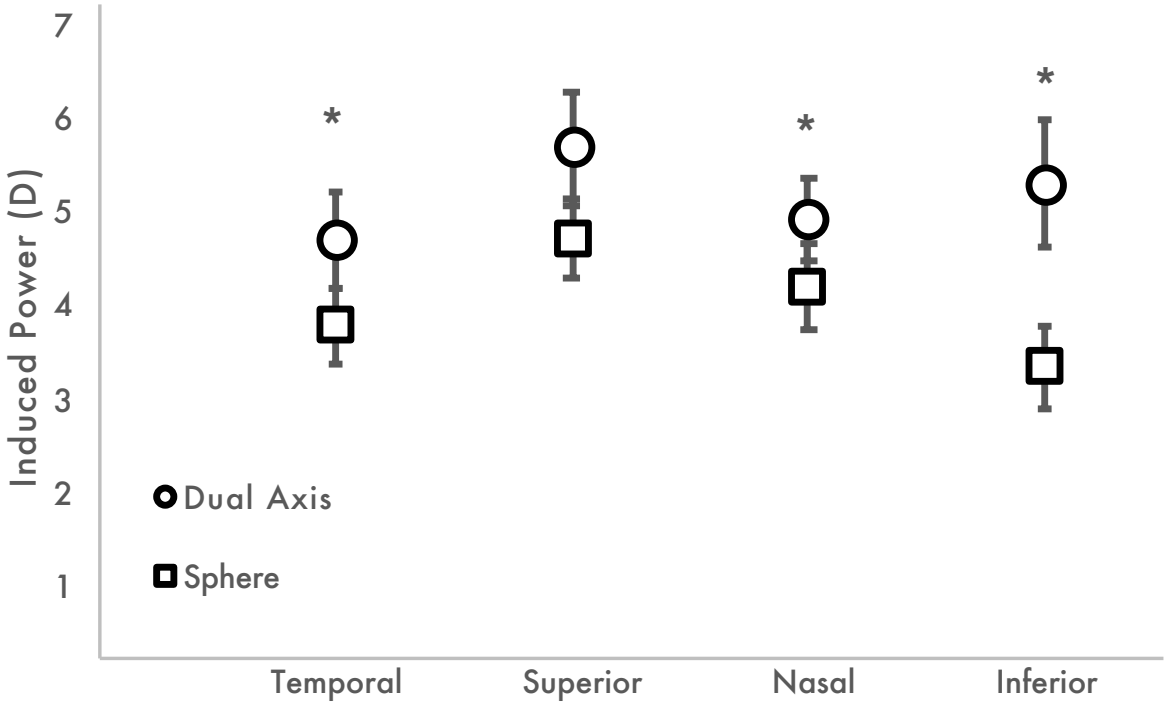

Figure A.6: The magnitude of the induced paracentral corneal steepening is shown in each of the four quadrants measured. Error bars indicate one standard deviation. Asterisks indicate statistical significance ($P<0.05$). The DA lenses induced more paracentral steepening in all quadrants and was significantly different from the spherical lenses in three of the four quadrants.

A.4 Discussion

The shape of a regular cornea has traditionally been defined by K readings and eccentricity, both of which are critical indices for the depiction of corneal shape in the central region. However, more recent studies have demonstrated that peripheral corneal shape, which plays a critical role in the fitting of larger diameter overnight ortho-k lenses, may not be reliably reflected by central corneal indices. Moreover, corneal elevation analysis, which provides additional information on the asymmetry of peripheral cornea, is a relatively new technique that awaits further validation among various topographers with different imaging technologies and computing algorithms. As a result, the initial design and parameter selection of ortho-k lenses based on corneal astigmatism and/or corneal elevation differences may not be able to provide an ideal fit in all patients.

The purpose of this study was to investigate differences in Paragon CRT DA lenses compared to spherical CRT lenses on patients with minimal corneal astigmatism. These participants would not necessarily be initially considered as candidates for DA lens design in routine clinical practice. Our clinical experience using these lenses lead us to believe that

the DA lens design could improve initial centration of the lenses and lead to faster, better correction of myopia by being a more precise match to the natural corneal curvature.

The decrease in central corneal power and increase in paracentral corneal power found in this study is consistent with previous reports of central corneal flattening and paracentral corneal steepening with ortho-k lens wear. Previous studies have found that ortho-k induced asymmetric power changes along different areas of the cornea [83]. Because the cornea is rarely symmetric, wearing a rotationally thing will result in (1) asymmetric weight distribution, (2) less efficacious distribution of of the hydraulic pressure in post-lens tear compartment, and (3) asymmetric refractive changes. We did observe this asymmetry in our spherical CRT lens-wearing eyes, with induced corneal steepening measuring 4.74D ($\pm$ 0.43), 4.22D ($\pm$ 0.46), 3.38D ($\pm$ 0.44), and 3.80D ($\pm$ 0.40) in the superior, nasal, inferior, and temporal meridians, respectively. This asymmetric steepening is less dramatic for the DA lenses worn in this study: 5.70D ($\pm$ 0.59), 4.93D ($\pm$ 0.44), 5.32D ($\pm$ 0.68), and 4.73D ($\pm$ 0.50) in the superior, nasal, inferior, and temporal meridians, respectively, which are designed to be more conformable to the peripheral curvature of the cornea. These findings suggest that a non-rotationally symmetric lens, which better matches the peripheral corneal shape, may provide better consistency in induced paracentral corneal steepening.

For our current cohort of subjects with low with-the-rule corneal astigmatism, the DA design with the same base curve led to a slightly greater, albeit statistically insignificant, treatment after one day, but a similar correction of myopia at one week measured by autorefraction. The majority of subjects achieved over 70% of their target correction after one week, and visual acuity was also acceptable to most subjects by one week. This is consistent with previous longer-term studies of ortho-k. Nichols et al. found that most of the change in visual and refractive outcome variables occurred after 7 nights of overnight lens wear, but that improvements continued out to 30 days [123]. The central treatment area, width of paracentral steepening ring, and location of the greatest induced corneal power were similar between the two lens designs. However, the magnitude of the induced corneal steepening was significantly higher for the DA design.

In this cohort, we did not find a significant difference in initial lens centration between the DA and the spherical CRT lenses. This is likely due to the rigorous inclusion criteria of of both low corneal astigmatism and minimal peripheral elevation differences, which allowed the spherical CRT lenses to be centered satisfactorily. Based on our clinical experience, it would be worthwhile to study the long-term consistency of lens centration between the two designs, especially given that the lenses are worn in the close-lid condition with significant lid-lens interactions during REM sleep. In most cases of with-the-rule corneal toricity, the DA design would be more compatible with the natural shape of the mid-peripheral cornea, allowing for a more uniform distribution of the weight of the lens across the corneal surface, which could also lead to fewer long-term complications with lens wear.

Importantly, two subjects from this cohort reported increased difficulty removing the DA CRT lenses compared to the spherical design. This is a valid concern, particularly when working with a pediatric population. For patients that are fit with the DA design, practitioners should emphasize instilling artificial tears in the morning upon lens removal,

ensuring that the lens is moving well with each blink, and offsetting the DMV plunger so that it is closer to the lens edge, in order to minimize suction and discomfort when attempting to remove the lens.

To our knowledge, this is the first study to compare spherical and DA CRT designs in a population with minimal corneal toricity and minimal peripheral elevation differences. A unique advantage of this study design is that each subject had the opportunity to wear both types of lenses with masked and random allocation of the sequence of spherical versus DA designs, so that their subjective impression of their vision, lens comfort and ease of handling could be compared without bias. One limitation of the study was the short duration of lens wear for each design. It is possible that the differences reported here may reduce with longer lens wear. Only one participant required a base curve adjustment to the initial lens selected, but otherwise, no lenses required further adjustments during the trial. However, if we were to extend beyond one week of lens wear, we may expect further adjustments to achieve an ideal long-term fit. Anecdotal evidence from the UC Berkeley Myopia Control Clinic population suggests persistent differences in induced corneal morphological changes between the spherical and DA CRT designs with increased wear time. Longer studies are warranted to provide insight on the long-term benefit of the DA design in the consistency of lens centration and the stability of vision during the day. Another limitation of the study was that a uniform 50 microns of sagittal depth difference was incorporated in all DA lenses used, which greatly reduced its potential of being custom fitted based on the actual peripheral elevational difference of each cornea. With a more precise understanding of the peripheral corneal shape and more freedom in custom designing the depth differences in both the return zone and the landing zone of the CRT lenses in real clinical settings, we would be able to achieve faster and better treatment, as well as better long-term consistency in lens performance. While this study used CRT lenses, many ortho-k lenses incorporate back surface toricity in order to improve lens fit and centration.

Implication for Myopia Control

Despite the use of ortho-k lenses for slowing progression of myopia, current ortho-k lenses are designed for optimal visual performance while correcting myopia, rather than myopia control. The exact mechanism of ortho-k lenses in myopia retardation is still unclear and the optimal optical myopia control design, if one exists, remains unknown. It has been suggested that the location, area, and magnitude of paracentral corneal steepening causes myopic defocus to be imposed to the peripheral retina. The induced spherical aberration, as well as associated behavioral changes, may all contribute to the efficacy of these lenses for myopia control. Results from animal studies suggest that increasing the retinal area and/or the magnitude exposed to myopic defocus are positively associated with stronger myopia inhibiting effect [174, 103]. However, caution needs to be made in translating evidence from experimental models to human myopia control. Nonetheless, the results of this study suggest that if increased paracentral corneal steepening (i.e., more positive spherical aberration and stronger myopic defocus projected to peripheral retina) is a goal of treatment, then DA CRT

lenses could be considered over the spherical CRT lenses whenever appropriate for better myopia control efficacy. This study aimed to investigate the comparative efficacy of two CRT designs on myopia correction instead of that on myopia control, which requires a much longer observational period and a larger sample size.

A.5 Summary and Conclusion

In summary, we found that even in patients with low astigmatism and elevation differences in the mid-peripheral cornea, DA CRT lenses induced a greater magnitude of paracentral steepening compared to spherical CRT lenses. It remains largely unknown the complex interactions between the area, location, and magnitude of the imposed defocus on the efficacy for myopia control. This study suggests that a lens design such as the DA CRT is an important consideration when fitting patients with not only moderate-high corneal astigmatism but also for those showing minimal peripheral elevation difference.

Appendix B

Participant Questionnaire

Questionnaire to be administered at the BASELINE visit prior to removing the subjects habitually worn correction. The patient must be wearing the correction while filling out the questionnaire.

Patient Questionnaire

Habitual Correction

1. What, if anything, do you like about your current correction for your vision?
2. What, if anything, do you dislike about your current correction for your vision?
3. On average, how many days per week do your wear correction for your vision?
4. On average, how many hours per day do you wear your correction for your vision?
5. Please rate the current correction for your vision on the following visual attributes:

Circle one number per line (10 = Excellent, 1 = Poor)

Overall visual sharpness and clarity

10 9 8 7 6 5 4 3 2 1

Night vision/low or dim light situations (such as driving at night or reading a menu in a dark restaurant

10 9 8 7 6 5 4 3 2 1

Consistent vision throughout the day (stable or variable vision while wearing your correction?)

10 9 8 7 6 5 4 3 2 1

Vision while participating in sport activities (if applicable) Which sports?

10 9 8 7 6 5 4 3 2 1

Vision while working (such as working at a computer, reading fine print, long periods of close work)

10 9 8 7 6 5 4 3 2 1

6. Please rate your unaided vision on the following visual attributes

Circle one number per line (10 = Excellent, 1 = Poor)

Overall visual sharpness and clarity

10 9 8 7 6 5 4 3 2 1

Night vision/low or dim light situations (such as driving at night or reading a menu in a dark restaurant

10 9 8 7 6 5 4 3 2 1

Consistent vision throughout the day (stable or variable vision while wearing your correction?)

10 9 8 7 6 5 4 3 2 1

Vision while participating in sport activities (if applicable) Which sports?

10 9 8 7 6 5 4 3 2 1

Vision while working (such as working at a computer, reading fine print, long periods of close work)

10 9 8 7 6 5 4 3 2 1

7. Overall, how satisfied are you with the correction for your vision you currently wear? (10 = very satisfied, 1 = not at all satisfied)

10 9 8 7 6 5 4 3 2 1

8. Overall, how satisfied are you with you unaided vision?

10 9 8 7 6 5 4 3 2 1

Questionnaire to be administered at the ONE-WEEK follow-up visit prior to clinical testing

Patient Questionnaire

Study Lenses after One Week of Lens Wear

1. What, if anything, do you like about this pair of study lenses?
2. What, if anything, do you dislike about this pair of study lenses?
3. On average, how many nights per week did your wear your study lenses?
4. On average, how many hours per night did you wear your study lenses?
5. Please rate the study contact lenses on the following visual attributes:

Circle only one number per line (10 = excellent, 1 = poor)

Overall visual sharpness and clarity

10 9 8 7 6 5 4 3 2 1

6. Please rate the contact lenses used during the study on the following comfort attributes.

Circle only one number per line

Comfort of the lenses when you first put them in

10 9 8 7 6 5 4 3 2 1

Comfort of the lenses at the end of the wear time

10 9 8 7 6 5 4 3 2 1

Overall Comfort

10 9 8 7 6 5 4 3 2 1

7. Please rate your unaided vision on the following visual attributes

Circle only one number per line

Overall visual sharpness and clarity

10 9 8 7 6 5 4 3 2 1

Night vision/low or dim light situations (such as driving at night or reading a menu in a dark restaurant

10 9 8 7 6 5 4 3 2 1

Consistent vision throughout the day (stable or variable vision while wearing your correction?)

10 9 8 7 6 5 4 3 2 1

Vision while participating in sport activities (if applicable) Which sports?

10 9 8 7 6 5 4 3 2 1

Vision while working (such as working at a computer, reading fine print, long periods of close work)

10 9 8 7 6 5 4 3 2 1

8. Overall, how satisfied are you with the correction for your vision with the study lenses? (10 = very satisfied, 1 = not at all satisfied)

10 9 8 7 6 5 4 3 2 1

9. Overall, how satisfied are you with you unaided vision?

10 9 8 7 6 5 4 3 2 1

Appendix C

One Week Post-Treatment Topography Images

The following table displays the 1-week topography images for the right and left eyes for each phase of treatment. The eye that was wearing the dual axis lens is outlined in green. Of note, for subjects 12 (right eye, lens 1) and 16 (both eyes, lens 1), the original baseline measurement was not available due to topography software issues, so the second baseline (prior to the start of phase 2) was used for comparison. Therefore, the color map is reversed.

Three subjects were excluded from topography treatment analysis: **Subject 17** was excluded from topography analysis due to the inconsistent treatment area. **Subject 18** was excluded because phase 1 images were not available (due to the same topography software issues mentioned above which resulted in the images not being saved). **Subject 20** was excluded because the nasal treatment area for the left eye could not be defined.

Subject	Right Eye, Lens 1	Left Eye, Lens 1	Right Eye, Lens 2	Left Eye, Lens 2
1	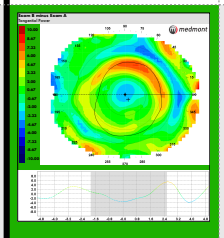	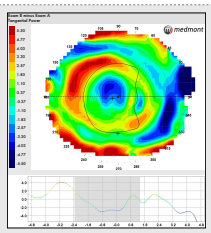	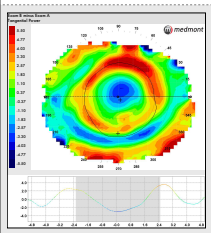	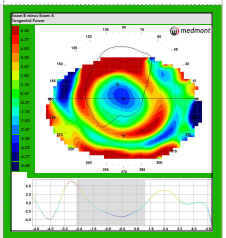
2	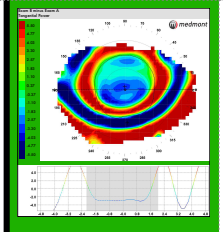	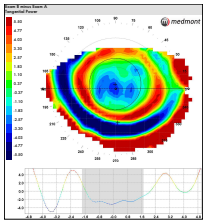	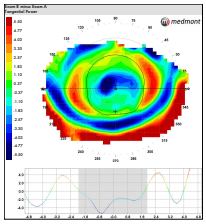	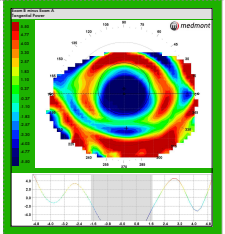
3	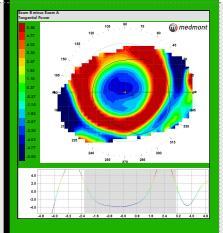	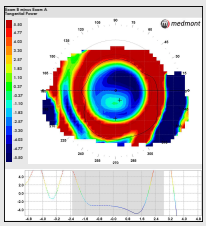	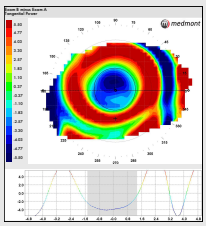	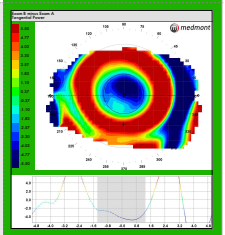
4	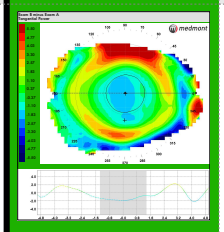	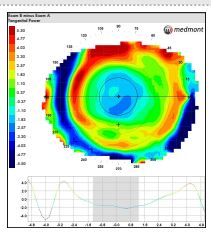	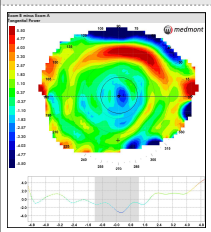	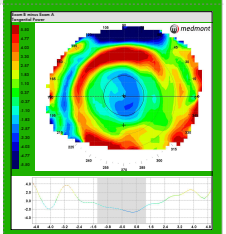
5	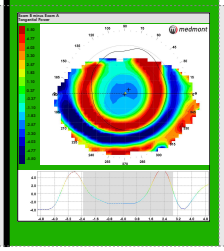	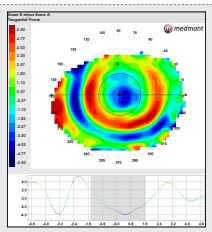	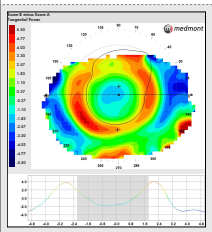	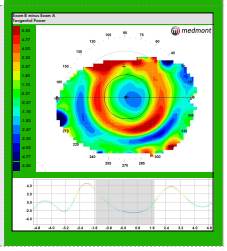

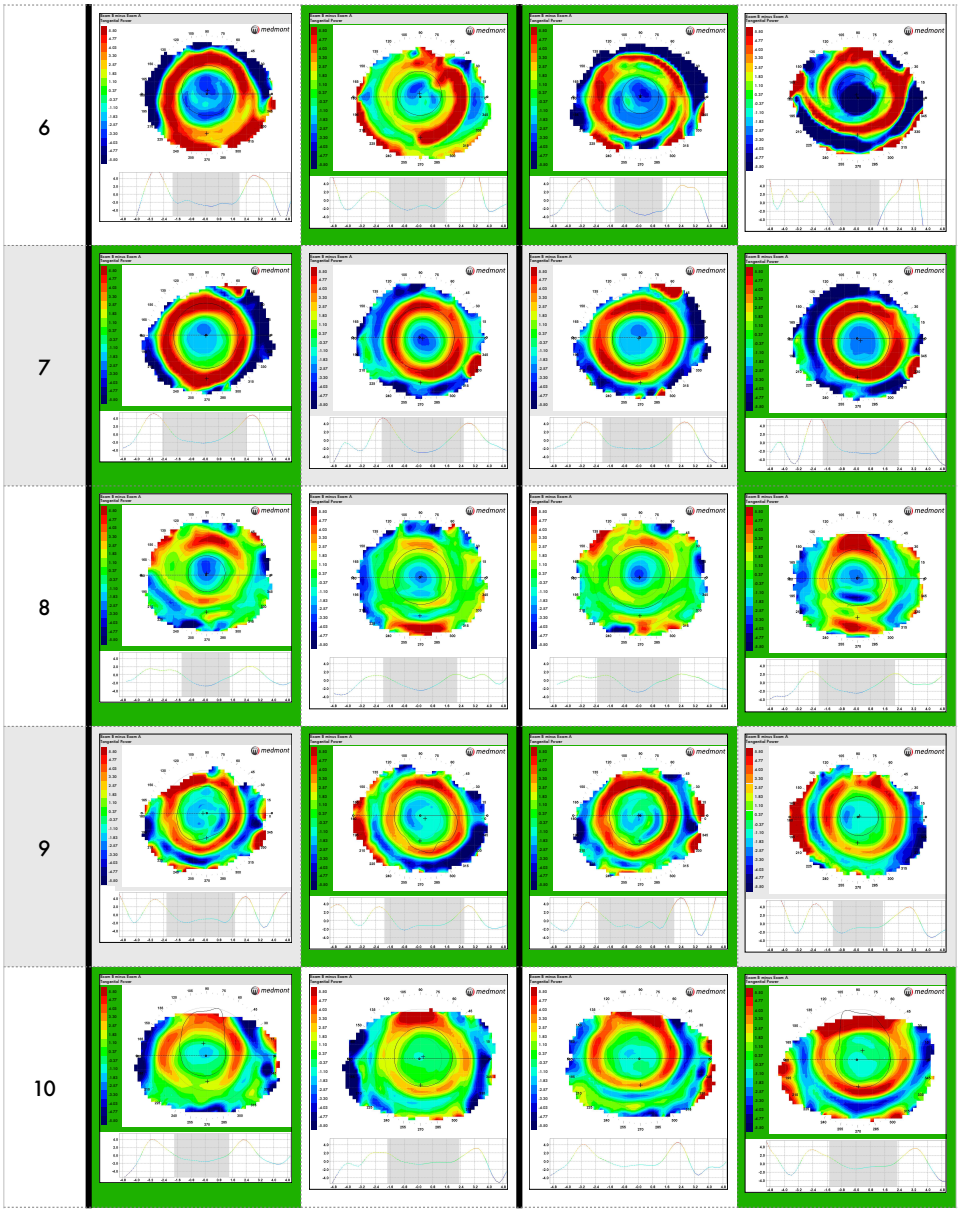
6
7
8
9
10

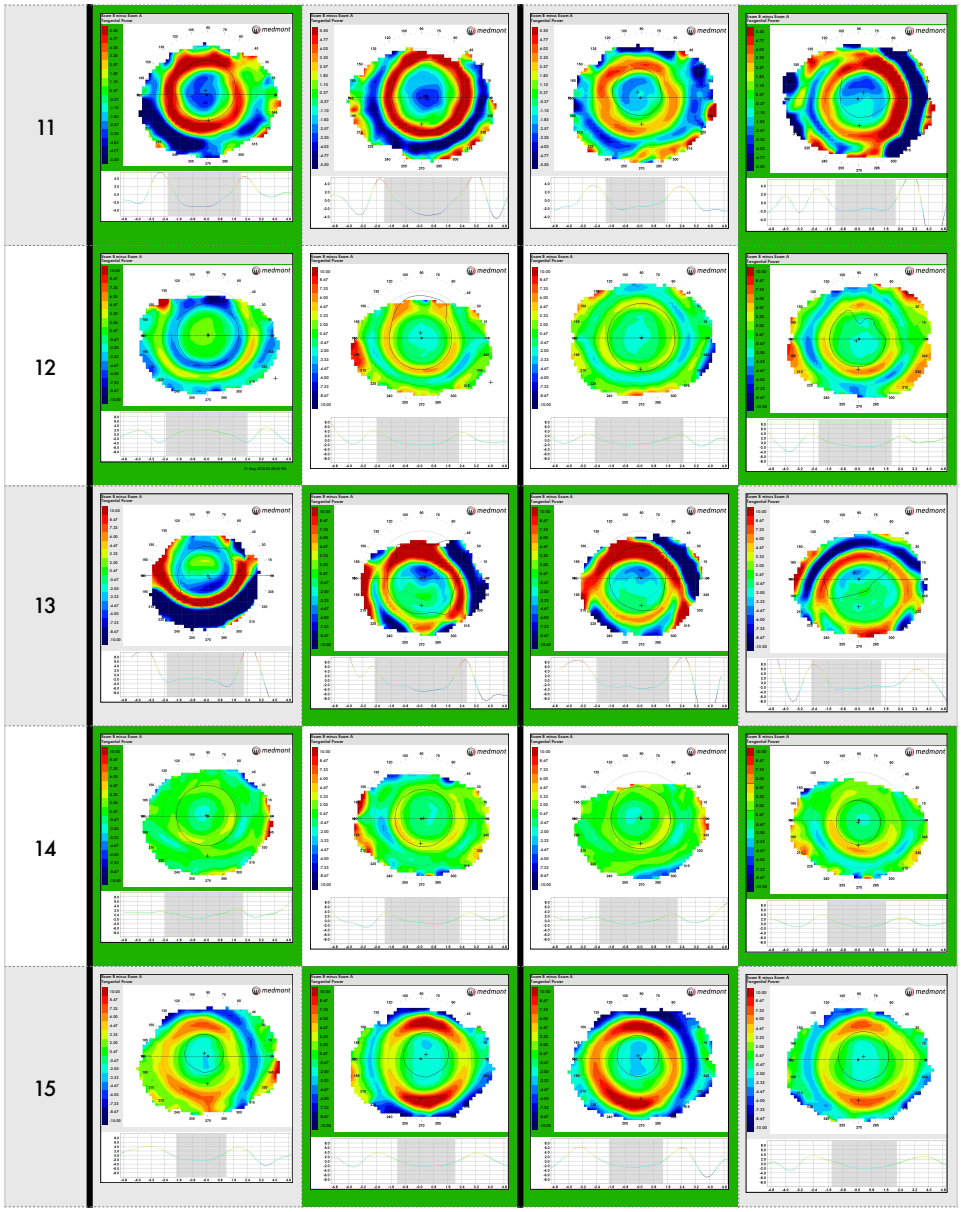
11
12
13
14
15

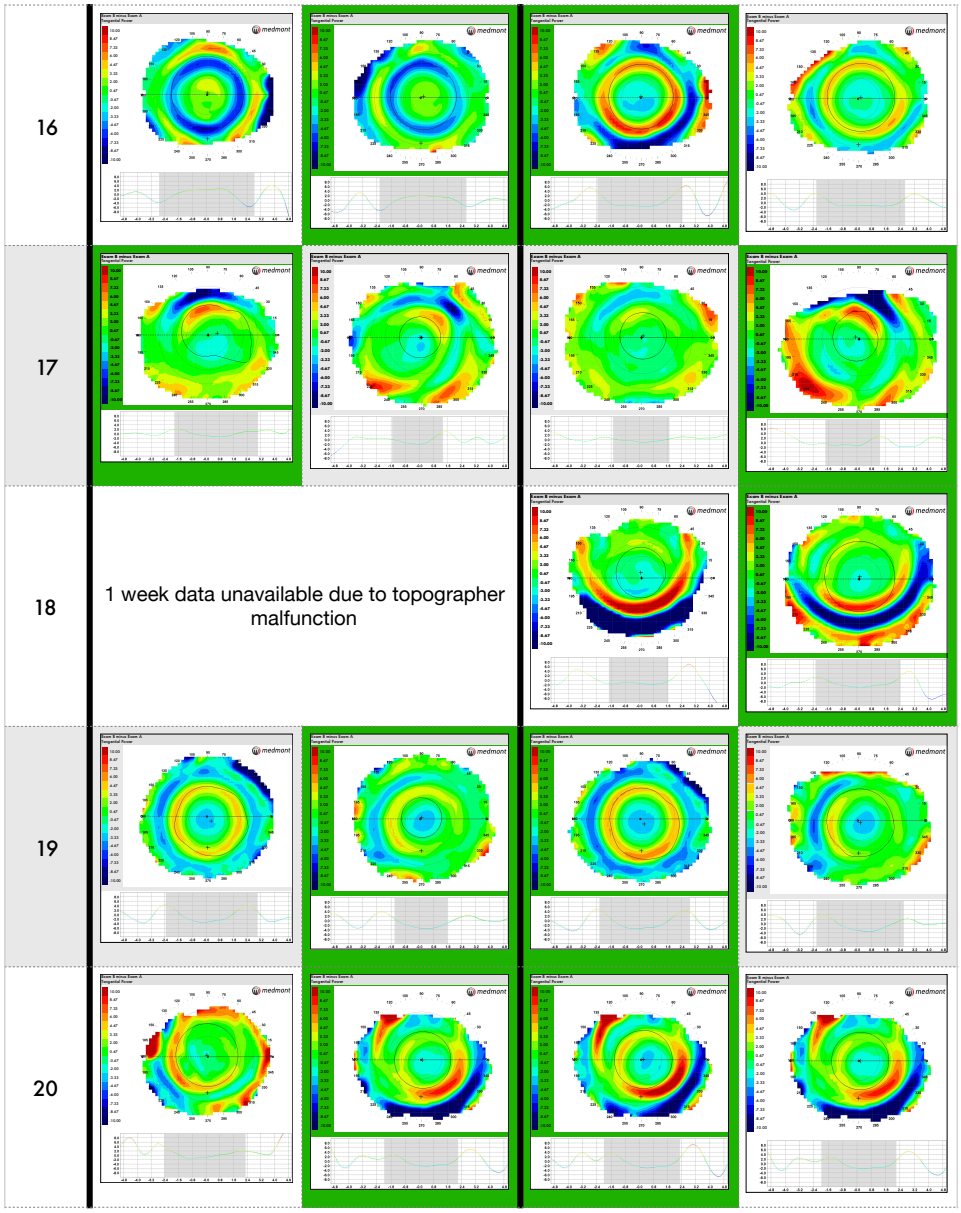
16
17
18
1 week data unavailable due to topographer malfunction
19
20

21	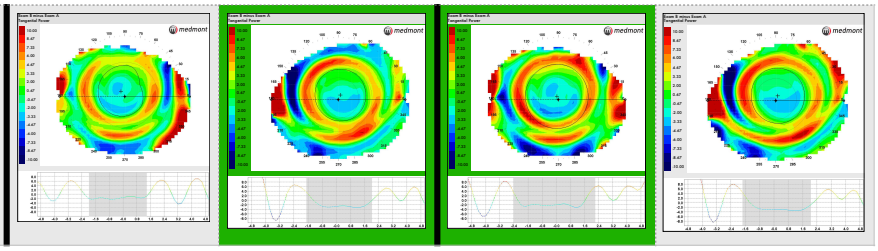

Bibliography

[1] Pablo Artal et al. "Compensation of corneal aberrations by the internal optics in the human eye". In: *Journal of Vision* 1.1 (2001), pp. 1–1.

[2] Pablo Artal et al. "Retinal image quality in the rodent eye". In: *Visual neuroscience* 15.4 (1998), pp. 597–605.

[3] Regan Ashby et al. "A muscarinic cholinergic antagonist and a dopamine agonist rapidly increase ZENK mRNA expression in the form-deprived chicken retina". In: *Experimental eye research* 85.1 (2007), pp. 15–22.

[4] Simon Backhouse and John R Phillips. "Effect of induced myopia on scleral myofibroblasts and in vivo ocular biomechanical compliance in the guinea pig". In: *Investigative ophthalmology & visual science* 51.12 (2010), pp. 6162–6171.

[5] Christophe Baudouin et al. "Preservatives in eyedrops: the good, the bad and the ugly". In: *Progress in retinal and eye research* 29.4 (2010), pp. 312–334.

[6] RH Bedrossian. "The effect of atropine on myopia." In: *Annals of ophthalmology* 3.8 (1971), pp. 891–897.

[7] Robert H Bedrossian. "The effect of atropine on myopia". In: *Ophthalmology* 86.5 (1979), pp. 713–717.

[8] Anna Rita Bentivoglio et al. "Analysis of blink rate patterns in normal subjects". In: *Movement disorders* 12.6 (1997), pp. 1028–1034.

[9] Rupert RA Bourne et al. "Causes of vision loss worldwide, 1990–2010: a systematic analysis". In: *The lancet global health* 1.6 (2013), e339–e349.

[10] Hannah E Bowrey et al. "The effect of spectacle lenses containing peripheral defocus on refractive error and horizontal eye shape in the guinea pig". In: *Investigative ophthalmology & visual science* 58.5 (2017), pp. 2705–2714.

[11] Hannah E Bowrey et al. "The relationship between image degradation and myopia in the mammalian eye". In: *Clinical and Experimental Optometry* 98.6 (2015), pp. 555–563.

[12] Dolores V Bradley et al. "Emmetropization in the rhesus monkey (Macaca mulatta): birth to young adulthood." In: *Investigative ophthalmology & visual science* 40.1 (1999), pp. 214–229.

[13] Cecil David Bethell Bridges. "Visual pigments of some common laboratory mammals". In: *Nature* 184.4700 (1959), p. 1727.

[14] Robert S Brodstein et al. "The treatment of myopia with atropine and bifocals: a long-term prospective study". In: *Ophthalmology* 91.11 (1984), pp. 1373–1378.

[15] Thamara A Cafaro et al. "The cornea of Guinea pig: structural and functional studies". In: *Veterinary ophthalmology* 12.4 (2009), pp. 234–241.

[16] Yun-Lin Cai et al. "The investigation on the role of mitochondrial fusion protein 1 in the development of myopia". In: *Indian journal of ophthalmology* 64.7 (2016), p. 500.

[17] Ignasi Cardelús et al. "Anticholinergic effects of desloratadine, the major metabolite of loratadine, in rabbit and guinea-pig iris smooth muscle". In: *European journal of pharmacology* 374.2 (1999), pp. 249–254.

[18] E Garcia de la Cera et al. "Emmetropization and optical aberrations in a myopic corneal refractive surgery chick model". In: *Vision research* 47.18 (2007), pp. 2465–2472.

[19] E García de la Cera, Guadalupe Rodríguez, and Susana Marcos. "Longitudinal changes of optical aberrations in normal and form-deprived myopic chick eyes". In: *Vision Research* 46.4 (2006), pp. 579–589.

[20] Elena García de la Cera et al. "Optical aberrations in the mouse eye". In: *Vision Research* 46.16 (2006), pp. 2546–2553.

[21] Jessie Charm and Pauline Cho. "High myopia-partial reduction orthokeratology (HM-PRO): study design". In: *Contact Lens and Anterior Eye* 36.4 (2013), pp. 164–170.

[22] Connie Chen, Sin Wan Cheung, and Pauline Cho. "Myopia control using toric orthokeratology (TO-SEE study)". In: *Investigative ophthalmology & visual science* 54.10 (2013), pp. 6510–6517.

[23] Bo-Yu Chen et al. "Mechanical behavior of scleral fibroblasts in experimental myopia". In: *Graefe's Archive for Clinical and Experimental Ophthalmology* 250.3 (2012), pp. 341–348.

[24] Han Cheng et al. "A population study on changes in wave aberrations with accomodation". In: *Journal of Vision* 4.4 (2004), pp. 3–3.

[25] Audrey Chia, Qing-Shu Lu, and Donald Tan. "Five-year clinical trial on atropine for the treatment of myopia 2: myopia control with atropine 0.01% eyedrops". In: *Ophthalmology* 123.2 (2016), pp. 391–399.

[26] Audrey Chia et al. "Atropine for the treatment of childhood myopia: changes after stopping atropine 0.01%, 0.1% and 0.5%". In: *American journal of ophthalmology* 157.2 (2014), pp. 451–457.

[27] Audrey Chia et al. "Atropine for the treatment of childhood myopia: safety and efficacy of 0.5%, 0.1%, and 0.01% doses (Atropine for the Treatment of Myopia 2)". In: *Ophthalmology* 119.2 (2012), pp. 347–354.

[28] Pauline Cho, Sin Wan Cheung, and Marion Edwards. "The longitudinal orthokeratology research in children (LORIC) in Hong Kong: a pilot study on refractive changes and myopic control". In: *Current eye research* 30.1 (2005), pp. 71–80.

[29] Pauline Cho and Sin-Wan Cheung. "Retardation of myopia in Orthokeratology (ROMIO) study: a 2-year randomized clinical trial". In: *Investigative ophthalmology & visual science* 53.11 (2012), pp. 7077–7085.

[30] Wei-Han Chua et al. "Atropine for the treatment of childhood myopia". In: *Ophthalmology* 113.12 (2006), pp. 2285–2291.

[31] Nancy J Coletta, Susana Marcos, and David Troilo. "Ocular wavefront aberrations in the common marmoset Callithrix jacchus: effects of age and refractive error". In: *Vision research* 50.23 (2010), pp. 2515–2529.

[32] Martin E Coster et al. "Results of diagnostic ophthalmic testing in healthy guinea pigs". In: *Journal of the American Veterinary Medical Association* 232.12 (2008), pp. 1825–1833.

[33] Sigrid Diether et al. "Effects of intravitreally and intraperitonally injected atropine on two types of experimental myopia in chicken". In: *Experimental eye research* 84.2 (2007), pp. 266–274.

[34] Meihua Ding et al. "Effects of glucocorticoid on the eye development in guinea pigs". In: *Steroids* 139 (2018), pp. 1–9.

[35] Mohamed Dirani et al. "Prevalence of refractive error in Singaporean Chinese children: the strabismus, amblyopia, and refractive error in young Singaporean Children (STARS) study". In: *Investigative ophthalmology & visual science* 51.3 (2010), pp. 1348–1355.

[36] Elie Dolgin. "The myopia boom". In: *Nature News* 519.7543 (2015), p. 276.

[37] Feng Dong et al. "Inhibition of experimental myopia by a dopamine agonist: different effectiveness between form deprivation and hyperopic defocus in guinea pigs". In: *Molecular vision* 17 (2011), p. 2824.

[38] Li Dong et al. "Amphiregulin and ocular axial length". In: *Acta ophthalmologica* 97.3 (2019), e460–e470.

[39] Li Dong et al. "Ocular size and shape in lens-induced Myopization in young Guinea pigs". In: *BMC ophthalmology* 19.1 (2019), p. 102.

[40] Dorothy SP Fan et al. "Change in vision disorders among Hong Kong preschoolers in 10 years". In: *Clinical & experimental ophthalmology* 39.5 (2011), pp. 398–403.

[41] Dorothy SP Fan et al. "Prevalence, incidence, and progression of myopia of school children in Hong Kong". In: *Investigative ophthalmology & visual science* 45.4 (2004), pp. 1071–1075.

[42] Dorothy SP Fan et al. "Topical atropine in retarding myopic progression and axial length growth in children with moderate to severe myopia: a pilot study". In: *Japanese journal of ophthalmology* 51.1 (2007), pp. 27–33.

[43] Fang Fang et al. "Effects of muscarinic receptor modulators on ocular biometry of guinea pigs". In: *Ophthalmic and Physiological Optics* 35.1 (2015), pp. 60–69.

[44] DI Flitcroft. "The complex interactions of retinal, optical and environmental factors in myopia aetiology". In: *Progress in retinal and eye research* 31.6 (2012), pp. 622–660.

[45] Prema Ganesan and Christine F Wildsoet. "Pharmaceutical intervention for myopia control". In: *Expert review of ophthalmology* 5.6 (2010), pp. 759–787.

[46] Ting-Ting Gao, Qin Long, and Xue Yang. "Complement factors C1q, C3 and C5b-9 in the posterior sclera of guinea pigs with negative lens-defocused myopia". In: *International journal of ophthalmology* 8.4 (2015), p. 675.

[47] Mariana Garcia. "Myopia control in guinea pigs". PhD thesis. UC Berkeley, 2014.

[48] Timothy J Gawne, Alexander H Ward, and Thomas T Norton. "Long-wavelength (red) light produces hyperopia in juvenile and adolescent tree shrews". In: *Vision research* 140 (2017), pp. 55–65.

[49] Timothy J Gawne et al. "The wavelength composition and temporal modulation of ambient lighting strongly affect refractive development in young tree shrews". In: *Experimental eye research* 155 (2017), pp. 75–84.

[50] Ying Geng et al. "Optical properties of the mouse eye". In: *Biomedical optics express* 2.4 (2011), pp. 717–738.

[51] HV Gimbel. "The control of myopia with atropine". In: *Can J Ophthalmol* 8 (1973), pp. 527–532.

[52] Lydia Giordano et al. "Prevalence of refractive error among preschool children in an urban population: the Baltimore Pediatric Eye Disease Study". In: *Ophthalmology* 116.4 (2009), pp. 739–746.

[53] Qianwen Gong et al. "Efficacy and adverse effects of atropine in childhood myopia: a meta-analysis". In: *JAMA ophthalmology* 135.6 (2017), pp. 624–630.

[54] Dilraj S Grewal, Gagandeep S Brar, and Satinder PS Grewal. "Assessment of central corneal thickness in normal, keratoconus, and post-laser in situ keratomileusis eyes using Scheimpflug imaging, spectral domain optical coherence tomography, and ultrasound pachymetry". In: *Journal of Cataract & Refractive Surgery* 36.6 (2010), pp. 954–964.

[55] Li Guoping et al. "Alterations of Glutamate and γ-Aminobutyric Acid Expressions in Normal and Myopic Eye Development in Guinea Pigs". In: *Investigative ophthalmology & visual science* 58.2 (2017), pp. 1256–1265.

[56] Mingguang He et al. "Refractive error and visual impairment in urban children in southern China". In: *Investigative ophthalmology & visual science* 45.3 (2004), pp. 793–799.

[57] Ichijima Hideji et al. "Swelling and deswelling of rabbit corneas in response to rigid gas permeable, hydrogel and elastomer contact lens wear." In: *The CLAO journal: official publication of the Contact Lens Association of Ophthalmologists, Inc* 15.4 (1989), pp. 290–297.

[58] Brien A Holden et al. "Global prevalence of myopia and high myopia and temporal trends from 2000 through 2050". In: *Ophthalmology* 123.5 (2016), pp. 1036–1042.

[59] B Holden et al. "Myopia, an underrated global challenge to vision: where the current data takes us on myopia control". In: *Eye* 28.2 (2014), p. 142.

[60] Howard C Howland, Stacey Merola, and Jennifer R Basarab. "The allometry and scaling of the size of vertebrate eyes". In: *Vision research* 44.17 (2004), pp. 2043–2065.

[61] Marcus HC Howlett and Sally A McFadden. "Emmetropization and schematic eye models in developing pigmented guinea pigs". In: *Vision Research* 47.9 (2007), pp. 1178–1190.

[62] Marcus HC Howlett and Sally A McFadden. "Form-deprivation myopia in the guinea pig (Cavia porcellus)". In: *Vision research* 46.1-2 (2006), pp. 267–283.

[63] Marcus HC Howlett and Sally A McFadden. "Spectacle lens compensation in the pigmented guinea pig". In: *Vision research* 49.2 (2009), pp. 219–227.

[64] Creig S Hoyt et al. "Monocular axial myopia associated with neonatal eyelid closure in human infants". In: *American journal of ophthalmology* 91.2 (1981), pp. 197–200.

[65] Jinhai Huang et al. "Efficacy comparison of 16 interventions for myopia control in children: a network meta-analysis". In: *Ophthalmology* 123.4 (2016), pp. 697–708.

[66] Austin Hughes. "The topography of vision in mammals of contrasting life style: comparative optics and retinal organisation". In: *The visual system in vertebrates*. Springer, 1977, pp. 613–756.

[67] Li-Fang Hung, Morris LJ Crawford, and Earl L Smith. "Spectacle lenses alter eye growth and the refractive status of young monkeys". In: *Nature medicine* 1.8 (1995), p. 761.

[68] RM Ingram and A Barr. "Changes in refraction between the ages of 1 and 3 1/2 years." In: *British Journal of Ophthalmology* 63.5 (1979), pp. 339–342.

[69] EL Irving, JG Sivak, and MG Callender. "Refractive plasticity of the developing chick eye". In: *Ophthalmic and Physiological Optics* 12.4 (1992), pp. 448–456.

[70] Jason J Ivanusic, Rhiannon J Wood, and James A Brock. "Sensory and sympathetic innervation of the mouse and guinea pig corneal epithelium". In: *Journal of Comparative Neurology* 521.4 (2013), pp. 877–893.

[71] Aiko Iwase et al. "Prevalence and causes of low vision and blindness in a Japanese adult population: the Tajimi Study". In: *Ophthalmology* 113.8 (2006), pp. 1354–1362.

[72] Gerald H Jacobs. "The distribution and nature of colour vision among the mammals". In: *Biological Reviews* 68.3 (1993), pp. 413–471.

[73] Gerald H Jacobs and Jess F Deegan. "Spectral sensitivity of macaque monkeys measured with ERG flicker photometry". In: *Visual neuroscience* 14.5 (1997), pp. 921–928.

[74] Gerald H Jacobs and Jess F Deegan. "Spectral sensitivity, photopigments, and color vision in the guinea pig (Cavia porcellus)." In: *Behavioral neuroscience* 108.5 (1994), p. 993.

[75] Chang-Jin Jeon, Enrica Strettoi, and Richard H Masland. "The major cell populations of the mouse retina". In: *Journal of Neuroscience* 18.21 (1998), pp. 8936–8946.

[76] Liqin Jiang et al. "Spontaneous axial myopia and emmetropization in a strain of wild-type guinea pig (Cavia porcellus)". In: *Investigative ophthalmology & visual science* 50.3 (2009), pp. 1013–1019.

[77] Liqin Jiang et al. "Strain-Dependent Differences in Sensitivity to Myopia-Inducing Stimuli in Guinea Pigs and Role of Choroid". In: *Investigative ophthalmology & visual science* 60.4 (2019), pp. 1226–1233.

[78] Wen Jun Jiang et al. "Amphiregulin antibody and reduction of axial elongation in experimental myopia". In: *EBioMedicine* 17 (2017), pp. 134–144.

[79] Ashutosh Jnawali, Krista M Beach, and Lisa A Ostrin. "In vivo imaging of the retina, choroid, and optic nerve head in guinea pigs". In: *Current eye research* 43.8 (2018), pp. 1006–1018.

[80] Su-Kyung Jung et al. "Prevalence of myopia and its association with body stature and educational level in 19-year-old male conscripts in Seoul, South Korea". In: *Investigative ophthalmology & visual science* 53.9 (2012), pp. 5579–5583.

[81] Cynthia M Kahn. *The Merck veterinary manual*. Whitehouse Station N.J. [Great Britain]: Merck & Co, 2005.

[82] Tetsuhiko Kakita, Takahiro Hiraoka, and Tetsuro Oshika. "Influence of overnight orthokeratology on axial elongation in childhood myopia". In: *Investigative ophthalmology & visual science* 52.5 (2011), pp. 2170–2174.

[83] Pauline Kang and Helen Swarbrick. "New perspective on myopia control with orthokeratology". In: *Optometry and Vision Science* 93.5 (2016), pp. 497–503.

[84] John A King. "Social relations of the domestic guinea pig living under semi-natural conditions". In: *Ecology* 37.2 (1956), pp. 221–228.

[85] Marsha L Kisilak et al. "Aberrations of chick eyes during normal growth and lens induction of myopia". In: *Journal of Comparative Physiology A* 192.8 (2006), pp. 845–855.

[86] Helga Kolb, Eduardo Fernandez, and Ralph Nelson. "Photoreceptors–Webvision: The Organization of the Retina and Visual System". In: (1995).

[87] Jay H Krachmer and David A Palay. *Cornea Atlas E-Book: Expert Consult-Online and Print*. Elsevier Health Sciences, 2013.

[88] Weizhong Lan et al. "Refractive errors in 3–6 year-old Chinese children: a very low prevalence of myopia?" In: *PLoS One* 8.10 (2013), e78003.

[89] Jin Hae Lee et al. "Prevalence and risk factors for myopia in a rural Korean population". In: *Investigative ophthalmology & visual science* 54.8 (2013), pp. 5466–5471.

[90] Jong-Jer Lee et al. "Prevention of myopia progression with 0.05% atropine solution". In: *Journal of Ocular Pharmacology & Therapeutics* 22.1 (2006), pp. 41–46.

[91] Bo Lei. "The ERG of guinea pig (*Cavis porcellus*): comparison with I-type monkey and E-type rat". In: *Documenta ophthalmologica* 106.3 (2003), pp. 243–249.

[92] Amelia J Leotta et al. "Temporal properties of the myopic response to defocus in the guinea pig". In: *Ophthalmic and Physiological Optics* 33.3 (2013), pp. 227–244.

[93] Honghui Li et al. "BMP-2 is involved in scleral remodeling in myopia development". In: *PloS one* 10.5 (2015), e0125219.

[94] Honghui Li et al. "Retinal and choroidal expression of BMP-2 in lens-induced myopia and recovery from myopia in guinea pigs". In: *Molecular medicine reports* 13.3 (2016), pp. 2671–2676.

[95] Wentao Li et al. "The effect of spectral property and intensity of light on natural refractive development and compensation to negative lenses in guinea pigs". In: *Investigative ophthalmology & visual science* 55.10 (2014), pp. 6324–6332.

[96] Junzhong Liang and David R Williams. "Aberrations and retinal image quality of the normal human eye". In: *JOSA A* 14.11 (1997), pp. 2873–2883.

[97] Luke Long-Kuang Lin et al. "Prevalence of myopia in Taiwanese schoolchildren: 1983 to 2000". In: *Annals Academy of Medicine Singapore* 33.1 (2004), pp. 27–33.

[98] Georgia J Lind et al. "Muscarinic acetylcholine receptor antagonists inhibit chick scleral chondrocytes." In: *Investigative ophthalmology & visual science* 39.12 (1998), pp. 2217–2231.

[99] Shaohui Liu et al. "Expression and function of muscarinic receptor subtypes on human cornea and conjunctiva". In: *Investigative ophthalmology & visual science* 48.7 (2007), pp. 2987–2996.

[100] Shuai Liu et al. "Scleral cross-linking using riboflavin UVA irradiation for the prevention of myopia progression in a guinea pig model: blocked axial extension and altered scleral microstructure". In: *PloS one* 11.11 (2016), e0165792.

[101] Yan Liu et al. "α-adrenergic agonist brimonidine control of experimentally induced myopia in guinea pigs: A pilot study". In: *Molecular vision* 23 (2017), p. 785.

[102] Yue M Liu and Peiying Xie. "The safety of orthokeratology: a systematic review". In: *Eye & contact lens* 42.1 (2016), p. 35.

[103] Yue Liu and Christine Wildsoet. "The effect of two-zone concentric bifocal spectacle lenses on refractive error development and eye growth in young chicks". In: *Investigative ophthalmology & visual science* 52.2 (2011), pp. 1078–1086.

[104] D Lovell, D King, and MFW Festing. "Breeding performance of specific pathogen free guinea-pigs". In: *Guinea-pig News Letter* 6 (1972), pp. 6–11.

[105] Fan Lu et al. "Axial myopia induced by a monocularly-deprived facemask in guinea pigs: A non-invasive and effective model". In: *Experimental eye research* 82.4 (2006), pp. 628–636.

[106] Fan Lu et al. "Axial myopia induced by hyperopic defocus in guinea pigs: A detailed assessment on susceptibility and recovery". In: *Experimental eye research* 89.1 (2009), pp. 101–108.

[107] W Alana Luft, Yan Ming, and William K Stell. "Variable effects of previously untested muscarinic receptor antagonists on experimental myopia". In: *Investigative ophthalmology & visual science* 44.3 (2003), pp. 1330–1338.

[108] Yingyan Ma et al. "Age-specific prevalence of visual impairment and refractive error in children aged 3–10 years in Shanghai, China". In: *Investigative ophthalmology & visual science* 57.14 (2016), pp. 6188–6196.

[109] Jason D Marsack, Larry N Thibos, and Raymond A Applegate. "Metrics of optical quality derived from wave aberrations predict visual performance". In: *Journal of Vision* 4.4 (2004), pp. 8–8.

[110] Daniel Marzani and Josh Wallman. "Growth of the two layers of the chick sclera is modulated reciprocally by visual conditions." In: *Investigative ophthalmology & visual science* 38.9 (1997), pp. 1726–1739.

[111] Neville A McBrien, HO Moghaddam, and AP Reeder. "Atropine reduces experimental myopia and eye enlargement via a nonaccommodative mechanism." In: *Investigative ophthalmology & visual science* 34.1 (1993), pp. 205–215.

[112] SA McFadden and J Wallman. "Guinea-pig eye growth compensates for spectacle lenses". In: *Investigative Ophthalmology & Visual Science*. Vol. 36. 4. LIPPINCOTT-RAVEN PUBL 227 EAST WASHINGTON SQUARE, PHILADELPHIA, PA 19106. 1995, S758–S758.

[113] Sally A McFadden. "Partial occlusion produces local form deprivation myopia in the guinea pig eye". In: *Investigative ophthalmology & visual science* 43.13 (2002), pp. 189–189.

[114] Sally A McFadden, Marc HC Howlett, and James R Mertz. "Retinoic acid signals the direction of ocular elongation in the guinea pig eye". In: *Vision research* 44.7 (2004), pp. 643–653.

[115] Sally A McFadden et al. "Integration of defocus by dual power Fresnel lenses inhibits myopia in the mammalian eye". In: *Investigative ophthalmology & visual science* 55.2 (2014), pp. 908–917.

[116] JA McKanna and VA Casagrande. "Atropine affects lid-suture myopia development". In: *Third International Conference on Myopia Copenhagen, August 24–27, 1980*. Springer. 1981, pp. 187–192.

[117] Ian G Morgan and Kathryn A Rose. "Myopia and international educational performance". In: *Ophthalmic and Physiological Optics* 33.3 (2013), pp. 329–338.

[118] Ian Morgan and Kathryn Rose. "How genetic is school myopia?" In: *Progress in retinal and eye research* 24.1 (2005), pp. 1–38.

[119] John Morrison et al. "Structure and composition of the rodent lamina cribrosa". In: *Experimental eye research* 60.2 (1995), pp. 127–135.

[120] Donald O Mutti et al. "Axial growth and changes in lenticular and corneal power during emmetropization in infants". In: *Investigative ophthalmology & visual science* 46.9 (2005), pp. 3074–3080.

[121] Kovin S Naidoo et al. "Potential lost productivity resulting from the global burden of myopia: Systematic review, meta-analysis, and modeling". In: *Ophthalmology* 126.3 (2019), pp. 338–346.

[122] JL Do-Nascimento et al. "The neurons of the retinal ganglion cell layer of the guinea pig: quantitative analysis of their distribution and size". In: *Braz J Med Biol Res* 24.2 (1991), p. 199214.

[123] Jason J Nichols et al. "Overnight orthokeratology". In: *Optometry and Vision Science* 77.5 (2000), pp. 252–259.

[124] Debora L Nickla and Falk Schroedl. "Parasympathetic influences on emmetropization in chicks: evidence for different mechanisms in form deprivation vs negative lens-induced myopia". In: *Experimental eye research* 102 (2012), pp. 93–103.

[125] Debora L Nickla and Kristen Totonelly. "Dopamine antagonists and brief vision distinguish lens-induced-and form-deprivation-induced myopia". In: *Experimental eye research* 93.5 (2011), pp. 782–785.

[126] Debora L Nickla and Josh Wallman. "The multifunctional choroid". In: *Progress in retinal and eye research* 29.2 (2010), pp. 144–168.

[127] Debora L Nickla, Christine Wildsoet, and Josh Wallman. "Visual influences on diurnal rhythms in ocular length and choroidal thickness in chick eyes". In: *Experimental eye research* 66.2 (1998), pp. 163–181.

[128] Debora L Nickla, Yekaterina Yusupova, and Kristen Totonelly. "The muscarinic antagonist MT3 distinguishes between form deprivation-and negative lens-induced myopia in chicks". In: *Current eye research* 40.9 (2015), pp. 962–967.

[129] Thomas T Norton. "Animal models of myopia: learning how vision controls the size of the eye". In: *Ilar Journal* 40.2 (1999), pp. 59–77.

[130] Thomas T Norton and Neville A McBrien. "Normal development of refractive state and ocular component dimensions in the tree shrew (Tupaia belangeri)". In: *Vision Research* 32.5 (1992), pp. 833–842.

[131] TT Norton and Jr JT Siegwart. "Animal models of emmetropization: matching axial length to the focal plane." In: *Journal of the American Optometric Association* 66.7 (1995), pp. 405–414.

[132] Timothy W Olsen et al. "Human sclera: thickness and surface area". In: *American journal of ophthalmology* 125.2 (1998), pp. 237–241.

[133] Lisa A Ostrin, Janine Mok-Yee, and Christine F Wildsoet. "Behavioral Measures of Spatial Vision during Early Development in Pigmented and Albino Guinea Pigs". In: *Investigative Ophthalmology & Visual Science* 52.14 (2011), pp. 6296–6296.

[134] Lisa A Ostrin and Christine F Wildsoet. "Optic nerve head and intraocular pressure in the guinea pig eye". In: *Experimental eye research* 146 (2016), pp. 7–16.

[135] Lisa A Ostrin et al. "Pharmacologically stimulated pupil and accommodative changes in Guinea pigs". In: *Investigative ophthalmology & visual science* 55.8 (2014), pp. 5456–5465.

[136] Chen-Wei Pan et al. "The age-specific prevalence of myopia in Asia: a meta-analysis". In: *Optometry and Vision Science* 92.3 (2015), pp. 258–266.

[137] Georgios I Papastergiou et al. "Induction of axial eye elongation and myopic refractive shift in one-year-old chickens". In: *Vision research* 38.12 (1998), pp. 1883–1888.

[138] Juliet WL Parry and James K Bowmaker. "Visual pigment coexpression in guinea pig cones: a microspectrophotometric study". In: *Investigative ophthalmology & visual science* 43.5 (2002), pp. 1662–1665.

[139] Pablo Pérez-Merino et al. "Three-dimensional OCT based guinea pig eye model: relating morphology and optics". In: *Biomedical optics express* 8.4 (2017), pp. 2173–2184.

[140] Heywood M Petry, Robert Fox, and Vivien A Casagrande. "Spatial contrast sensitivity of the tree shrew". In: *Vision research* 24.9 (1984), pp. 1037–1042.

[141] Stacy L Pineles et al. "Atropine for the prevention of myopia progression in children: a report by the American Academy of Ophthalmology". In: *Ophthalmology* 124.12 (2017), pp. 1857–1866.

[142] Andrew D Pucker et al. "Ciliary muscle cell changes during guinea pig development". In: *Investigative ophthalmology & visual science* 56.13 (2015), pp. 7691–7696.

[143] Andrew D Pucker et al. "Guinea pig ciliary muscle development". In: *Optometry and vision science* 91.7 (2014), p. 730.

[144] Liu Qiong et al. "Changes in muscarinic acetylcholine receptor expression in form deprivation myopia in guinea pigs". In: *Mol Vis* 13 (2007), pp. 1234–1244.

[145] Jeff Rabin, RC Van Sluyters, and R Malach. "Emmetropization: a vision-dependent phenomenon." In: *Investigative ophthalmology & visual science* 20.4 (1981), pp. 561–564.

[146] J Racine et al. "The photopic ERGs of guinea pigs and humans are almost identical." In: *Investigative Ophthalmology & Visual Science* 45.13 (2004), pp. 814–814.

[147] Jody A Summers Rada, Setareh Shelton, and Thomas T Norton. "The sclera and myopia". In: *Experimental eye research* 82.2 (2006), pp. 185–200.

[148] Ramkumar Ramamirtham et al. "Monochromatic ocular wave aberrations in young monkeys". In: *Vision research* 46.21 (2006), pp. 3616–3633.

[149] Elio Raviola and Torsten N Wiesel. "An animal model of myopia". In: *New England Journal of Medicine* 312.25 (1985), pp. 1609–1615.

[150] Scott A Read et al. "The topography of the central and peripheral cornea". In: *Investigative ophthalmology & visual science* 47.4 (2006), pp. 1404–1415.

[151] Lee Ann Remington and Denise Goodwin. *Clinical anatomy of the visual system E-Book*. Elsevier Health Sciences, 2011.

[152] DG Reynolds and DH Rapaport. "Organisation of the retinal ganglion cell layer of the adult guinea pig". In: *Neuroscience Letters* 27 (1987), S114.

[153] Julia Rodriguez-Ramos Fernandez and Richard R Dubielzig. "Ocular comparative anatomy of the family R odentia". In: *Veterinary ophthalmology* 16 (2013), pp. 94–99.

[154] P Röhlich, Th Van Veen, and A Szel. "Two different visual pigments in one retinal cone cell". In: *Neuron* 13.5 (1994), pp. 1159–1166.

[155] John P Rood. "Ecological and behavioural comparisons of three genera of Argentine cavies." In: *Animal Behaviour Monographs* (1972).

[156] Serge G Rosolen et al. "Comparing the photopic ERG i-wave in different species". In: *Veterinary ophthalmology* 7.3 (2004), pp. 189–192.

[157] Alicja R Rudnicka et al. "Global variations and time trends in the prevalence of childhood myopia, a systematic review and quantitative meta-analysis: implications for aetiology and early prevention". In: *British Journal of Ophthalmology* 100.7 (2016), pp. 882–890.

[158] Florian Rüfer, Anke Schröder, and Carl Erb. "White-to-white corneal diameter: normal values in healthy humans obtained with the Orbscan II topography system". In: *Cornea* 24.3 (2005), pp. 259–261.

[159] Benjamin S Sajdak et al. "Noninvasive imaging of the tree shrew eye: Wavefront analysis and retinal imaging with correlative histology". In: *Experimental eye research* (2019).

[160] Thomas O Salmon and Corina van de Pol. "Normal-eye Zernike coefficients and root-mean-square wavefront errors". In: *Journal of Cataract & Refractive Surgery* 32.12 (2006), pp. 2064–2074.

[161] Jacinto Santodomingo-Rubido et al. "Long-term efficacy of orthokeratology contact lens wear in controlling the progression of childhood myopia". In: *Current eye research* 42.5 (2017), pp. 713–720.

[162] Jacinto Santodomingo-Rubido et al. "Myopia control with orthokeratology contact lenses in Spain: refractive and biometric changes". In: *Investigative ophthalmology & visual science* 53.8 (2012), pp. 5060–5065.

[163] SM Saw et al. "Myopia: attempts to arrest progression". In: *British Journal of Ophthalmology* 86.11 (2002), pp. 1306–1311.

[164] Frank Schaeffel and Marita Feldkaemper. "Animal models in myopia research". In: *Clinical and Experimental Optometry* 98.6 (2015), pp. 507–517.

[165] Frank Schaeffel and Howard C Howland. "Mathematical model of emmetropization in the chicken". In: *JOSA A* 5.12 (1988), pp. 2080–2086.

[166] KL Schmid et al. "Inhibitory effect of atropine on myopia development in the chick: mode of application and unilateral versus bilateral lens wear." In: *Investigative Ophthalmology & Visual Science* 45.13 (2004), pp. 1239–1239.

[167] Hartmut N Schwahn, Hakan Kaymak, and Frank Schaeffel. "Effects of atropine on refractive development, dopamine release, and slow retinal potentials in the chick". In: *Visual neuroscience* 17.2 (2000), pp. 165–176.

[168] F Sha et al. "Effects of electroacupuncture on the levels of retinal gamma-aminobutyric acid and its receptors in a Guinea pig model of lens-induced myopia". In: *Neuroscience* 287 (2015), pp. 164–174.

[169] Adam W Shaikh, Jr JT Siegwart, and Thomas T Norton. "Effect of interrupted lens wear on compensation for a minus lens in tree shrews." In: *Optometry and vision science* 76.5 (1999), pp. 308–315.

[170] Yung-Feng Shih et al. "An intervention trial on efficacy of atropine and multi-focal glasses in controlling myopic progression". In: *Acta Ophthalmologica Scandinavica* 79.3 (2001), pp. 233–236.

[171] Yung-Feng Shih et al. "Effects of different concentrations of atropine on controlling myopia in myopic children". In: *Journal of ocular pharmacology and therapeutics* 15.1 (1999), pp. 85–90.

[172] Jun-Kang Si et al. "Orthokeratology for myopia control: a meta-analysis". In: *Optometry and Vision Science* 92.3 (2015), pp. 252–257.

[173] John T Siegwart Jr and Thomas T Norton. "The susceptible period for deprivation-induced myopia in tree shrew". In: *Vision research* 38.22 (1998), pp. 3505–3515.

[174] Earl L Smith III. "The Charles F. Prentice award lecture 2010: a case for peripheral optical treatment strategies for myopia". In: *Optometry and Vision Science* 88.9 (2011), p. 1029.

[175] Earl L Smith III, Melanie CW Campbell, and Elizabeth Irving. "Does peripheral retinal input explain the promising myopia control effects of corneal reshaping therapy (CRT or ortho-k) & multifocal soft contact lenses?" In: *Ophthalmic and Physiological Optics* 33.3 (2013), pp. 379–384.

[176] Earl L Smith III and Li-Fang Hung. "The role of optical defocus in regulating refractive development in infant monkeys". In: *Vision research* 39.8 (1999), pp. 1415–1435.

[177] Earl L Smith et al. "Effects of brief periods of unrestricted vision on the development of form-deprivation myopia in monkeys". In: *Investigative ophthalmology & visual science* 43.2 (2002), pp. 291–299.

[178] Earl L Smith et al. "Hemiretinal form deprivation: evidence for local control of eye growth and refractive development in infant monkeys". In: *Investigative ophthalmology & visual science* 50.11 (2009), pp. 5057–5069.

[179] Molly J Smith and Jeffrey J Walline. "Controlling myopia progression in children and adolescents". In: *Adolescent health, medicine and therapeutics* 6 (2015), p. 133.

[180] A Sorsby, GA Leary, and M Joan Richards. "Correlation ametropia and component ametropia". In: *Vision research* 2.9-10 (1962), pp. 309–313.

[181] Arnold Sorsby. "Refraction and its components during the growth of the eye from the age of three". In: *Medical Research Council* 301 (1991), pp. 1–67.

[182] Arnold Sorsby, GA Leary, and GR Fraser. "Family studies on ocular refraction and its components". In: *Journal of medical genetics* 3.4 (1966), p. 269.

[183] Richard A Stone, Ton Lin, and Alan M Laties. "Muscarinic antagonist effects on experimental chick myopia." In: *Experimental eye research* 52.6 (1991), p. 755.

[184] Richard A Stone et al. "Pharmacology of myopia and potential role for intrinsic retinal circadian rhythms". In: *Experimental eye research* 114 (2013), pp. 35–47.

[185] Jing Sun et al. "High prevalence of myopia and high myopia in 5060 Chinese university students in Shanghai". In: *Investigative ophthalmology & visual science* 53.12 (2012), pp. 7504–7509.

[186] Ágoston Szél et al. "Photoreceptor distribution in the retinas of subprimate mammals". In: *JOSA A* 17.3 (2000), pp. 568–579.

[187] Larry N Thibos et al. "Accuracy and precision of objective refraction from wavefront aberrations". In: *Journal of vision* 4.4 (2004), pp. 9–9.

[188] Larry N Thibos et al. "Standards for reporting the optical aberrations of eyes". In: *Journal of refractive surgery* 18.5 (2002), S652–S660.

[189] Margarete Tigges et al. "Effects of muscarinic cholinergic receptor antagonists on postnatal eye growth of rhesus monkeys." In: *Optometry and vision science* 76.6 (1999), pp. 397–407.

[190] Louis Tong et al. "Atropine for the treatment of childhood myopia: effect on myopia progression after cessation of atropine". In: *Ophthalmology* 116.3 (2009), pp. 572–579.

[191] David Troilo, Michael D Gottlieb, and Josh Wallman. "Visual deprivation causes myopia in chicks with optic nerve section". In: *Current eye research* 6.8 (1987), pp. 993–999.

[192] David Troilo, Debora L Nickla, and Christine F Wildsoet. "Choroidal thickness changes during altered eye growth and refractive state in a primate". In: *Investigative ophthalmology & visual science* 41.6 (2000), pp. 1249–1258.

[193] David Troilo et al. "IMI–Report on Experimental Models of Emmetropization and Myopia". In: *Investigative ophthalmology & visual science* 60.3 (2019), pp. M31–M88.

[194] Katrin Trost, M Skalicky, and Barbara Nell. "Schirmer tear test, phenol red thread tear test, eye blink frequency and corneal sensitivity in the guinea pig". In: *Veterinary ophthalmology* 10.3 (2007), pp. 143–146.

[195] Susan Vitale, Robert D Sperduto, and Frederick L Ferris. "Increased prevalence of myopia in the United States between 1971-1972 and 1999-2004". In: *Archives of ophthalmology* 127.12 (2009), pp. 1632–1639.

[196] Sujiv Vurgese, Songhomitra Panda-Jonas, and Jost B Jonas. "Scleral thickness in human eyes". In: *PloS one* 7.1 (2012), e29692.

[197] Joseph E Wagner. *The biology of the guinea pig*. Academic Press, 2014.

[198] Jeffrey J Walline, Lisa A Jones, and Loraine T Sinnott. "Corneal reshaping and myopia progression". In: *British Journal of Ophthalmology* 93.9 (2009), pp. 1181–1185.

[199] Jeffrey J Walline et al. "Interventions to slow progression of myopia in children". In: *Cochrane Database of Systematic Reviews* 12 (2011).

[200] Josh Wallman. "Retinal control of eye growth and refraction". In: *Progress in retinal research* 12 (1993), pp. 133–153.

[201] Josh Wallman and Jonathan Winawer. "Homeostasis of eye growth and the question of myopia". In: *Neuron* 43.4 (2004), pp. 447–468.

[202] Gordon Lynn Walls. *The vertebrate eye and its adaptive radiation*. LWW, 1944.

[203] I-Jong Wang et al. "The effect of intravitreal injection of atropine on the proliferation of scleral chondrocyte in vivo". In: *Journal of ocular pharmacology and therapeutics* 14.4 (1998), pp. 337–343.

[204] Lan Wang et al. "Prevalence of and Factors Associated with Myopia in Inner Mongolia Medical Students in China, a cross-sectional study". In: *BMC ophthalmology* 17.1 (2017), p. 52.

[205] Qing Wang et al. "Form-deprivation myopia induces decreased expression of bone morphogenetic protein-2, 5 in guinea pig sclera". In: *International journal of ophthalmology* 8.1 (2015), p. 39.

[206] Sha Wang et al. "Effect of retinoic acid on the tight junctions of the retinal pigment epithelium-choroid complex of guinea pigs with lens-induced myopia in vivo". In: *International journal of molecular medicine* 33.4 (2014), pp. 825–832.

[207] Yiyi Wang et al. "Human Foveal Cone Photoreceptor Topography and its Dependence on Eye Length". In: *BioRxiv* (2019), p. 589135.

[208] Ge Wen et al. "Prevalence of myopia, hyperopia, and astigmatism in non-Hispanic white and Asian children: multi-ethnic pediatric eye disease study". In: *Ophthalmology* 120.10 (2013), pp. 2109–2116.

[209] Andrew R Whatham and Stuart J Judge. "Compensatory changes in eye growth and refraction induced by daily wear of soft contact lenses in young marmosets". In: *Vision Research* 41.3 (2001), pp. 267–273.

[210] Torsten N Wiesel and Elio Raviola. "Myopia and eye enlargement after neonatal lid fusion in monkeys". In: *Nature* 266.5597 (1977), p. 66.

[211] CF Wildsoet. "Active emmetropization: evidence for its existence and ramifications for clinical practice". In: *Ophthalmic and Physiological Optics* 17.4 (1997), pp. 279–290.

[212] Christine F Wildsoet and Katrina L Schmid. "Optical correction of form deprivation myopia inhibits refractive recovery in chick eyes with intact or sectioned optic nerves". In: *Vision Research* 40.23 (2000), pp. 3273–3282.

[213] Christine F Wildsoet et al. "IMI–Interventions for Controlling Myopia Onset and Progression Report". In: *Investigative ophthalmology & visual science* 60.3 (2019), pp. M106–M131.

[214] Christine Wildsoet and Josh Wallman. "Choroidal and scleral mechanisms of compensation for spectacle lenses in chicks". In: *Vision research* 35.9 (1995), pp. 1175–1194.

[215] David Williams and Ann Sullivan. "Ocular disease in the guinea pig (Cavia porcellus): a survey of 1000 animals". In: *Veterinary ophthalmology* 13 (2010), pp. 54–62.

[216] Barry Winn et al. "Factors affecting light-adapted pupil size in normal human subjects." In: *Investigative ophthalmology & visual science* 35.3 (1994), pp. 1132–1137.

[217] James S Wolffsohn et al. "Global trends in myopia management attitudes and strategies in clinical practice". In: *Contact Lens and Anterior Eye* 39.2 (2016), pp. 106–116.

[218] Daniel Woolf. "A comparative cytological study of the ciliary muscle". In: *The Anatomical Record* 124.2 (1956), pp. 145–163.

[219] Robert J Wordinger et al. "Effects of TGF-β2, BMP-4, and gremlin in the trabecular meshwork: implications for glaucoma". In: *Investigative ophthalmology & visual science* 48.3 (2007), pp. 1191–1200.

[220] Hao Wu et al. "Scleral hypoxia is a target for myopia control". In: *Proceedings of the National Academy of Sciences* 115.30 (2018), E7091–E7100.

[221] Li Juan Wu et al. "Prevalence and associated factors of myopia in high-school students in Beijing". In: *PLoS One* 10.3 (2015), e0120764.

[222] Pei-Chang Wu et al. "Outdoor activity during class recess reduces myopia onset and progression in school children". In: *Ophthalmology* 120.5 (2013), pp. 1080–1085.

[223] Samuel M Wu. "Synaptic organization of the vertebrate retina: general principles and species-specific variations: the Friedenwald lecture". In: *Investigative ophthalmology & visual science* 51.3 (2010), pp. 1264–1274.

[224] Hui Xiao et al. "Comparison of form-deprived myopia and lens-induced myopia in guinea pigs". In: *International journal of ophthalmology* 7.2 (2014), p. 245.

[225] Jason C Yam et al. "Low-concentration Atropine for Myopia Progression (LAMP) study: a randomized, double-blinded, placebo-controlled trial of 0.05%, 0.025%, and 0.01% atropine eye drops in myopia control". In: *Ophthalmology* 126.1 (2019), pp. 113–124.

[226] MY Yen et al. "Comparison of the effect of atropine and cyclopentolate on myopia". In: *Ann Ophthalmol* 21.5 (1989), pp. 180–182.

[227] Lu Yin et al. "Chromatic properties of horizontal and ganglion cell responses follow a dual gradient in cone opsin expression". In: *Journal of Neuroscience* 26.47 (2006), pp. 12351–12361.

[228] Qi Sheng You et al. "Prevalence of myopia in school children in greater Beijing: the Beijing Childhood Eye Study". In: *Acta ophthalmologica* 92.5 (2014), e398–e406.

[229] Francis A Young. "The effect of atropine on the development of myopia in monkeys". In: *Optometry and Vision Science* 42.8 (1965), pp. 439–449.

[230] Dao-Yi Yu and Stephen J Cringle. "Oxygen distribution and consumption within the retina in vascularised and avascular retinas and in animal models of retinal disease". In: *Progress in retinal and eye research* 20.2 (2001), pp. 175–208.

[231] Yan Zhang and Christine F Wildsoet. "RPE and choroid mechanisms underlying ocular growth and myopia". In: *Progress in molecular biology and translational science*. Vol. 134. Elsevier, 2015, pp. 221–240.

[232] Wen Zhao et al. "GABA and GABA receptors alterations in the primary visual cortex of concave lens-induced myopic model". In: *Brain research bulletin* 130 (2017), pp. 173–179.

[233] Xiangtian Zhou et al. "Normal development of refractive state and ocular dimensions in guinea pigs". In: *Vision research* 46.18 (2006), pp. 2815–2823.